Master's Theses

Master's Theses and Graduate Research

1995

Investigation of the structure - property - processing relationships of 316L stainless steel hypotubing

Mazdak Rooein
San Jose State University

Follow this and additional works at: https://scholarworks.sjsu.edu/etd_theses

INFORMATION TO USERS

This manuscript has been reproduced from the microfilm master. UMI films the text directly from the original or copy submitted. Thus, some thesis and dissertation copies are in typewriter face, while others may be from any type of computer printer.

The quality of this reproduction is dependent upon the quality of the copy submitted. Broken or indistinct print, colored or poor quality illustrations and photographs, print bleedthrough, substandard margins, and improper alignment can adversely affect reproduction.

In the unlikely event that the author did not send UMI a complete manuscript and there are missing pages, these will be noted. Also, if unauthorized copyright material had to be removed, a note will indicate the deletion.

Oversize materials (e.g., maps, drawings, charts) are reproduced by sectioning the original, beginning at the upper left-hand corner and continuing from left to right in equal sections with small overlaps. Each original is also photographed in one exposure and is included in reduced form at the back of the book.

Photographs included in the original manuscript have been reproduced xerographically in this copy. Higher quality 6" x 9" black and white photographic prints are available for any photographs or illustrations appearing in this copy for an additional charge. Contact UMI directly to order.

INVESTIGATION OF THE
STRUCTURE - PROPERTY - PROCESSING RELATIONSHIPS
OF 316L STAINLESS STEEL HYPOTUBING

A Thesis

presented to

the Faculty of the Department of Materials Engineering

San Jose State University

In Partial Fulfillment

of the Requirements for the Degree

Master of Science

by

Mazdak Rooein

August 1995

UMI Number: 1375722

Copyright 1995 by
Rooein, Mazdak
All rights reserved.
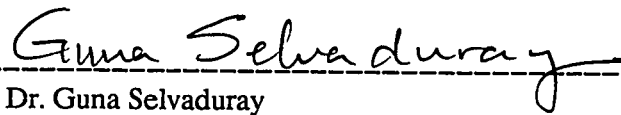
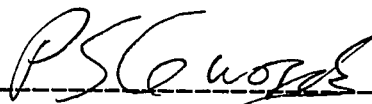# UMI
300 North Zeeb Road
Ann Arbor, MI 48103

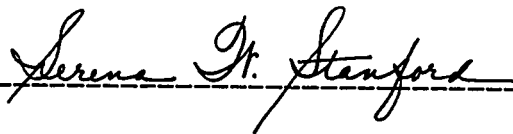APPROVED FOR THE DEPARTMENT OF MATERIALS

ENGINEERING

Dr. Guna Selvaduray

Dr. Sepehr Fariabi

Dr. Peter Gwozdz

APPROVED FOR THE UNIVERSITY

ABSTRACT

INVESTIGATION IN
STRUCTURE - PROPERTY - PROCESSING RELATIONSHIPS
OF 316L STAINLESS STEEL HYPOTUBING

by Mazdak Rooein

The effects of thermomechanical processes on the microstructure and the mechanical properties of 316L stainless steel hypotubing, used as an intravascular implant device, were studied by employing statistically designed experiments. The heat treatment temperature (in the range of 720°C to 920°C), the initial cold working of the material (in the range of 10% to 24%), and the wall thickness of the hypotubings (in the range of 0.06 mm and 0.10 mm) were the variables. The study showed that up to 35% of residual stress can be released, and the ductility of the material can be increased up to 60% by heat treating at 920°C, without any grain growth and chromium carbide precipitation. The wall thickness affected the ductility of the material - thinner hypotubings had lower elongations. Mathematical equations correlating the mechanical properties of the material to the variables were developed.

ACKNOWLEDGMENTS

TABLE OF CONTENTS

LIST OF TABLES

LIST OF FIGURES

x

CHAPTER 1
INTRODUCTION

1.1. History

It was 1821 when a Frenchman named Berthier found that iron highly alloyed with chromium becomes more resistant to acid attack and that its resistance improves with increasing chromium content. Another Frenchman, Brustlein, developed the first chromium steels between 1877 and 1886. These later became known as stainless steels and are classified into three categories: martensitic stainless steels with 12-16% Cr and 0.1-0.4%C, ferritic stainless steels with 16-30% Cr, and austenitic stainless steels with 12-30%Cr and 7-25% Ni. Austenitic stainless steels, or so-called 18-8 (18Cr-8Ni) steels, were first introduced and used as implants in orthopedic surgery in 1926 and eventually became one of the alloys that replaced the more corrosion-prone steels. Today, austenitic stainless steels are the predominant implant alloys. This is mainly due to their early introduction and development, history of comparative successes, ease of fabrication, and good mechanical properties and corrosion behavior.[1]

One of the materials that is used for implantable surgical devices is 316LVM stainless steel†, or simply 316L. It is one of the alloys in the 302 stainless steel family, standard austenitic stainless steels, which have been modified for different improvements. For example, silicon is added to 302 stainless steel to obtain 302B, which has improved scaling resistance. Molybdenum is added to increase corrosion resistance to obtain the 316 grade, and carbon is reduced to obtain the 316L grade, which has better welding characteristics and reduced carbide precipitation. Table 1. shows the chemical composition of the 302 stainless steel family.[2]

1

Table 1. Chemical composition of 302 stainless steel family

Grade	C	Mn	Si	Cr	Ni	P	S	Fe	Other
302	0.15	2.00	1.0	17.0-19.0	8.0-10.0	0.045	0.03	Balance	-
302B	0.15	2.00	2.0-3.0	17.0-19.0	8.0-10.0	0.045	0.03	Balance	-
316	0.08	2.00	1.0	16.0-18.0	10.0-14.0	0.045	0.03	Balance	2-3 Mo
316L	0.03	2.00	1.0	16.0-18.0	10.0-14.0	0.045	0.03	Balance	2-3 Mo

316L stainless steel has shown outstanding reliability in surgical implant applications and was approved by the U.S. Food and Drug Administration (FDA) as the standard grade to be used for this purpose because of the combination of compatibility with bodily fluids, wear behavior, malleability, low notch sensitivity, and reasonable material and manufacturing costs.[3]

1.2. What is Hypotubing?

Tubular products are generally divided into three categories: tubes, pipes, and tubings. The term "tube" refers to tubular products that are made in a variety of sizes, whereas the term "pipe" refers to tubular products that are made only in standard sizes. "Tubings" are tubular products that are made to exact specifications with regard to dimensions, chemical composition, mechanical properties, surface finish, etc. Hypotubing is a tubing of small dimensions, with an outside diameter (O.D.) typically less than 6 mm (1/4"). Hypotubing is manufactured in two varieties: seamless and welded. For seamless products, the tubing is made by forging a solid rod, piercing it by simultaneously rotating and forcing it over a piercer point, and further reducing it by rolling and drawing. A

welded tubing is made from a rolled strip with a typical width of 5.8 cm (2.3") and a thickness of 1.3 mm (0.05") formed into a cylinder and welded by various heating methods. In both cases the product is tubing with a typical O.D. of 16 mm (0.5" - 0.8"). To produce hypotubings, the tubing is rolled and drawn down to a typical O.D. of 1.3 - 1.8 mm (0.06") by drawing (cold working) and heat treating. Figure 1 is a schematic diagram of the process for manufacturing seamless and welded hypotubing.
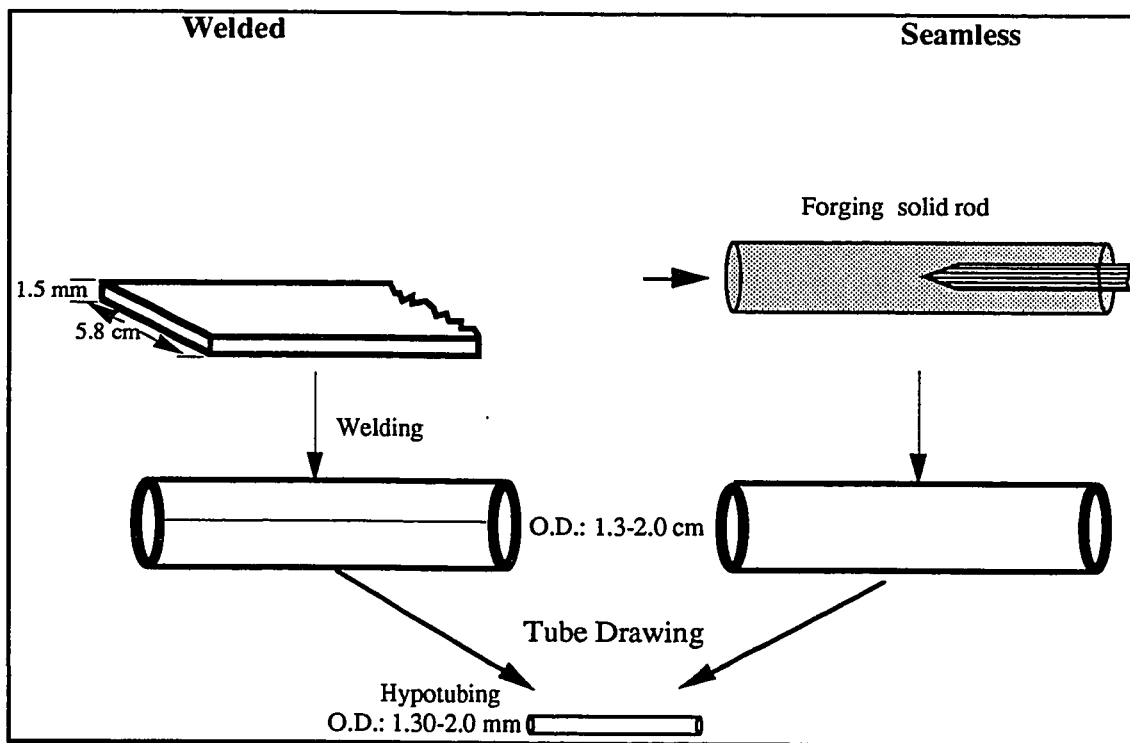
Figure 1. Schematic diagram of manufacturing seamless and welded hypotubing

The amount of cold work that is introduced into the final hypotubing product during the tube drawing process affects the properties of the material. The strength and ductility of the material are affected significantly. As is shown schematically in Figure 2, increasing the amount of cold work decreases the ductility of the material, and at the same time this effect increases the strength of the material. The percent cold work, which represents the residual stress in the material, can be reduced by heat treatment. Therefore, depending on the application and the required mechanical properties the percent of initial cold work and heat treatment process variables can be specified.
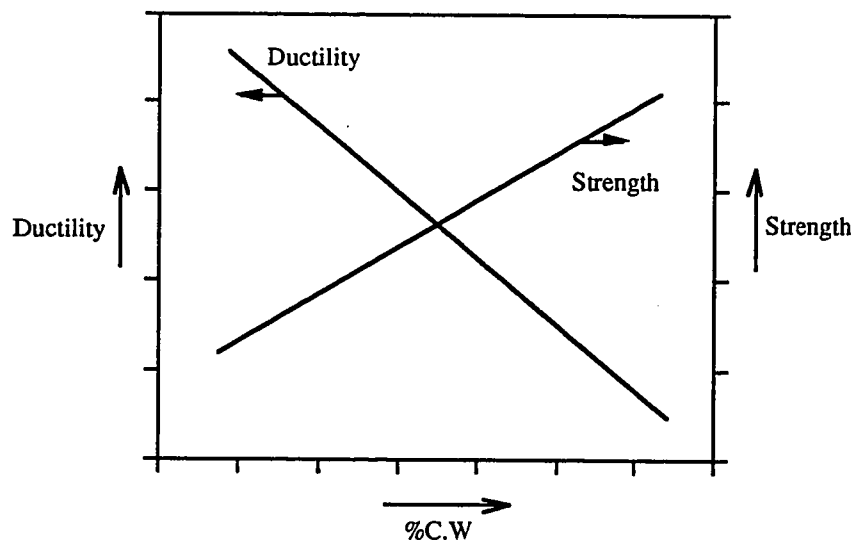
Figure 2. A schematic of the effect of cold work on the strength and ductility of stainless steel

1.3. Application of 316L Stainless Steel Hypotubing in Cardiovascular Devices

A particular application of austenitic stainless steels in the field of implantable surgical devices is their use in cardiology procedures. Coronary artery disease (CAD) is a major health problem. This disease is usually cured by coronary bypass surgery. During the past decade, angioplasty has become an alternative to surgery. In coronary artery disease, the coronary arteries become narrowed or blocked by a gradual build-up of fat (cholesterol) within the artery wall. This build-up is called atherosclerotic plaque or simply plaque. Figure 3 shows a narrowed artery due to plaque formation.
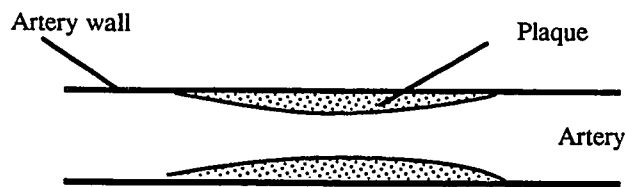
Figure 3. Schematic of an artery narrowed by built-up plaque

If the plaque narrows the channel of the artery significantly, it becomes difficult for an adequate quantity of blood to flow to the heart's muscles. Generally there are three ways to treat CAD: medication, coronary bypass surgery, and precutaneous transluminal coronary angioplasty (PTCA) or simply angioplasty. Angioplasty is a technique that is used to widen the plaque-filled coronary artery without surgery. In this process a small inflatable balloon is sent within the narrowed section of the coronary artery by means of a

5

guide wire. Figure 4 shows the placing of an inflatable balloon in the narrowed section and expanding it during the process of angioplasty.

a

b
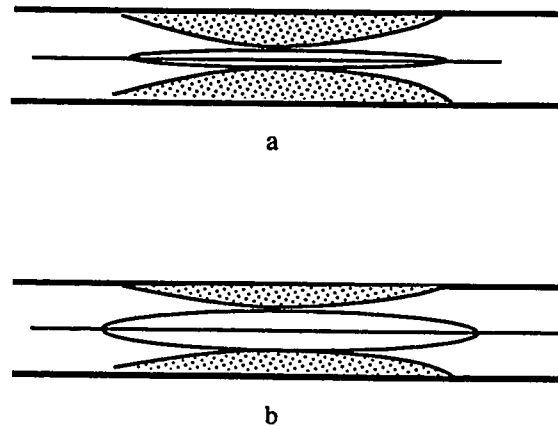
Figure 4. A schematic of angioplasty procedure: a: Insertion of guide wire and balloon in the narrowed coronary artery b: Widening of artery by expansion of balloon

The success rate of angioplasty is not as high as it should be because of reclosure of the artery either while the procedure is being performed or sometime later. This problem has led cardiovascular industries to use an implantable surgical device called an intravascular stent, or simply stent. This is a mesh type 316L stainless steel hypotubing that can be expanded and made to retain its expanded shape. By placing this small tubing in the narrowed section of the artery and expanding it, the plaque is pushed back and the artery remains open, with less chance for reclosure of the vessel. A guide wire is sent through the narrowed section as was shown in Figure 4, and a balloon, which holds the stent, is passed over the guide wire. Then the balloon, and therefore the stent, is expanded and the stent is implanted in the artery. The balloon is then pulled out. Figure 5 illustrates the process of expanding a stent in a narrowed artery.

6
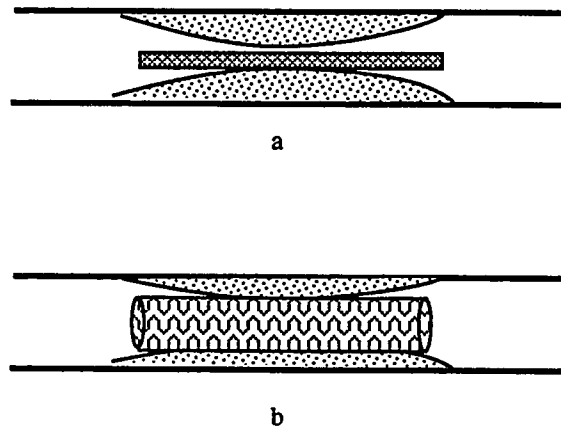
Figure 5. Schematic of implantation of intravascular stent:
a: Non-expanded stent b: Expanded stent

Of critical importance here are the strength and ductility of the material. In an ideal case, sufficient ductility is needed to provide the deformation during the process of expansion of the stent without fracture, while at the same time retaining sufficient strength to support the vessel against reclosure.

1.4. Corrosion of 316L Stainless Steel when used as an Implant

Corrosion is one of the main concerns when using metallic implants. Depending on the materials involved, the corroded species may be toxic, carcinogenic, or allergenic, and may cause self-tissue reactions, inflammation, or bone necrosis.[3] As mentioned before, 316L stainless steel has very good corrosion properties, especially in bodily fluids. There are four principal types of corrosion mechanisms of interest to the biomedical field: uniform attack, crevice corrosion, pitting corrosion, and intergranular corrosion.

In intergranular corrosion (IGC) passivating elements such as chromium are depleted at the grain boundaries, and as a result, the grain boundaries or adjacent regions

7

are often less corrosion resistant. In some cases the preferential corrosion at the grain boundaries may be severe enough to drop the grains out of the surface. This is due to the high surface energy of the grain boundaries, making these boundaries the preferred sites for solid-state reactions such as diffusion, phase transformations, and precipitation reactions. The high energy of grain boundaries usually results in a higher concentration of solute atoms at the boundary, compared to the interior of the grain. Therefore, if the austenite grain size in stainless steel is coarse, fewer nucleation sites would be available and diffusion controlled transformation of the austenite would be retarded. The intergranular attack may also be deep and rapid, leading to abrupt failure by fracture of the implants. Austenitic stainless steels are susceptible to this kind of corrosion when they are heat treated in the range of 425°C to 815°C, and regions of the grains adjacent to the grain boundaries are depleted of chromium by metallurgical reaction with carbon and form chromium carbides at the grain boundaries.[4] This is called chromium carbide precipitation. Ti, Nb, Mo, and Cr are examples of elements that are carbide formers. Chromium is the most important carbide former in stainless steels.

1.5. Scope of Research

The objective of this project was to investigate the structure-properties-processing relationships in 316L stainless steel hypotubing and to develop the characterization techniques for verifying the relationships. The main focus was to identify the effects and interactions of the manufacturing process parameters of the hypotubing on the properties of the final product. The parameters under study included the amount of cold working, the heat treatment temperature, and the wall thickness of the hypotubing. The hypotubing properties included mechanical properties, grain size, and intergranular corrosion susceptibility of the material.

8

CHAPTER 2

APPLICATION OF STAINLESS STEELS IN CARDIOLOGY

Because of the relatively recent development and use of surgically implanted devices in the field of cardiology, most of the research results are still not available in the open literature. Grade 316L stainless steel has been extensively studied, mostly regarding its biocompatibility, corrosion properties, and mechanical defects in the area of orthopedic implants. In this chapter, the available literature on the use of 316L in surgical implants are reviewed.

After metallographic examinations of bone pins, which support the other implant parts, Gray[5] reported that the amount of cold working, and therefore the hardness of the 316L implant parts, contributed to the failure of the implants due to stress corrosion cracking or corrosion fatigue. He measured the hardness of the material in the area of the failure and correlated the amount of the hardness to the excessive amount of cold working done on the material due to the applied stress during the service. Hardness measurements were used because of the inability of measuring the tensile properties of the implant parts. The hardness values were then correlated to the tensile properties and the amount of residual stress in the material. This study illustrated that the amount of cold working, and therefore the residual stress, in the as-received material must not exceed its ultimate tensile strength. Gray also found that lack of good surface finish resulted in the occurrence of localized stress concentration.

Cahoon et al[6] and Weinstein et al[7] also studied the failure of orthopedic implants. They examined the area of the materials that had been under maximum stress during service. The orthopedic parts that they examined included bone plates, screws, and nails.

They measured the inclusion content and the grain size, and analyzed the chemical composition using microprobe x-ray analysis. They found high inclusion contents and small grain size primarily in the areas of maximum stress. They reported that these inclusions provide the preferred sites for stress corrosion. In both cases, the researchers found another cause for the failure of the implants: formation of delta ferrite in the welded structure.

In their research on the quality of stainless steel surgical implants, Procter and Seaton[8] compared the corrosion resistance of heavily cold worked (above 50%) with annealed (less than 15% cold work) stainless steel parts. They concluded that the materials with more cold-working were more susceptible to corrosion. They also emphasized the importance of the heating or cooling rate for the manufacturing of austenitic stainless steel. They reported that slow heating or cooling of austenitic stainless steel at around 550-850°C results in precipitation of chromium carbide in the grain boundaries.

In another related research, Advani et al[9] studied the effects of deformation of the material during the manufacturing process on intergranular carbide precipitation and transgranular chromium depletion. They reported that thermomechanical treatments that especially introduce strains above 20% cause carbide formation at the intersections of faults, dislocation lines, and strain-induced martensite boundaries, especially in type 304 stainless steel.

In the area of effects of chemical composition, Procter and Seaton examined the primary effect of Mo addition to austenitic stainless steels.[8] They compared the corrosion resistance of parts made of 302 stainless steel, with no molybdenum, and 316L stainless steel, with 2-3% Mo. They found that this alloying of 316L greatly improved its resistance to pitting attack in chloride containing environments.

Eckenrod and Kovach studied the effect of nitrogen content on the properties of austenitic stainless steels.[10] They examined the anodic polarization characteristics of these stainless steels in sodium chloride and sulfuric acid solutions, and found that the corrosion resistance of the stainless steels was improved with increasing nitrogen content. They also measured the yield strength of the stainless steels for different nitrogen contents and found that nitrogen increases the yield strength of the stainless steel by 5.5 to 6.2 MPa for each 0.01 percent increase in the nitrogen content. Figure 6. shows the effect of increasing the nitrogen content on the mechanical strength of the material.
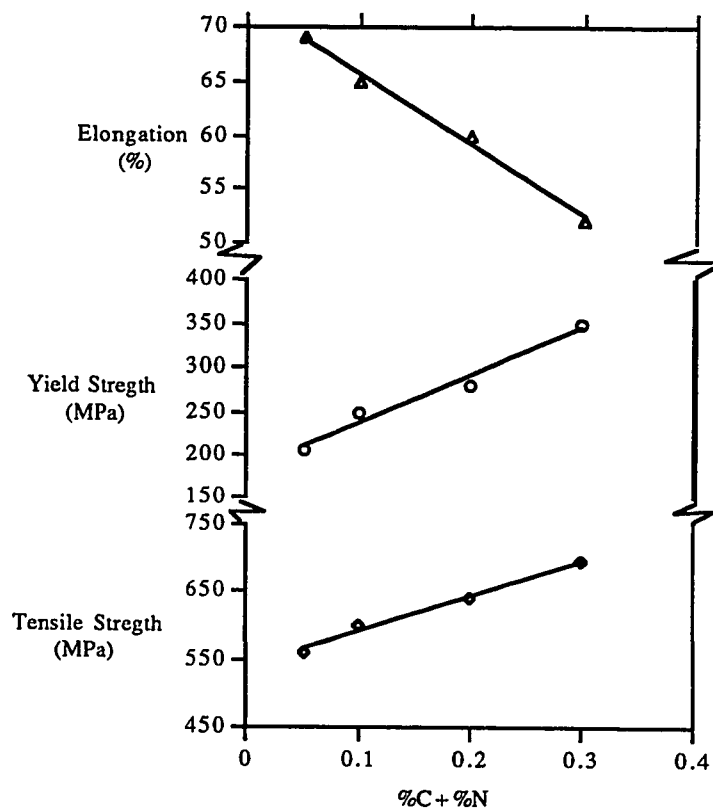
Figure 6. Effect of nitrogen on the room-temperature mechanical properties of austenitic stainless steels[10]

11

CHAPTER 3
OBJECTIVE AND METHODOLOGY

3.1. Objective

The overall objective of this study was to determine the effects of manufacturing operation variables on the properties of 316L stainless steel hypotubings, so that the latter can meet the requirements of an implant material (stent). A secondary objective was to develop characterization techniques for evaluation of incoming hypotubings before they are subjected to the manufacturing operations of the implant device, so that the properties of the manufactured hypotubing could be correlated to the raw material properties. The effects of thermomechanical processing on the microstructure, mechanical properties, and intergranular corrosion resistance of the material were therefore studied, and an empirical relationship between the manufacturing parameters and the mechanical properties was developed by employing designed experiments.

3.2. Test Methods

Because of the relatively recent development of stent parts, new test methods needed to be developed. These included methods for mounting the cross section of the hypotubing, metallographic procedures, grain size measurement method, inclusion rating methodology for raw materials, and tensile testing procedure.

Chemical analyses of the samples were done by outside laboratories. Since these analyses provided acceptance or rejection information of the hypotubing as an implant

material, per ASTM standard specifications,[17,18] they were performed as on-going processes throughout the course of this project.

The main effort of this investigation focused on studying the effects of thermomechanical processing (heat treatment factors) on the microstructure, intergranular corrosion resistance, and mechanical properties of the material. Designed experiments were used for this purpose. The heat treatment temperature, percent initial cold-work, and wall thickness of the hypotubing were the factors (input variables) studied.

The response variables were the tensile properties of the hypotubings, including ultimate tensile strength (UTS), yield strength (Y.S.), and ductility. In addition to these responses, the effects of the heat treatment process on the microstructure of the material, including grain size and intergranular precipitation, which makes the material susceptible to intergranular corrosion, were also studied. These responses were evaluated according to the procedures presented in following sections. Finally, correlations between the heat treatment process factors and the mechanical properties of the stainless steel hypotubing were derived.

Since the material was subjected to heat treatment process, intergranular corrosion resistance of the material was tested according to "Standard Practices for Detecting Susceptibility to Intergranular Attack in Austenitic Stainless Steels".[14]

This project did not evaluate the overall corrosion resistance of the material in detail. Although 316L stainless steel has been approved as one of the materials used for surgical implants by the Food and Drug Administration (FDA), a thorough corrosion study of the material is beyond the scope of this project, and is recommended for future study.

The raw materials used in this study are first described. Then, the methodology for the microstructure analysis, and the mechanical properties measurements; the heat treatment

13

process, the heat treatment factors, the design of experiments, and methodology for intergranular corrosion testing are presented.

3.3. Raw Materials and Methodology

The raw materials used for this investigation were 316L stainless steel hypotubings provided by two outside suppliers with very close chemical composition. These hypotubings were obtained with various extent of cold works and dimensions. The physical properties of these hypotubings are given in Table 2.

Table 2. Physical properties of incoming 316L stainless steel hypotubings

Lot #	Cold work %	UTS (MPa)	Y.S. (MPa)	Elongation %	I.D. (mm)	Wall Thick. (mm)
2	25	975.6	827.5	13.7	1.40	0.09
4	10	861.9	729	25.5	1.40	0.09
6	10	649.7	536	24.0	1.40	0.06
8	10	711.0	577.4	38.3	1.50	0.10
9	10	779.3	664.9	29.7	1.50	0.10
14	24	850.2	673.2	7.0	1.50	0.10
15	17	753.8	596.7	23.0	1.50	0.10
16	10	708.3	560.8	31.0	1.50	0.10

3.3.1. Metallography of 316L Stainless Steel Hypotubing

A methodology for the metallography procedure needed to be developed. Since the materials specification must conform to FDA requirements, the developed test procedures

were in accordance with ASTM test methods.[11,12] However, because of the extremely thin wall of the hypotubings (0.10 mm), procedures for mounting the specimen, optical observations, inclusion rating, and grain size measurements were modified.

For each mount a 3.8 cm section of the hypotubings was used. Because of the thin wall of the hypotubings and work hardenability of the austenitic stainless steels, sectioning was performed with a low-speed diamond saw, which according to Vander Voot, introduces a depth of deformation of approximately 30 μm for austenitic stainless steels.[15]

A cold-setting epoxy resin was used for mounting the samples. In order to avoid air trapping in the middle of the hypotubing, it was mounted vertically with an outside support and with one side out of the epoxy resin, with the bottom edge slightly higher than the bottom of the mold. Thus, it was ensured that the epoxy resin would flow inside the hypotubing from the bottom. Use of a vacuum chamber during filling made sure that the inside of the hypotubing was filled. Figure 7 shows a schematic of a mounted hypotubing.
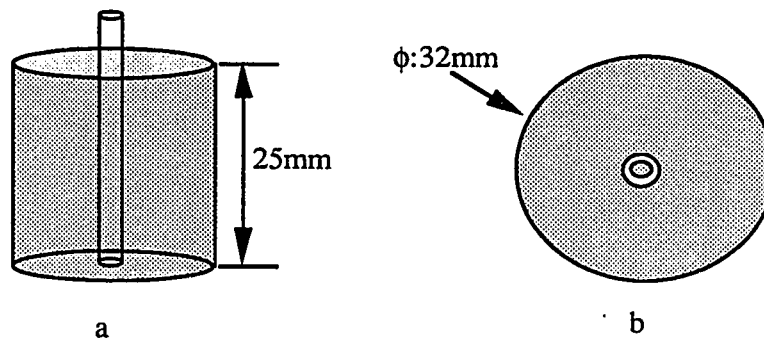
Figure 7. Schematic of mounted hypotubing for metallography procedure:
a: side view b: top view

After mounting, the specimen was ground with water-cooled silicon carbide papers starting with 600-grit and finishing with 4000-grit. A grinding wheel rotating at 300 rpm

and a moderate-firm pressure for about thirty seconds was used. The specimen was ultrasonically cleaned, between each step, for three minutes in order to avoid cross contamination. The specimen was then washed with alcohol and dried under a stream of hot air before optical microscopy. If any scratches from the previous steps were observed, extra grinding time, up to two minutes, was spent in order to remove them.

The sample was then mechanically polished using low-nap polishing cloths, with 3 and 1 micron diamond paste as abrasive particles. Ethylene Glycol was used as the lubricant extender to moisten the cloth and reduce drag. A grinding wheel rotating at 300 rpm and a moderate pressure was used. The polishing process was then continued using a medium-nap cloth with 0.05 micron α-alumina slurry as abrasive particles. A medium-nap cloth soaked with distilled water was then used as the last polishing tool.

A summary of the grinding and polishing steps followed for the metallography procedure of the stainless steel hypotubings is contained in Table 3.

Table 3. Summary of grinding and polishing steps for metallography of
stainless steel hypotubings

	Size	Paper / Cloth	Paste	Dispenser	Time
1	320 grit	silicon carbide paper	-	tap water	30 sec
2	600 grit	silicon carbide paper	-	tap water	30 sec
3	1200 grit	silicon carbide paper	-	tap water	30-60 sec
4	4000 grit	silicon carbide paper	-	tap water	1-2 min.
5	3 micron	low-nap cloth	diamond	Ethylene Glycol	1-2 min.
6	1 micron	low-nap cloth	diamond		1-2 min.
7	0.05 micron	medium-nap cloth	α-alumina		1 min.
8	Final	medium-nap cloth	-	distilled water	1 min.

3.3.2. Grain Size Measurement

After the specimen was mounted, ground, and polished, it was electroetched with a 10% oxalic acid solution. This was followed by application of a potential of 3 V DC and 10 mm electrode spacing for 45 seconds. Figure 8 shows a schematic of the electrolytic etching process.

stainless steel hypotubing
mounted sample as the anode

power
supply

10% oxalic
acid solution

stainless steel container as the cathode
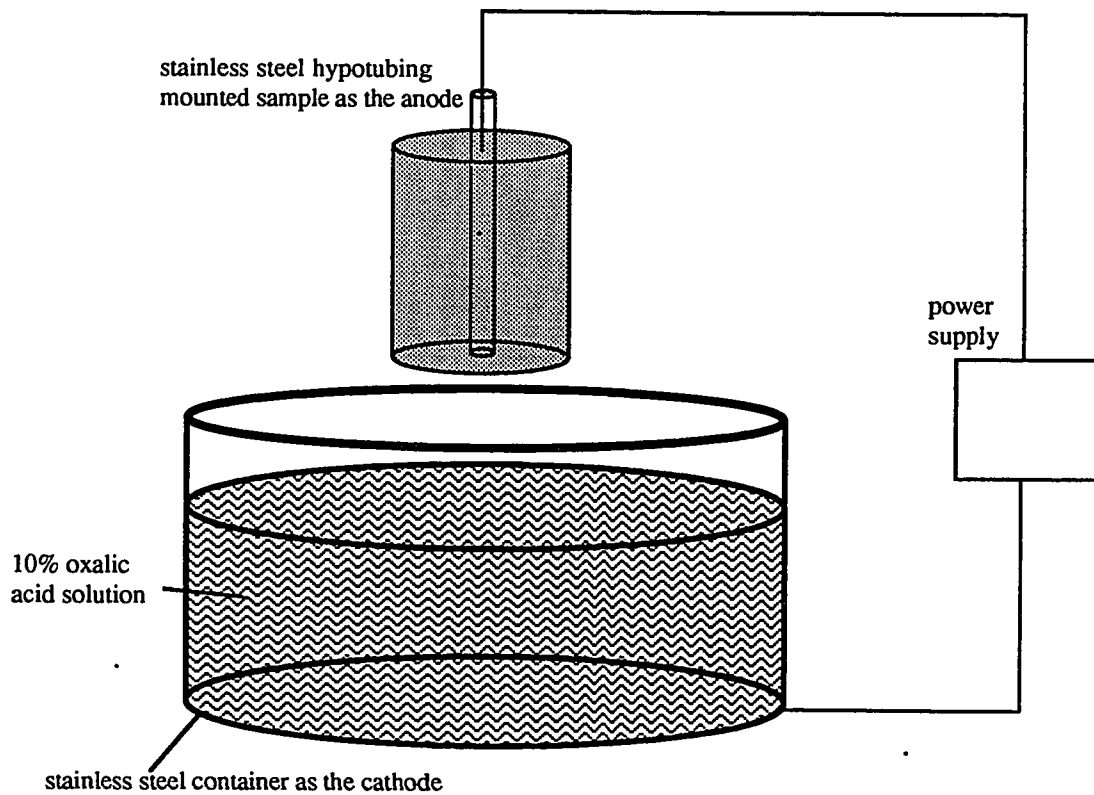
Figure 8. Schematic of electrolytic etching of stainless steel hypotubing in 10% oxalic acid solution

After electrolytic etching, the specimen was rinsed first with distilled water and then with alcohol, and finally dried with hot air. Photomicrographs at 100X and 400X magnification were then taken. On the 400X pictures, 5 random grain counts were performed within a 2.54 x 2.54 cm (1" x 1") square, and the numbers averaged (N_{400}). The ASTM grain size was then calculated from Equation 1, to the nearest 0.5.

$$\text{ASTM Grain Size: } G = (3.32 \times \log N_{400}) + 5 \qquad [1]$$

Equation 1 was derived from the ASTM standard grain size measurement relationship. Equation 2 shows the general relationship between ASTM grain size and the number of grains per 6.45 cm^2 (1 in^2) at 100X magnification (N).[11]

$$N = 2^{G-1} \qquad [2]$$

3.3.3.   Inclusion Rating

Ten 1 cm long pieces of stainless steel hypotubings were cut and mounted longitudinally. The mount was then ground until the hypotubing walls were exposed, as is shown in Figure 9. The specimen was then ground and polished as per the procedure described in Section 3.3.1. Assuming a hypotubing wall thickness of 0.09 mm, this mount provided a total area of 0.18 mm^2 of hypotubing walls.

18
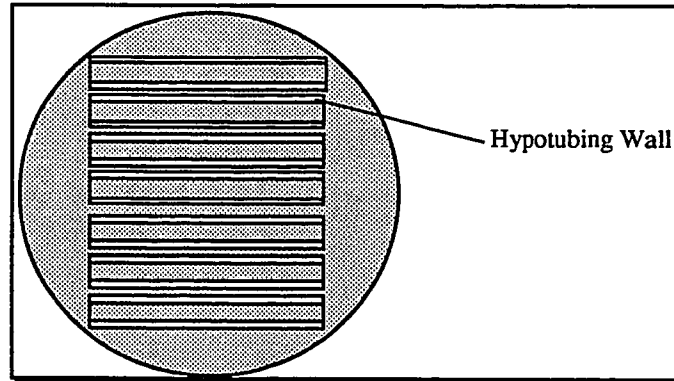
Figure 9. Schematic of mounted stainless steel hypotubings for inclusion rating

The specimen was inspected under an optical microscope, at 100X or larger magnification, to determine if any inclusions were presented. If any inclusion was found, the photomicrograph of the polished surface was first compared with the ASTM standard inclusion chart, namely, the JK chart Method D, which has been designed primarily for low inclusion content steels.[12] Selective etching was then done in order to identify the inclusion. Table 4 shows the etchants and the etching times employed for selective etching for three of the most common inclusions in stainless steels.

Table 4. Summary of selective etching process for stainless steel hypotubing

Solution	Time	Effect
100ml water 2 g KMnO4 12g KOH	5-15 sec	Attacks carbides (darken)
0.2g oxalic acid 100 ml water	20-30 sec	Attacks sulfides (darken)
15 CrO3 100 ml water	60 sec	Attacks sulfides (reddish)

3.3.4. Tensile Testing

One of the test methods developed was the tensile test procedure for stainless steel hypotubing. In a tensile test three parameters have to be specified, i.e., the strain rate, gage length, and specimen length. The gage length is the section of the specimen over which elongation measurements are done, and the specimen length is the total length of the specimen that is pulled during the test. In the ASTM standard tensile test method on steel tubular products,[13] the recommended gage length is four times the outside diameter of the tubular specimen. In the case of the hypotubings this length would be very small. Therefore, conventional 5.08 cm (2 in) and 25.4 cm (10 in) lengths were used as the gage length and the sample length, respectively, in order to obtain data consistent with currently available information, including those provided by the vendor and those reported by other researchers. The concern about the consistency of the data was mainly with regard to the total percent elongation value (including both uniform and localized), which depends on the gage and sample length. A comparison of the results of tensile tests with three different specimen lengths is presented in Appendix 1.

The strain rate sensitivity of the stainless steel hypotubing was calculated to be 0.0088. This calculation is also presented in Appendix 1. Therefore, because it was found that the strain rate had only a very minor effect, the conventional strain rate of 0.05 min^{-1} was used.

3.3.4.1. Procedure

Three 30.48 cm (12 inch) long pieces of each type of hypotubing were cut and used as specimens for each tensile test. The measured properties were averaged. The specimens were marked at every 1.27 cm (0.5 inch) interval along their length for elongation measurements. Two 2.54 cm (1 inch) long pieces of 304 stainless steel mandrels were inserted from both sides of the hypotubing to hold the specimen. Figure 10 shows the

20

tensile test specimen and the gripping jaws of the tensile test machine schematically. Table 5 is a summary of the conditions under which the tensile tests were done.
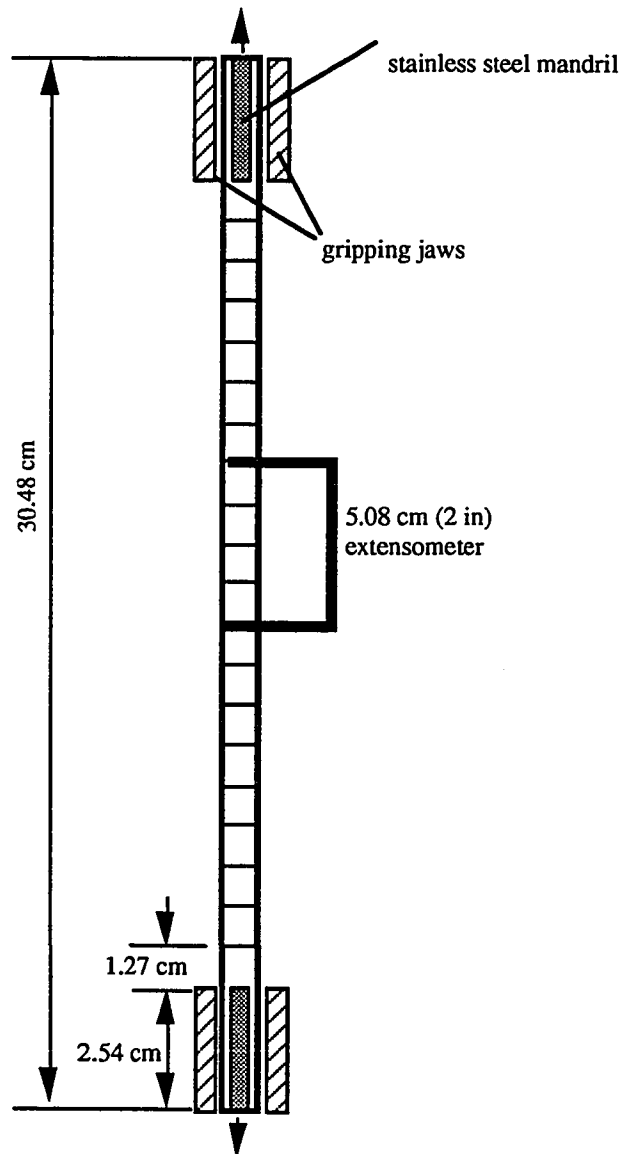
Figure 10. Schematic of stainless steel hypotubing tensile test

Table 5. Summary of tensile test conditions

Test Temperature	20-25°C
Grip Type	hydraulic jaws (0.5 MPa)
Grip face	knurled face
Sample length	25.4 cm (10")
Extensometer gage length	5.08 cm (2")
Mandrill	1" S.S.(O.D.= tubing's I.D. - 0.002)
Crosshead speed	1.27 cm/min.(0.5 in/min.)
Load cell	100N(220.4lb)
Cross head action at break	stop, then return
Sampling rate	2 pt/sec

The ultimate tensile strength (UTS) in MPa, and the yield strength (Y.S.) in MPa were measured using Instron software. After fracture, the specimen was removed from the machine and the ductility of the material, represented by total percent elongation, was calculated by measuring the amount of elongation over a 5.08 cm (2 in) span around the fracture area, as shown by Equation 3.

$$\% \text{ Elongation} = \frac{(\text{Distance between 2" marks around the fracture} - 2)}{2} \times 100 \qquad [3]$$

3.3.5. Heat Treatment and Annealing of Stainless Steel

In order to obtain material with different levels of cold working (different levels of strength and ductility) the stainless steel hypotubing samples were heat treated. The heat treatment process was done in a tube furnace with three heat zones. Figure 11 is a diagram of the heat treatment furnace configuration. To avoid surface oxidation, argon mixed with 3.5% hydrogen was used. The gas mixture was introduced through a 65 cm long ceramic tube at a flow rate of 4.7 l/min (10 CFH) and exhausted into air. Since there was a temperature gradient due to the gas flow along the ceramic tube, the temperature set point of the first heat zone was 100°C higher than the desired heat treatment temperature (By monitoring the temperature profile along the ceramic tube, one can make this adjustment for different conditions). The furnace temperature profile along the ceramic tube for heat treatment at 720°C is presented in Appendix 2.

The specimen was inserted in a porous ceramic sample holder, and the sample holder was put in the ceramic tube, as is shown in Figure 11. The pores were designed to avoid a pressure drop.

The specimen was heat treated for five minutes. The sample holder and the specimen were then water quenched. Tensile tests were subsequently performed to determine the effects of heat treatment on the mechanical properties of the material by measuring the ultimate tensile strength, yield strength, and ductility. The effect of heat treatment on the microstructure of the material was determined by optical metallography and grain size measurement. In addition, the microstructure of the material was examined for any chromium carbide precipitation due to the heat treatment process. The procedure for this examination is presented in Section 3.3.7.
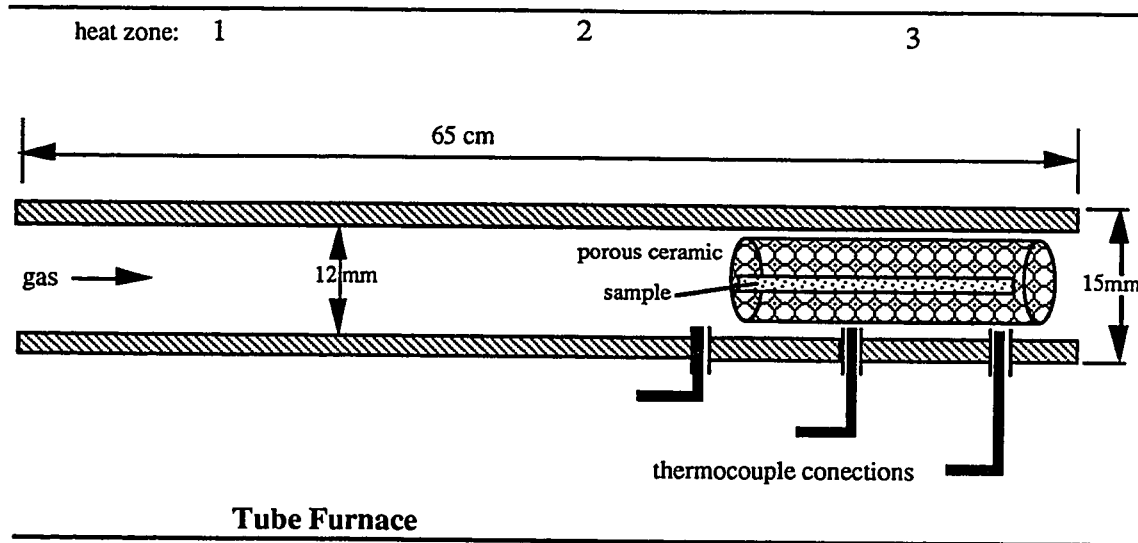
Figure 11. Schematic of heat treatment fixture: tube furnace,
ceramic tube for gas flow, porous ceramic as sample holder

3.3.6. Manufacturing Variables and Designed Experiments

A preliminary study was done to specify the heat treatment temperature range, time, environment, and cooling method. The goal of this study was to identify the heat treatment conditions such that the as received material may be heat treated to yield a product that would be stress relieved, more ductile, and would not exhibit grain growth, and surface oxidation. The necessity to relieve the stress from cold working was expected to determine the lower temperature limit for the heat treatment process. On the other hand, the higher temperature limit was determined to be the maximum temperature for the heat treatment process that causes no grain growth. The results of this study are presented in Appendix 4. Based on this study, the heat treatment time of 5 minutes, an argon-3.5% hydrogen environment, and water-quench cooling method were specified. In other words, these factors were blocked in the experiments. Also, the temperature range of 720°C to 920°C

24

was identified. The effect of this range of heat treatment temperature on the mechanical properties of stainless steel hypotubings from Lot #16 (Table 2) is illustrated in Figure 12, in Chapter 4. As a result, the heat treatment temperature was then considered to be one of the variables affecting the mechanical properties of the stainless steel hypotubing at 720°C and 920°C as the low and high levels, respectively.

The effect of the initial cold working on the extent of stress relief (% SR), due to the heat treatment process, was studied. For this study samples with different initial cold working (CW) were heat treated, and the extent of stress relief was calculated from Equation 5.

$$\% \text{ SR} = (\text{UTS}_{\text{As-received}} - \text{UTS}_{\text{Heat Treated}}) / \text{UTS}_{\text{As-received}} \qquad [5]$$

Samples from Lot # 14 (24% CW), Lot # 15 (16% CW), and Lot # 16 (10% CW) were used for this study. Three specimens from each lot were heat treated at 720°C, and the extent of stress relief of these samples was compared with that from the samples heat treated at 920°C. The results of this study are presented in Figure 13, in Chapter 4. As a result of this study, the percent cold work (initial cold working) of the incoming material was considered to be another manufacturing variable, at two levels of 10% and 24% as the low and high levels, respectively.

In another study for identifying the manufacturing variables, the effect of wall thickness on the mechanical properties of stainless steel hypotubing was studied. Hypotubings with 0.10 mm (0.004 in) wall thickness, from different lots and with different heat treatment history, were ground down to 0.06 mm (0.0025 in) wall thickness. The grinding procedure was performed by an outside vendor. The mechanical properties

25

of these samples were then measured by tensile testing. The stress-strain graphs for these tests are presented in Appendix 4. These tests showed no significant change in the strength of the hypotubings, but they did show a significant drop in ductility due to decrease in the wall thickness. A comparison of the ductility of the hypotubing samples for the two wall thicknesses is presented in Figure 15, in Chapter 4. As a result of this experiment, wall thickness was considered to be another factor at 0.06 mm as the low, and 0.10 mm as the high level.

3.3.6.1. Design of Experiments

After identifying the factors as: (A) heat treatment temperature, (B) percent cold-work, and (C) wall thickness, full factorial experiments at two levels were designed with the help of "Design Ease 3.01" software, with three replications. This made it necessary to have a total of twenty four experiments. Table 6 shows the matrix for this experiment design, including the factors and their levels.

Table 6. Matrix of DOE

	Low (-)	High (+)
heat treatment temperature (C)	720	920
cold-work (%)	10	24
wall thickness (mm)	0.06	0.10

The software randomly assigned the sequence of the experiments. The raw materials for these experiments were samples from Lot #14 and Lot #16 which had the

same chemical composition and same dimensions (1.50 mm I.D. and 0.10 mm wall thickness). Lot #14 had 24% initial cold-working and Lot #16 had 10% initial cold working. In order to obtain samples with 0.06 mm wall thickness, samples from Lot #14 and Lot #16 were ground, by an outside vendor. The samples were then heat treated at 720°C and 920°C. The layout of the experiments is presented in Table 7. In this table, A, B, and C represent the factors, and the positive (+) and negative (-) signs show the level of the corresponding factor, with "+" representing the high level and "-" representing the low level. For example, in order to perform Run #5, hypotubing samples with 0.06 mm wall thickness and 10% cold working would be heat treated at 920°C.

Table 7. Layout of designed experiments

DOE Information						Responses		
Design Id	Run #	Block	A	B	C	UTS (MPa)	Y.S. (MPa)	Elong. (%)
6	1	1	+	-	+			
2	2	1	+	-	-			
5	3	1	-	-	+			
1	4	1	-	-	-			
2	5	1	+	-	-			
5	6	1	-	-	+			
8	7	1	+	+	+			
6	8	1	+	-	+			
4	9	1	+	+	-			
3	10	1	-	+	-			
2	11	1	+	-	-			
7	12	1	-	+	+			
1	13	1	-	-	-			
6	14	1	+	-	+			
5	15	1	-	-	+			
1	16	1	-	-	-			
3	17	1	-	+	-			
4	18	1	+	+	-			
4	19	1	+	+	-			
8	20	1	+	+	+			
3	21	1	-	+	-			
7	22	1	-	+	+			
7	23	1	-	+	+			
8	24	1	+	+	+			

Samples for each run included three specimens for tensile test, one specimen for grain size measurement, and one specimen for corrosion testing. The responses of the experiment were: ultimate tensile strength, yield strength, and ductility of the material (total percent elongation). The DOE layout and the response values are presented in Table 9 in Chapter 4. The analyses of the variance (ANOVA) for each response variable, done by the software, are presented in Appendix 5.

The effect of each factor (A, B, and C), as the main effects, and their interactions (AB, AC, BC, and ABC), on the response variables were calculated for each response variable from Equation 6.

$$\text{Effect} = \left(\frac{\sum Y^+}{n^+} - \frac{\sum Y^-}{n^-} \right) \qquad [6]$$

In this equation Y is the response variable value in each run, n is the number of the experiments. In this case $n^+ = n^- = 12$. The positive and negative signs indicate the level of the corresponding factor or interaction. For example, in Run #5 the heat treatment temperature, A, has a positive sign, or interaction of the cold-working (negative) and the wall thickness (negative) has a positive sign. The results of these calculations for all the response values are presented in Table 10. Based on the ANOVA and value of the effects and interactions, the software provides equations for predicting the response variables in terms of the factors. The resultant equations are also presented in Chapter 4 (Equations 7, 8, and 9).

In order to study the effect of the heat treatment processes on the grain size, the microstructure of the materials was examined according to the procedure outlined in Section 3.3.1. Photomicrographs at 100X and 400X magnifications are presented in Figures 30 through 39, in Chapter 4. These include the microstructure of the specimens from the designed experiments, as well as the microstructure of the specimens in the as-received

28

condition. The grain size of these specimens was measured and the results of these measurements are presented in Table 11, in Chapter 4.

3.3.7.   Corrosion Testing

The intergranular corrosion susceptibility of all of the specimens in the designed experiments was tested according to ASTM A-262.[13] In this test method, each specimen was heat treated at 650°C for one hour. Then the specimen was mounted, ground, polished, and finally electroetched. Photomicrographs at 400X magnification were taken. These photomicrographs are presented in Figures 40 through 47, in Chapter 4. The material was considered to be susceptible to intergranular corrosion if any ditching (grain boundary thickening) was observed in these pictures. The results of these tests are presented in Table 11, in Chapter 4.

CHAPTER 4
RESULTS

4.1. Introduction

In this chapter the results of the tests and experiments performed are presented. First, the results of the preliminary study of the effects of the manufacturing variables (heat treatment temperature, percent initial cold working, and wall thickness) on the properties of the material are presented. Based on this study, experiments with the above manufacturing variables as the factors, at two levels, were statistically designed. The response variables of these experiments were the mechanical properties of the hypotubings. The layout and results of these experiments, including the effect of each manufacturing variable and the interactions among them, are then presented. Finally, the results of grain size measurements and tests for intergranular corrosion susceptibility of the material are presented.

4.2. Heat Treatment Temperature

Figure 12 illustrates the effect of heat treatment temperature on the mechanical properties of the samples from Lot #16. As can be seen from Figure 12, when the heat treatment temperature was increased, the ultimate tensile strength (UTS), and yield strength (Y.S.) decreased but ductility increased, as expected. Also shown in Figure 12 are the corresponding values for the Lot #16 material in the as-received condition, i.e. cold worked, but prior to heat treatment. The results shown graphically in Figure 12

demonstrates that the mechanical properties of the as-received material could be varied in the desired direction by heat treatment.
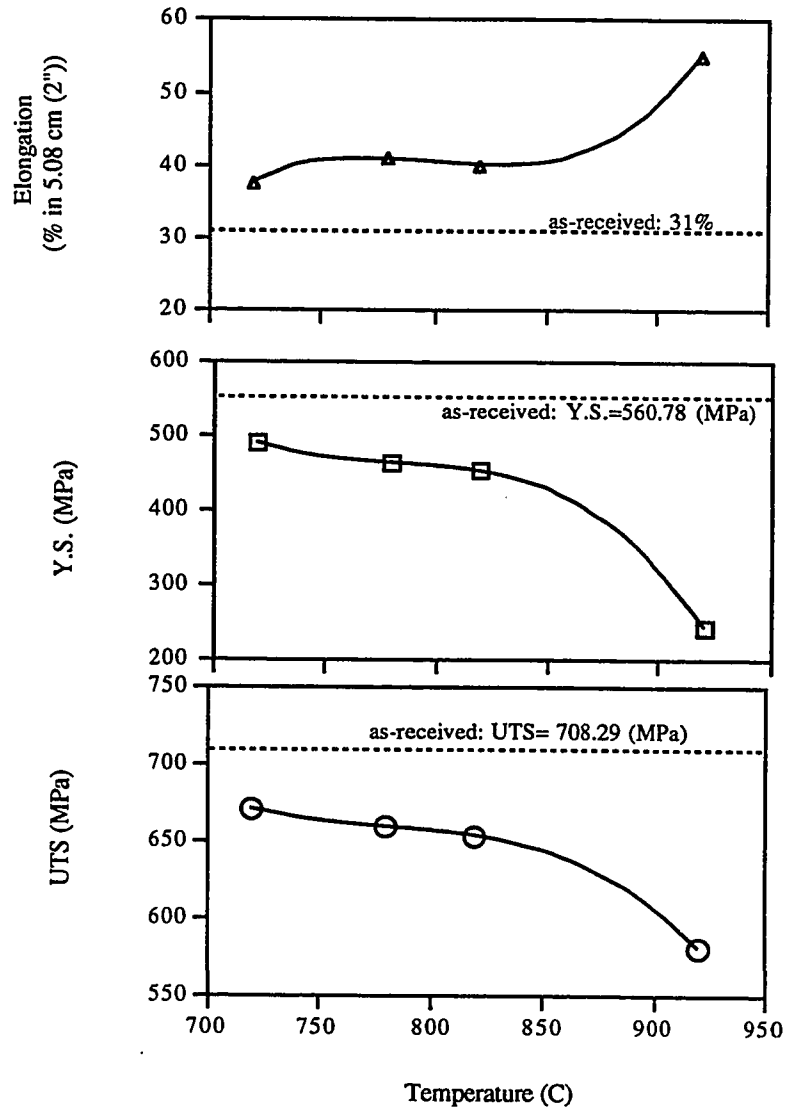
Figure 12. Effect of heat treatment temperature on the mechanical properties of stainless steel hypotubing (Samples from Lot #16, 5 minute, argon, and water quenched)

31

4.3. Cold Working

The effect of the percent initial cold working, or simply cold working, on the strength of the samples heat treated at 750°C and 950°C was studied by determining the extent of stress relief. The latter represents the reduction in the ultimate tensile strength of the material due to heat treatment, and was calculated from Equation 5. The results are illustrated in Figure 13, and show that the extent of stress relief is greater for materials with higher initial cold working. In other words, materials with higher initial cold working had a greater tendency to release the internal stress. Figure 13 also shows that this effect is more significant at higher temperatures, i.e. higher percent of stress is released by heat treatment at higher temperatures. Therefore the mechanical properties of the heat treated hypotubing depend on initial cold working as well as the heat treatment temperature.
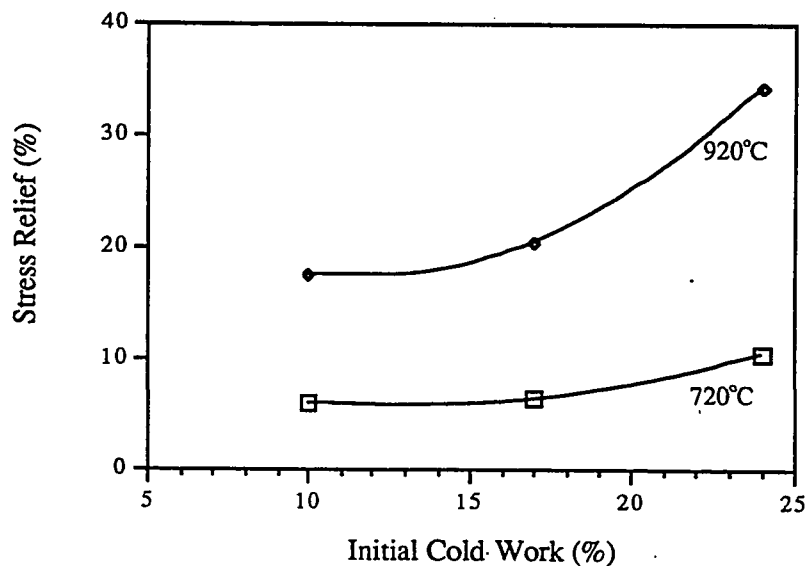
Figure 13. Effect of initial cold working on the extent of stress relief during heat treatment process at 720°C and 920°C for stainless steel hypotubing

32

4.4. Wall Thickness

In another part of the preliminary study, the effect of wall thickness on the mechanical properties of the hypotubings was investigated. Figure 14 shows the stress strain curves for samples from Lot #8, with two wall thicknesses. As can be seen from this figure, the wall thickness did not significantly affect the ultimate tensile strength and the yield strength of the material. However, Figure 14 does show that reducing the wall thickness did lower the ductility of the material. By reducing the wall thickness, the uniform elongation of the material is not changed. But once the localized elongation starts, in the case of thinner material, there is less material thickness available for this elongation. Therefore, the thinner material shows a lower total percent elongation. Figure 15 shows the effect of the wall thickness on the ductility of different hypotubings, for two wall thicknesses. Figure 15 confirms that by reducing the wall thickness of the hypotubings the total percent elongation will be reduced.
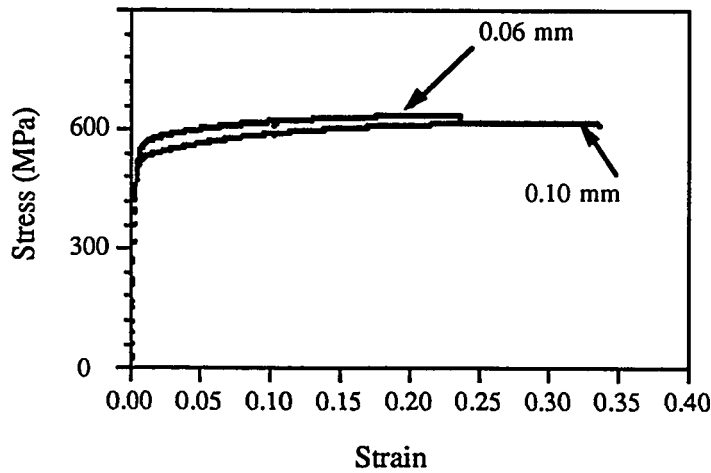
Figure 14. Stress strain curves for stainless steel hypotubings (Lot #8) with two wall thicknesses

33
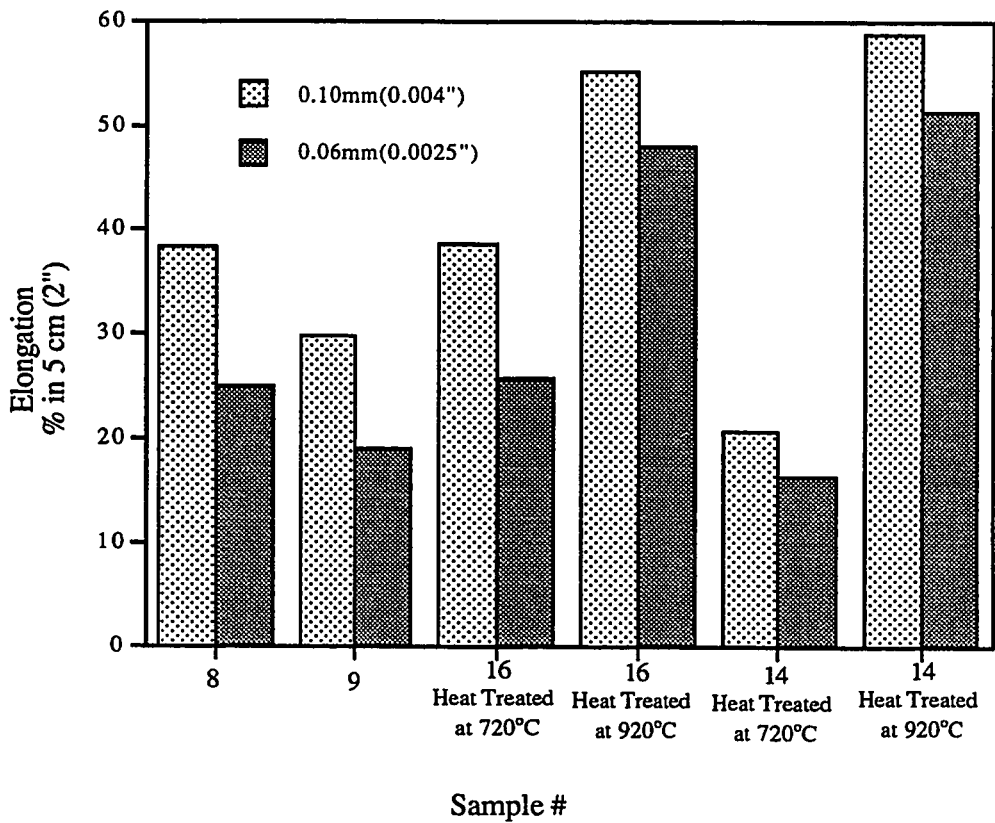
Figure 15. Effect of wall thickness on ductility of stainless steel hypotubing

4.5. Design of Experiment

The results of the preliminary study showed that heat treatment temperature, initial cold working, and wall thickness of the hypotubings affect the mechanical properties of the material. The preliminary study can be considered as single factor experiments where one variable was changed at the time. Therefore, in order to fully study the effects of these factors on the mechanical properties of the material, and to determine the corresponding correlations, the factors were considered as the variables in the designed experiments.

Full factorial experiments with three factors (heat treatment temperature, percent cold working, and wall thickness) at two levels were designed. Table 8 shows the design layout which includes $2^F = 2^3 = 8$ factor combinations (F: number of factors). Each combination was identified by "Design Id", and had three replications, which made for a total of twenty four runs.

Table 8. DOE layout

Design Id.	A: Heat T.Temp. (C)	B: Cold Work (%)	C: Wall Thick (mm)
1	720	10	0.0635
2	920	10	0.0635
3	720	24	0.0635
4	920	24	0.0635
5	720	10	0.1016
6	920	10	0.1016
7	720	24	0.1016
8	920	24	0.1016

The response variables were the mechanical properties of the hypotubings. Table 9 shows the layout of the 2^3 factorial experiments with the values of the response variables. The negative and positive signs, or codes, correspond to the low and high levels of the factors, respectively. The interaction of the factors[†], in coded units, are represented by the product of the factors with corresponding negative or positive sign, e.g., the interaction of

---

† When the effect of one factor depends on the level of another factor, there exists an interaction.

heat treatment temperature and wall thickness in Experiment 2 (Run #2) was shown by AC and has a negative sign.

.

Table 9. Layout of 2^3 factorial experiments in coded units with three replications and the response values

DOE Information			A	B	C	Responses		
Design Id	Run #	Block				UTS (MPa)	Y.S. (MPa)	Elong. (%)
6	1	1	+	-	+	590.75	259.75	55.20
2	2	1	+	-	-	591.16	265.47	46.50
5	3	1	-	-	+	668.40	494.98	38.50
1	4	1	-	-	-	716.56	542.31	25.70
2	5	1	+	-	-	607.70	283.11	48.00
5	6	1	-	-	+	668.54	501.18	34.00
8	7	1	+	+	+	560.78	251.42	58.75
6	8	1	+	-	+	582.07	253.28	56.30
4	9	1	+	+	-	615.97	278.56	51.80
3	10	1	-	+	-	821.98	690.38	16.20
2	11	1	+	-	_	602.19	277.94	46.80
7	12	1	-	+	+	767.55	653.17	20.50
1	13	1	-	-	-	710.36	538.04	28.70
6	14	1	+	-	+	586.00	249.56	59.50
5	15	1	-	-	+	667.92	495.74	38.00
1	16	1	-	-	-	706.91	535.15	24.30
3	17	1	-	+	-	839.89	741.40	13.00
4	18	1	+	+	-	603.01	274.29	51.20
4	19	1	+	+	-	591.23	267.61	50.00
8	20	1	+	+	+	558.85	249.35	58.50
3	21	1	-	+	-	824.73	706.91	16.20
7	22	1	-	+	+	761.35	659.17	20.00
7	23	1	-	+	+	757.90	653.86	19.20
8	24	1	+	+	+	558.44	248.66	58.75

.

36

From the results of these experiments, three main effects, three two-factor interactions, and one three-factor interaction were calculated for each response variable, according to Equation 6:

$$\text{Effect} = \left(\frac{\sum Y^{+}}{n^{+}} - \frac{\sum Y^{-}}{n^{-}} \right)$$

[6]

Y is the response variable value in each run, n is the number of the experiments, and the positive and negative signs indicate the sign of the corresponding factor or interaction in coded units. In this case $n^{+} = n^{-} = 12$. The results of these calculations for all the response values are presented in Table 10. For example the effect of heat treatment temperature on the yield strength of the material was calculated to be -338.00 MPa which indicates that by increasing the heat treatment temperature, in the designed range (from 720°C, as low, to 920°C, as high level), the ultimate tensile strength of the material decreases by 338.00 MPa.

Table 10. Calculated effects and interactions of the factors on the response variables

	Effect			Interaction			
	A	**B**	**C**	**AB**	**AC**	**BC**	**ABC**
UTS (MPa)	-155.33	46.93	-41.93	-58.86	12.87	-13.40	-1.59
Y.S.(MPa)	-338.00	81.52	-35.90	-84.73	13.43	-4.67	3.48
Elongation	28.9	-5.6	8.2	8.4	0.6	-2.0	0.9

If all the effects were zero, then all the response variable values would be like a random sample drawn from a normal distribution with a fixed mean, and it follows that all seven effects and interactions would be normally distributed about zero. The calculated effects and interaction values presented in Table 10 are further explained, for each response variable, in the following sections.

4.5.1.   Effect of Factors on Ultimate Tensile Strength

The effects of all the factors and their interactions on the ultimate tensile strength of the material are explained based on the calculated values presented in Table 10. The heat treatment temperature (Factor A) had the most significant effect on the ultimate tensile strength. By increasing the temperature from 720°C to 920°C (low level to high level), the ultimate tensile strength decreased by 155.33 MPa. Since the standard deviations of the measurements for the ultimate tensile strength were in the order of 20 - 30 MPa, those effects or interactions that were less than 30 MPa were not considered as significant. The tensile test data for all the specimens are presented in Appendix 4.

Figures 16 through 21 show the effect of heat treatment temperature (A), cold working (B), wall thickness (C) and their interactions on the ultimate tensile strength, individually. In these figures, the negative and positive signs for the factors indicate the low and high levels of the factors, respectively. Figure 16 shows the effect of heat treatment temperature on the ultimate tensile strength of the material. Increasing the temperature from 720°C to 920°C, resulted in the ultimate tensile strength decreasing from 743 MPa to 587 MPa.

38
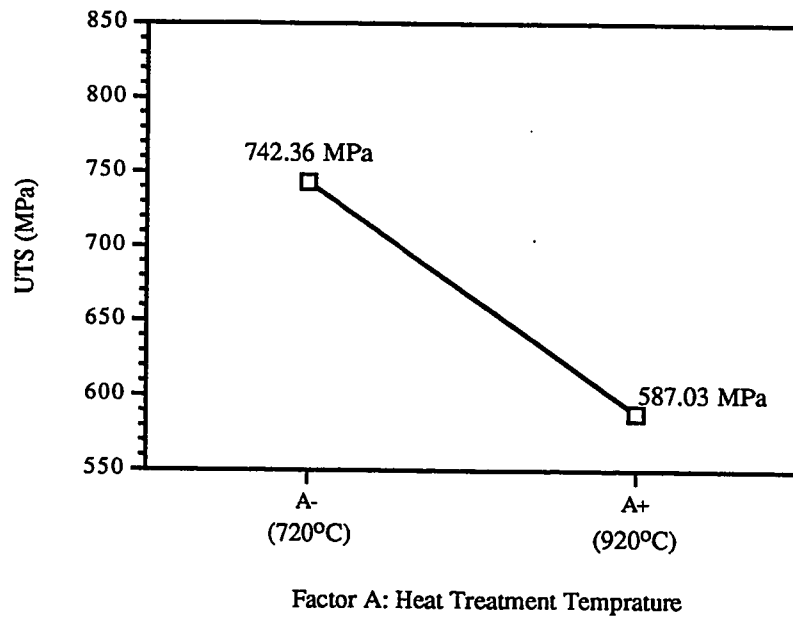
Figure 16. Effect of heat treatment temperature (720°C to 920°C) on the ultimate tensile strength of stainless steel hypotubing

In Figure 17, the effect of initial cold working on the ultimate tensile strength of the material is illustrated. These results confirmed the expectation that the material with higher cold working would have higher strength.
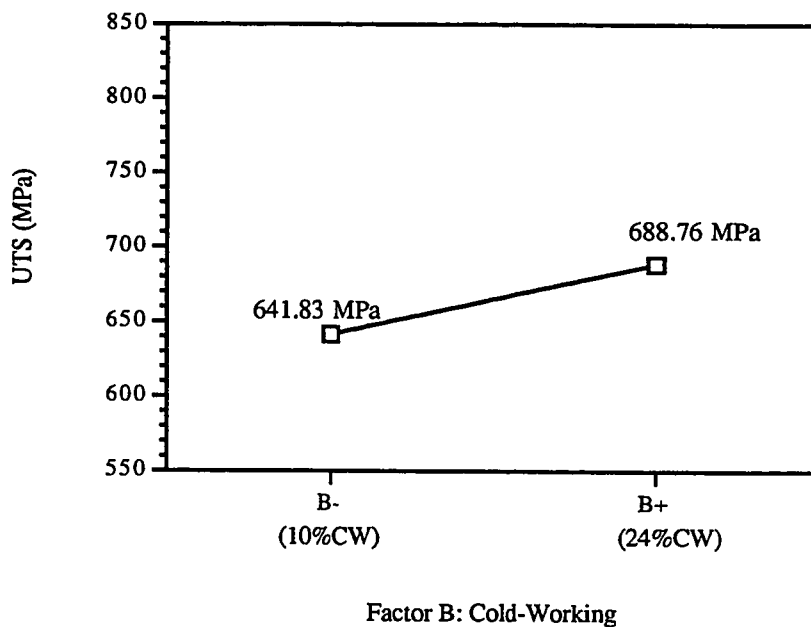
Figure 17. Effect of cold working (10% to 24%) on the ultimate tensile strength of stainless steel hypotubing

As can be seen from Figure 18, the wall thickness of the hypotubings had a negative effect, and the material with a thicker wall had lower strength. This effect was not as significant as the effect of the heat treatment temperature. The higher ultimate tensile strength for thinner walls most probably arised from the fact that the hypotubings with thinner walls were fabricated by grinding down the hypotubings. This grinding process ws thought to have induced a small amount of cold working, thus making the material "harder".

40
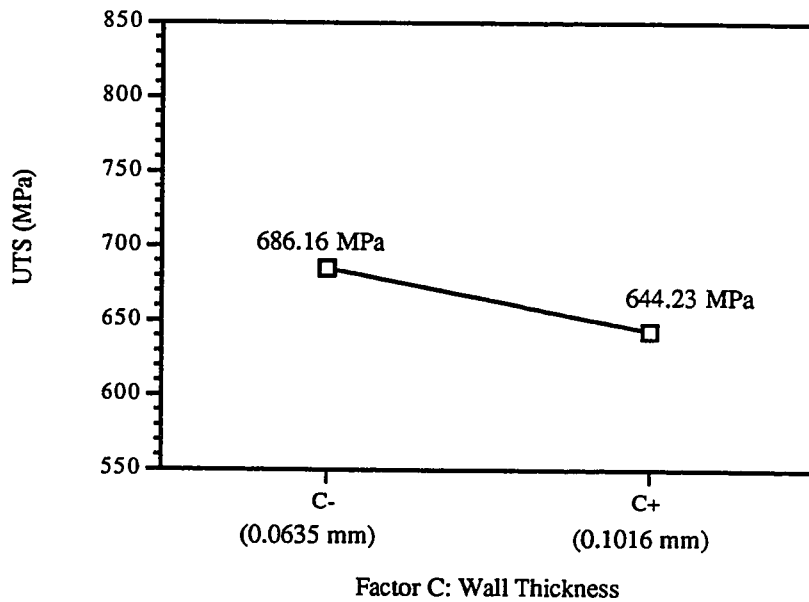
Figure 18. Effect of wall thickness (0.0635 mm to 0.1016 mm) on
the ultimate tensile strength of stainless steel hypotubing

The interactions of the factors on the ultimate tensile strength are shown in Figures 19 through 21. Figure 19 shows that at the high level of cold working (B+), the effect of heat treatment temperature was more significant in decreasing the ultimate tensile strength of the material than at the low level of cold working. In other words, the effect of heat treatment temperature depended on the level of cold working. This interaction was also found in the preliminary study where the material with a higher initial cold working showed a greater tendency to relieve the stresses (lowering the ultimate tensile strength) by heat treatment.

41
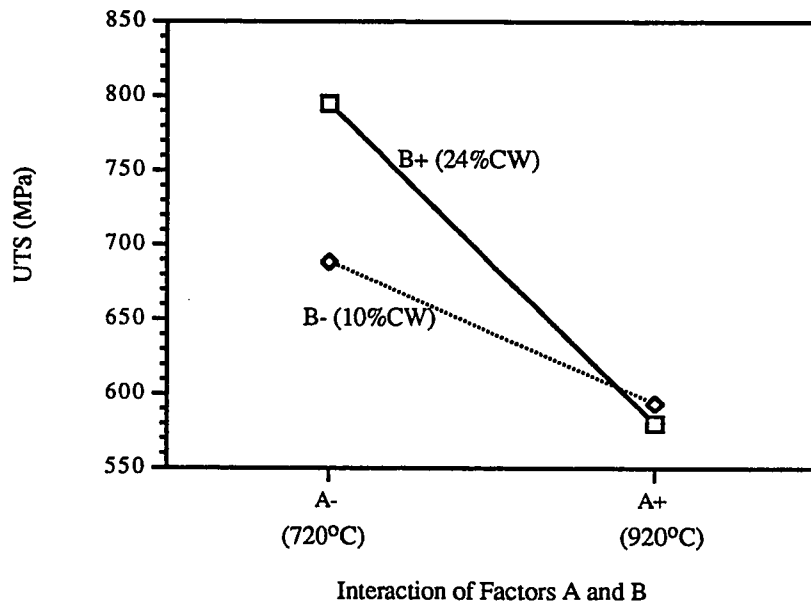
Figure 19. Interaction of heat treatment temperature (720°C to 920°C) and cold working (10% to 24%) on the ultimate tensile strength of stainless steel hypotubing

Figure 20 shows the interaction of the heat treatment temperature and wall thickness. As was seen in Table 10, this interaction (12.87 MPa) was not significant, and the two connecting lines at the two levels of wall thickness, shown in Figure 20, are almost parallel. In other words, the effect of heat treatment temperature on the ultimate tensile strength of the material did not significantly depend on the wall thickness.
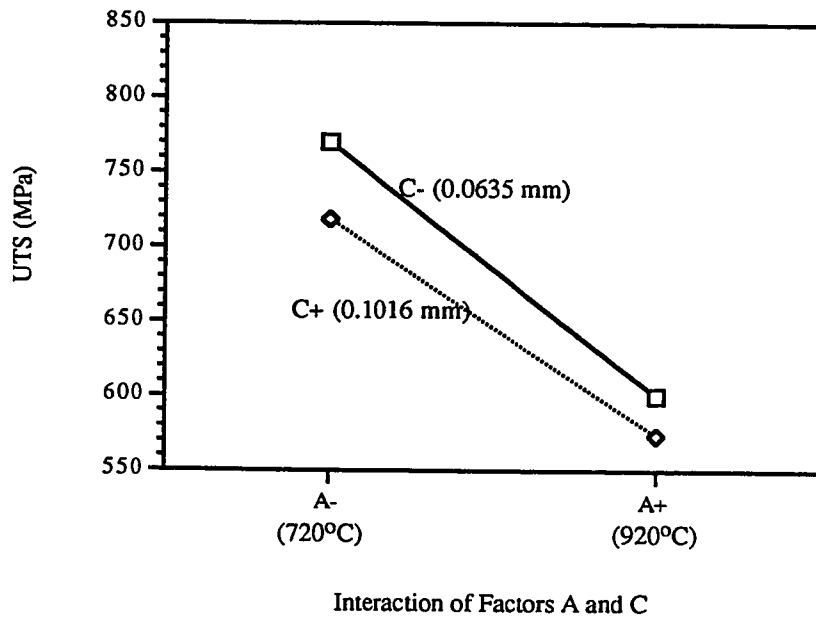
Figure 20. Interaction of heat treatment temperature (720°C to 920°C) and wall thickness (0.0635 mm to 0.1016 mm) on UTS of stainless steel hypotubing

Figure 21 shows the interaction of cold working and wall thickness of the hypotubings on the ultimate tensile strength. The calculated value for the effect of this interaction, as shown in Table 10, was -13.40 MPa. As a result, and as can be seen in Figure 21, no significant interaction existed between these two factors. In other words, the effect of cold working did not depend on the wall thickness.

43
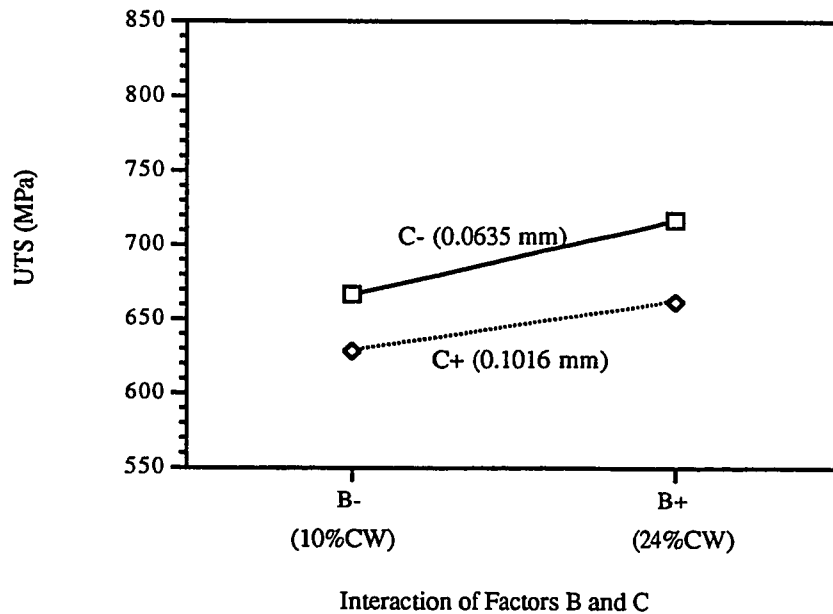
Figure 21. Interaction of cold working (10% to 24%) and wall thickness (0.0635 mm to 0.1016 mm) on UTS of stainless steel hypotubing

4.5.1.1. Mathematical Correlation

Based on the ANOVA, and the calculated effects and interactions, the software provided an equation for predicting each response variable in terms of the factors. This equation included a constant value, the intercept, which was an average of all the response variables, and terms of the factors with the coefficients that represented the significance of their effect. The predicted ultimate tensile strength, in terms of the DOE factors, is presented in Equation 7. For example, in this equation cold working has a coefficient of +41.972 which shows that cold working has a positive effect on the ultimate tensile strength of the material, but the combination of the heat treatment temperature (H.T.Temp.)

44

and cold working has a negative effect (interaction). In this equation, heat treatment temperature is in degree C, cold working in percent, and wall thickness in mm. By varying these factors one can obtain hypotubings with the desired ultimate tensile strength. However, it must be borne in mind that this equation can be used only for interpolating within the boundary conditions, and should not be used for extrapolations.

Equation 7. Predicted ultimate tensile strength value in terms of DOE factors

UTS (MPa) =	907.77 - 0.341 (H.T.Temp.)
	+ 41.972 (Cold work)
	- 3015.86 (Wall Thickness)
	- 0.042 (H.T.Temp.) (Cold work)
	+ 3.377 (H.T. Temp.) (Wall Thickness)
	- 50.225 (Cold work) (Wall Thickness)

4.5.2. Effect of Factors on Yield Strength

The effects of all the factors and their interactions on the yield strength of the material are explained based on the calculated values presented in Table 10. For example, the heat treatment temperature (Factor A) had the most significant effect on the yield strength. By increasing the temperature from 720°C to 920°C (low level to high level), the yield strength decreased by 338.00 MPa. The standard deviations of the measurements for the yield strength were in the order of 20 - 30 MPa; therefore, those effects or interactions that were less than 30 MPa were not considered to be significant. The tensile test data for all the specimens are presented in Appendix 4.

Figures 22 through 25 show the effect of heat treatment temperature (A), cold working (B), wall thickness (C) and their interactions on the yield strength, individually. In these figures, the negative and positive signs for the factors indicate the low and high levels of the factors, respectively. Figure 22 shows the effect of heat treatment temperature on the yield strength of the material. Increasing the temperature from 720°C to 920°C, resulted in the yield strength decreasing from 601 MPa to 263.3 MPa.
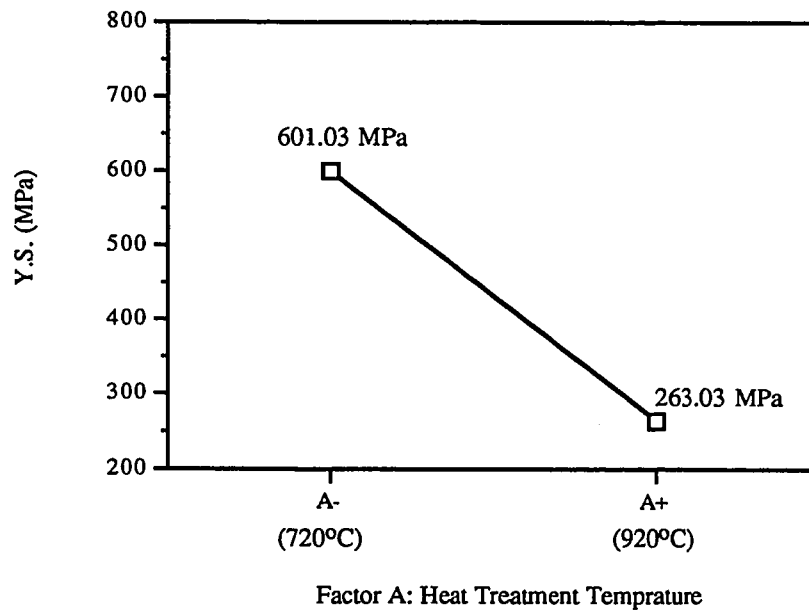
Figure 22. Effect of heat treatment temperature (720°C to 920°C) on the yield strength of stainless steel hypotubing

Figure 23 shows the effect of cold working on the yield strength. As expected, increasing the extent of cold working increased the yield strength of the material.

46
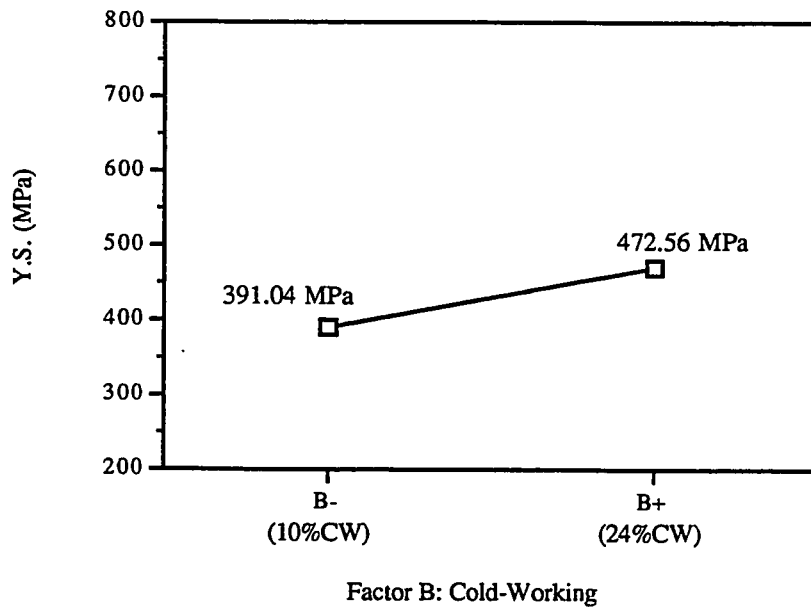
Figure 23. Effect of cold working (10% to 24%) on the yield strength of stainless steel hypotubing

As can be seen from Figure 24, the wall thickness of the hypotubings had a negative effect, and material with a thicker wall had a lower yield strength. Again, this effect was not as significant as the effect of heat treatment temperature. As was explained for the ultimate tensile strength, this effect was due to the grinding process for obtaining hypotubings with thinner walls.

47
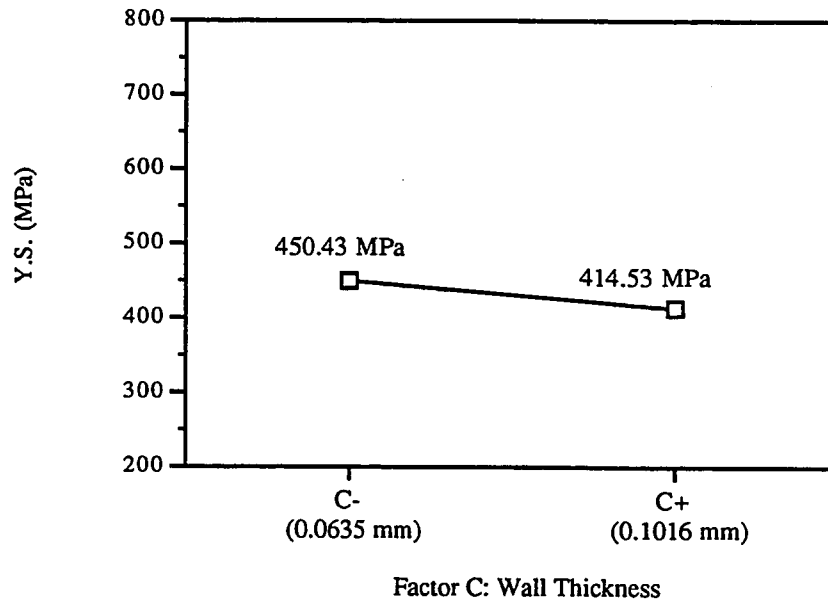
Figure 24. Effect of wall thickness (0.0635 mm to 0.1016 mm)
on the yield strength of stainless steel hypotubing

The interactions of heat treatment temperature and cold working, as the only significant interaction (Table 10), on the yield strength is shown in Figure 25. At high levels of cold working (B+), the effect of heat treatment temperature was more significant in decreasing the yield strength of the material than at low levels of cold working. In other words, the effect of heat treatment temperature depended on the level of cold working. This interaction can also be explained by the fact that the material with a higher extent of cold working has a greater tendency to lower its total free energy, as compared with the material with a lower extent of cold working.

48
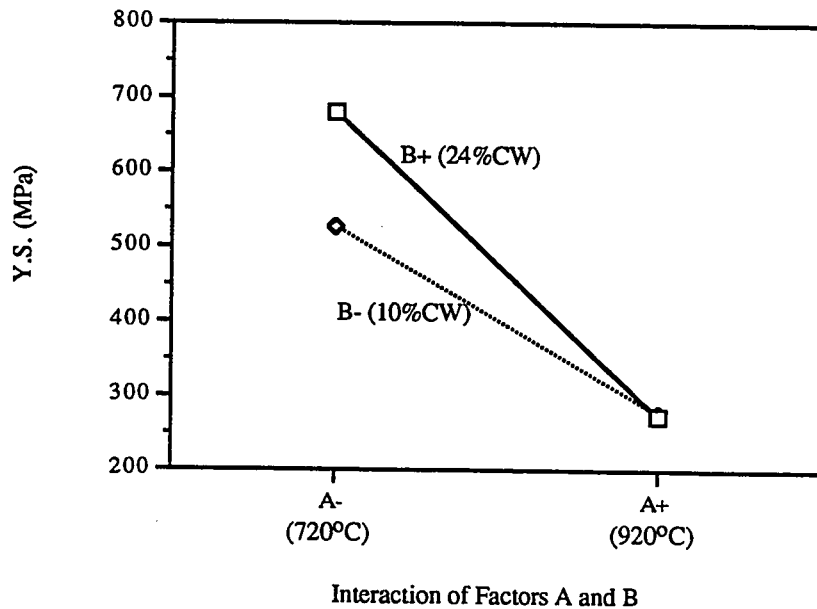
Figure 25. Interaction of heat treatment temperature (720°C to 920°C) and cold working (10% to 24%) on the yield strength of stainless steel hypotubing

4.5.2.1. Mathematical Correlation

The same procedures described in Section 4.5.1.1. was utilized to obtain a mathematical correlation between the yield strength and the DOE factors. This is shown in Equation 8. For example, in this equation cold working has a coefficient of -119.379 which shows that cold working has a negative effect on the yield strength of the material, but the combination of the heat treatment temperature (H.T.Temp.) and cold working has a positive effect (interaction). In this equation, the heat treatment temperature is in degree C, cold working in percent, and wall thickness is in mm. By varying these factors one can

obtain hypotubings with the desired yield strength. However, it must be borne in mind that this equation can be used only for interpolating within the boundary conditions, and should not be used for extrapolations.

Equation 8. Predicted yield strength value in terms of DOE factors

Y.S. (MPa) =	2867.068 - 2.78 (H.T.Temp.)
	- 119.379 (Cold work)
	- 19934.526 (Wall Thickness)
	+ 0.13 (H.T.Temp.) (Cold work)
	+ 21.108 (H.T.Temp.) (Wall Thickness)
	+ 1697.379 (Cold work) (Wall Thickness)
	- 1.85 (H.T.Temp.) (Cold work) (Wall Thickness)

4.5.3. Effect of Factors on Ductility

The effects of all the factors and their interactions on the ductility (percent elongation) of the materials are explained based on the calculated values presented in Table 10. For example the effect of the heat treatment temperature (A) on the ductility was 28.92% (as calculated from Equation 6). In other words, increasing the heat treatment temperature from 720°C to 920°C (low level to high level) increased the ductility by 28.92%. The standard deviations of the measurements for the ductility of the material were in the order of 5%; therefore, those effects or interactions that were less than 5% were not

50

considered as significant. The tensile test data for all the specimens are presented in Appendix 4.

Figures 26 through 32 show the effects of the heat treatment temperature, cold working, wall thickness, and their interactions on the ductility of the material. As presented in Table 10 and can be seen in Figure 26, the heat treatment temperature had the most significant effect on the ductility of the material. Increasing the heat treatment temperature from 720°C to 920°C, resulted in the ductility of the material increasing by 28.9%
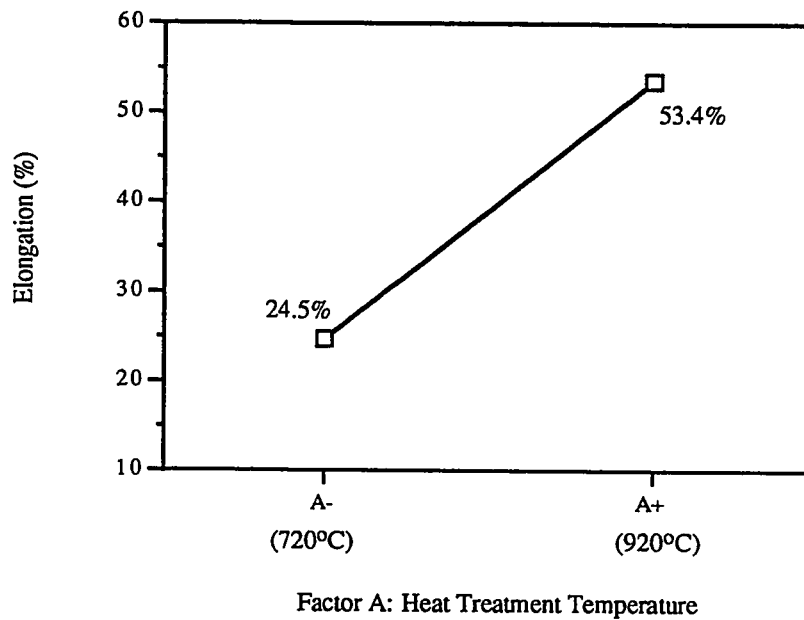
Figure 26. Effect of heat treatment temperature (720°C to 920°C) on the ductility of stainless steel hypotubing

Figure 27 shows the effect of cold working on the ductility of the material. As expected, increasing cold working made the material harder, or in other words, less ductile.
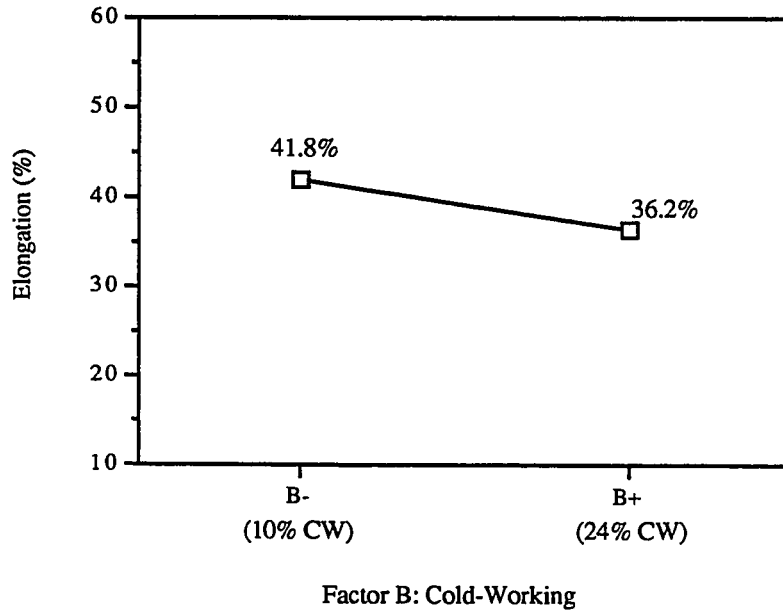
Figure 27. Effect of cold working (10% to 24%) on the ductility of stainless steel hypotubing

Figure 28 shows the effect of wall thickness on the ductility of the material. As was determined during the preliminary study, and can be seen from Figure 28, the hypotubing with smaller wall thickness was less ductile, or had a lower total percent of elongation.
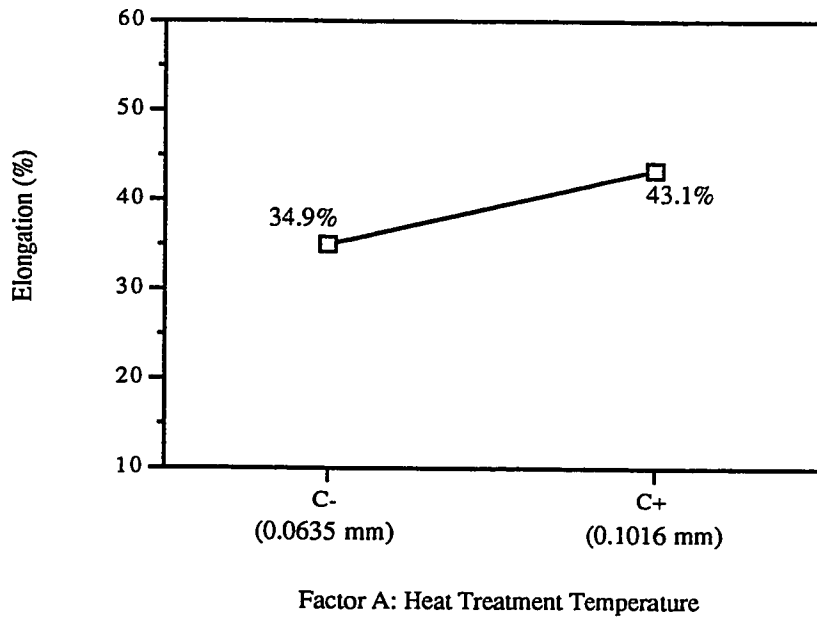
Figure 28. Effect of wall thickness (0.0635 mm to 0.1016 mm)
on the ductility of stainless steel hypotubing

Figure 29 shows the interaction effect of heat treatment temperature and cold working, as the most significant interaction, on the ductility of the material. As can be seen from this figure, the effect of the temperature depended on the level of cold working. Here, as was in the case of strength, the positive effect of the heat treatment temperature in increasing the ductility was more significant for the material with a higher initial cold working.
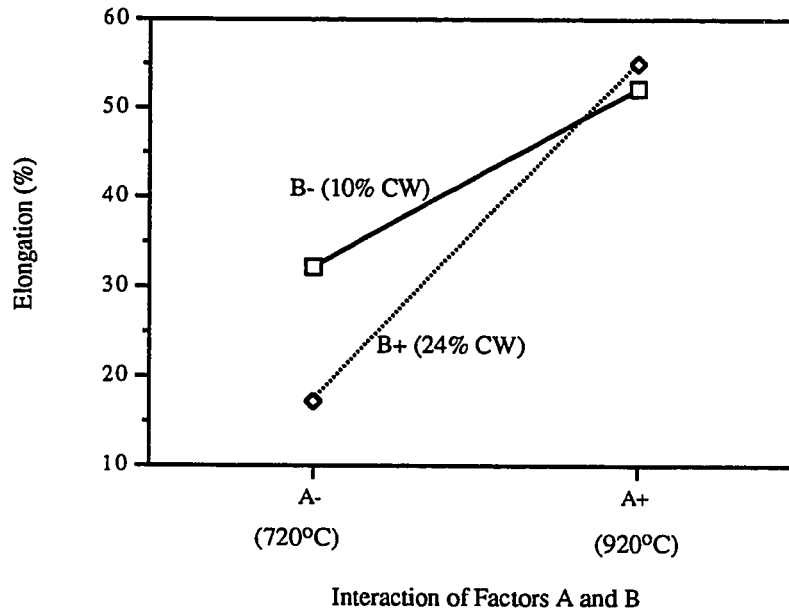
Figure 29. Interaction of heat treatment temperature (720°C to 920°C) and cold working (10% to 24%) on the ductility of stainless steel hypotubing

4.5.3.1. Mathematical Correlation

The predicted ductility of the material in terms of DOE factors can be calculated by Equation 9. In this equation, heat treatment temperature is in degree C, cold working in percent, and wall thickness is in mm. By varying these factors one can obtain hypotubings with desired ductility. Note that this equation can be used only for interpolating within the boundary conditions, and should not be used for extrapolations.

Equation 9. Predicted percent elongation value in terms of DOE factors

$$
\begin{aligned}
\text{Elongation (\%)} = \ & -46.63 + 0.078 \text{ (H.T.Temp.)} \\
& - 2.4127 \text{ (Cold work)} \\
& + 696.6879 \text{ (Wall Thickness)} \\
& + 0.0032 \text{ (H.T.Temp.) (Cold work)} \\
& - 0.4293 \text{ (H.T.Temp.) (Wall Thickness)} \\
& - 35.233 \text{ (Cold work) (Wall Thickness)} \\
& + 0.0337 \text{ (H.T.Temp.) (Cold work) (Wall Thickness)}
\end{aligned}
$$

4.6. Effect of Heat Treatment on Microstructure

Figures 30 and 31 are photomicrographs of cross sections of samples from Lot #14 (24% cold work) and Lot #16 (10% cold work), in the as-received condition, at 100X and 400X magnifications, respectively. Figures 32 through 39 are photomicrographs of specimens from the designed experiments, with their "Design Id." and the level of the three corresponding factors, at 100X and 400X magnifications. These photomicrographs were used for the grain size measurements. The results of these measurements are presented in Table 11, from which it can be seen that the grain size of the material did not increase due to the heat treatment procedures.

55
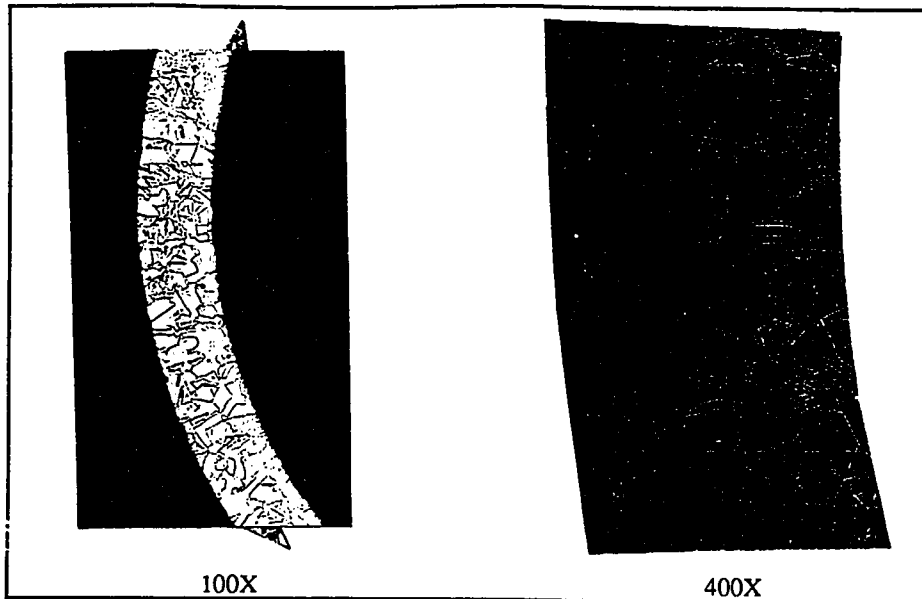
Figure 30. Microstructure of sample from Lot #14, in as-received condition
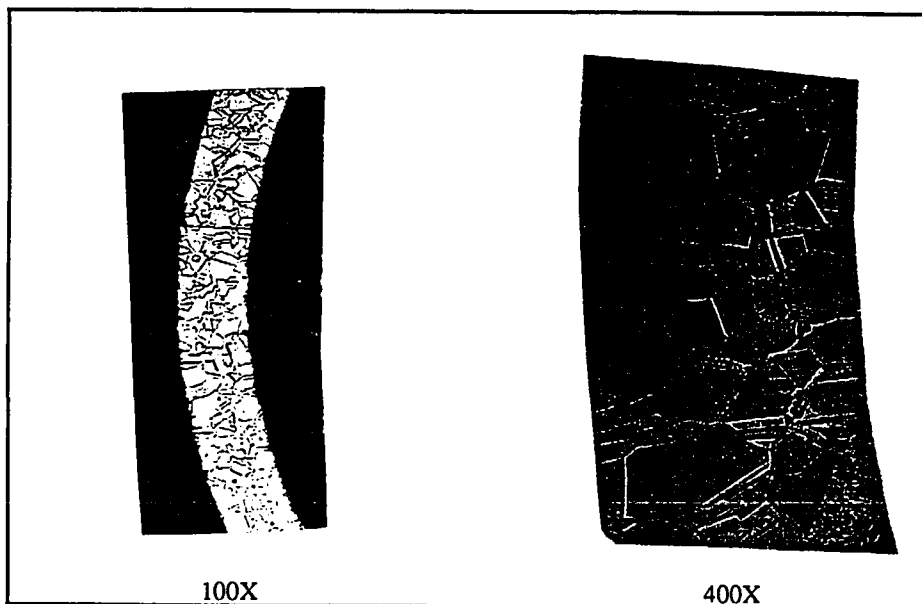
Figure 31. Microstructure of sample from Lot #16, in as-received condition

56
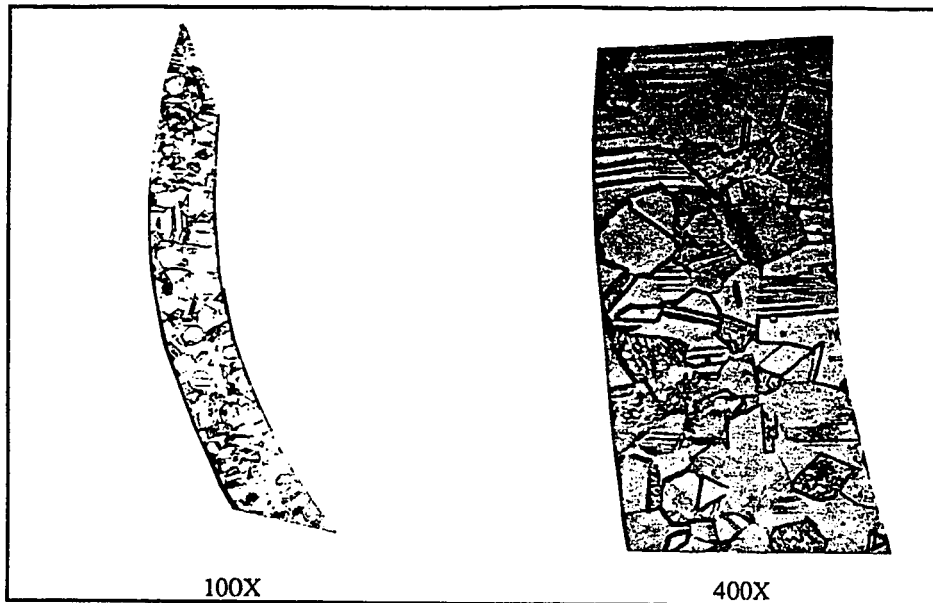
Figure 32. Microstructure of sample from Lot #16
(DOE ID: 1: A: Heat treated at 720°C   B: 10% CW   C: 0.0635 mm)
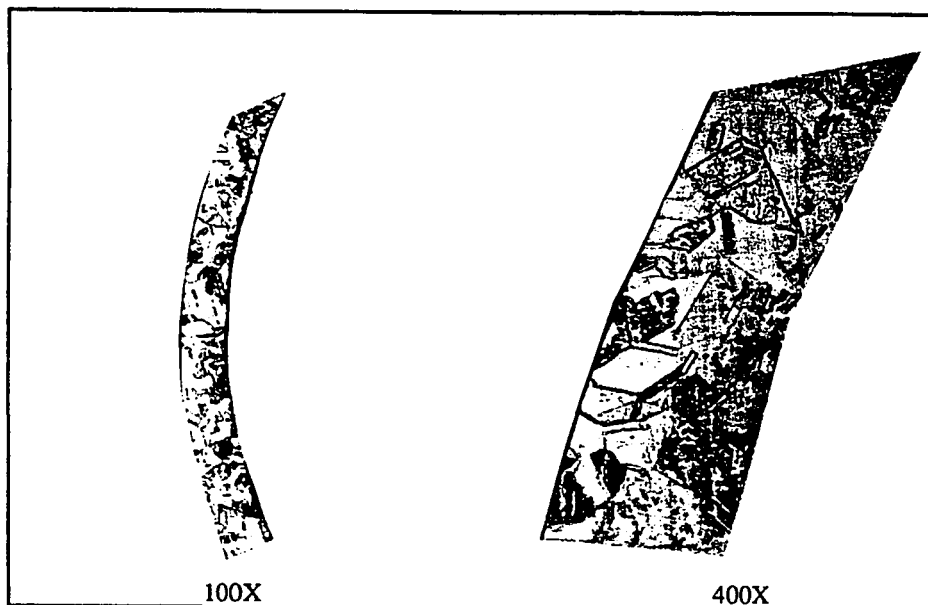
Figure 33. Microstructure of sample from Lot #16
(DOE ID: 2: A: Heat treated at 920°C   B: 10% CW   C: 0.0635 mm)

100X 400
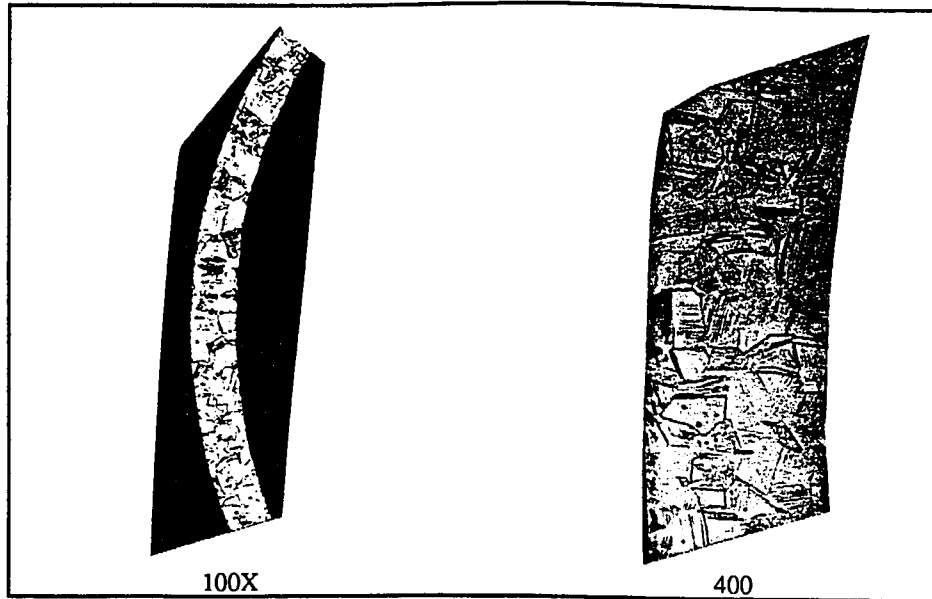
Figure 34. Microstructure of sample from Lot #14
(DOE ID: 3: A: Heat treated at 720°C B: 24%CW C: 0.0635 mm)

100X 400X
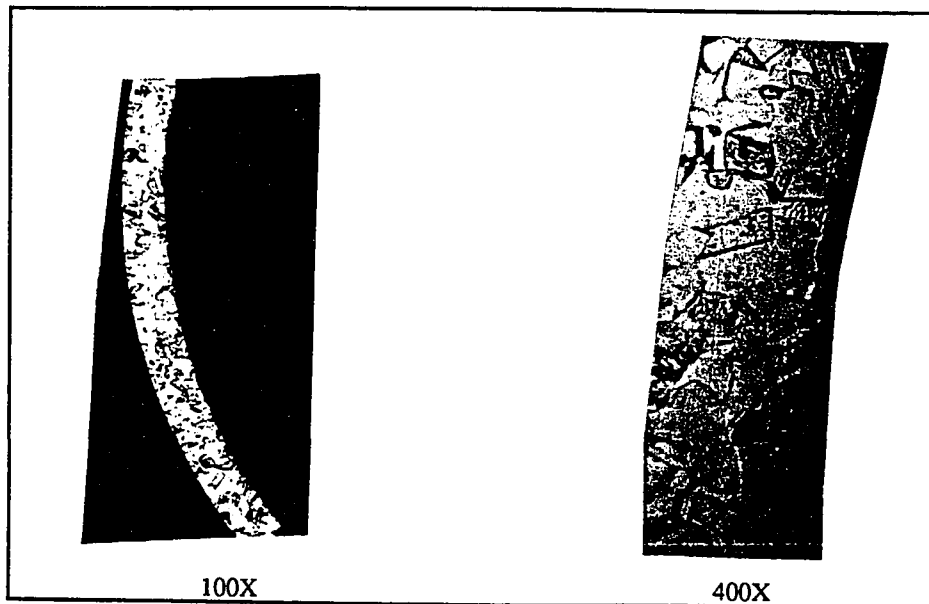
Figure 35. Microstructure of sample from Lot #14
(DOE ID: 4: A: Heat treated at 920°C B: 24%CW C: 0.0635 mm)
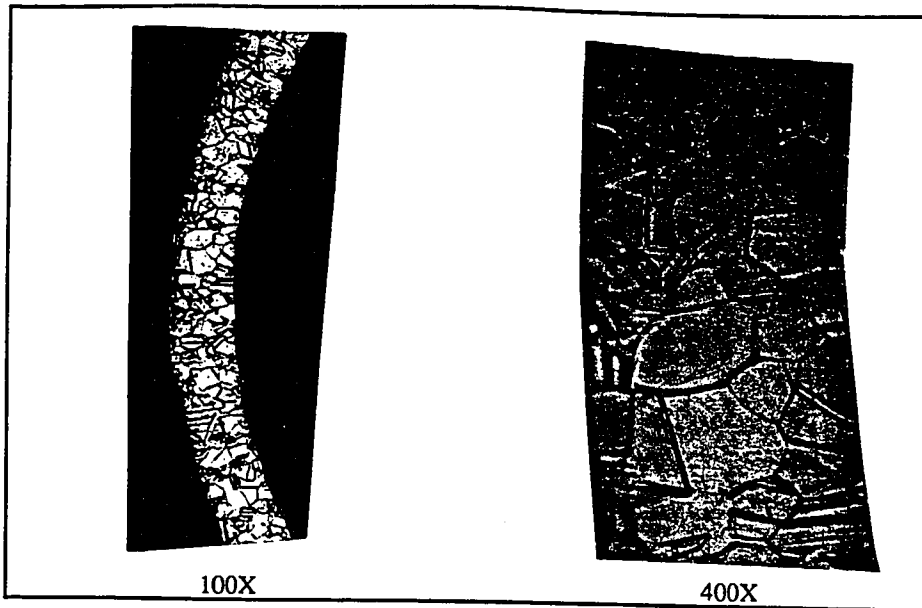
Figure 36. Microstructure of sample from Lot #16
(DOE ID: 5: A: Heat treated at 720°C   B: 10% CW   C: 0.1016 mm)
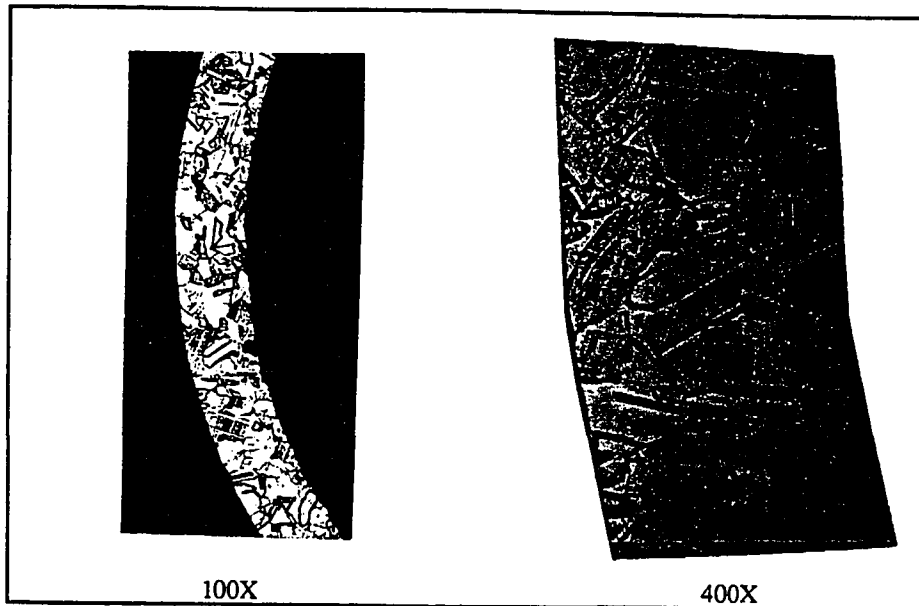
Figure 37. Microstructure of sample from Lot #16
(DOE ID: 6: A: Heat treated at 920°C   B: 10% CW   C: 0.1016 mm)

59
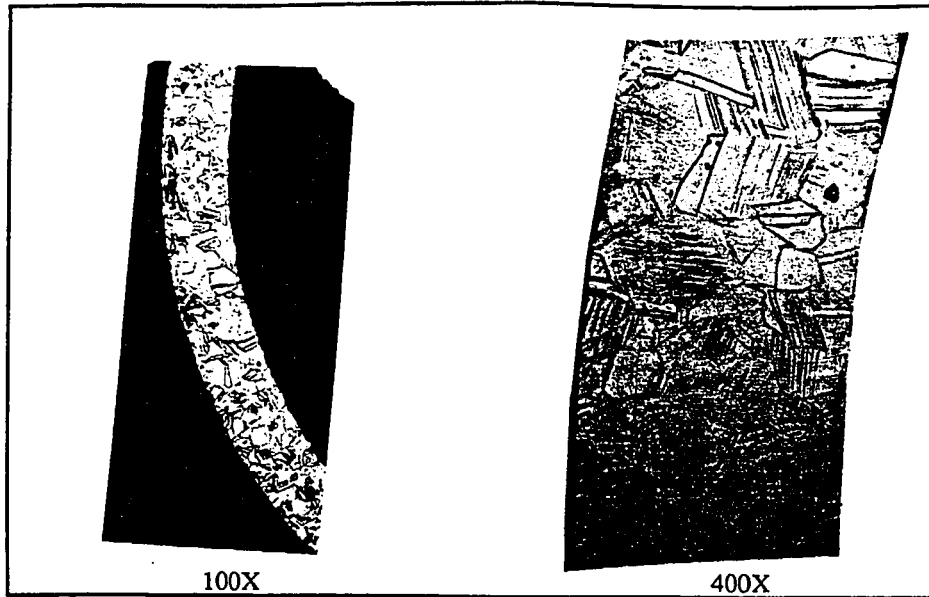
Figure 38. Microstructure of sample from Lot #14
(DOE ID: 7: A: Heat treated at 720°C B: 24% CW C: 0.1016 mm)
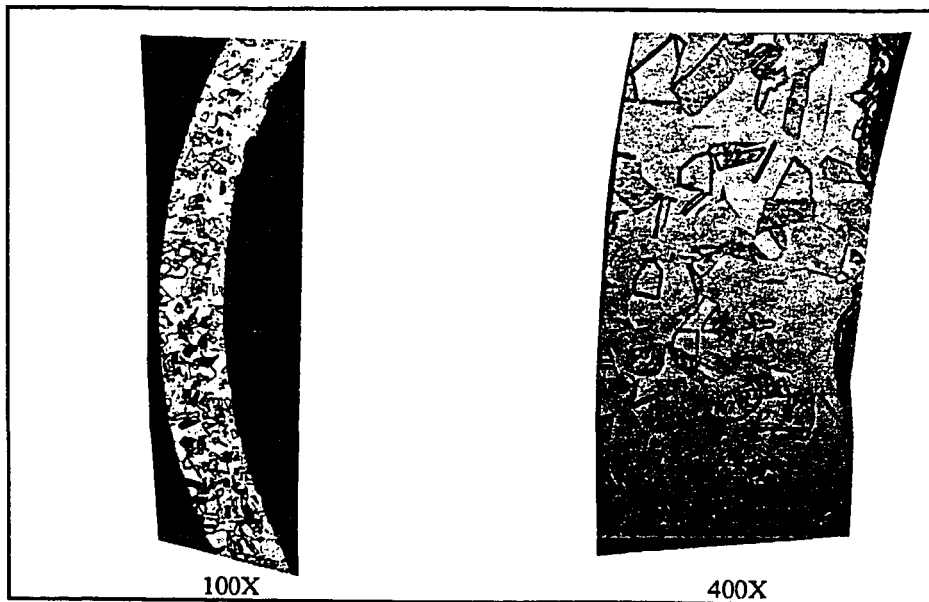
Figure 39. Microstructure of sample from Lot #14
(DOE ID: 8: A: Heat treated at 920°C B: 24% CW C: 0.1016 mm)

4.7. Corrosion Testing

Figures 40 through 47 are photomicrographs of the DOE samples that were tested for intergranular corrosion attack, at 100X and 400X magnifications. These photomicrographs were checked for ditching[†] on the grain boundaries. All the samples passed the test, and no chromium carbide precipitation was observed. The results of these tests (pass or fail) are presented in Table 11.
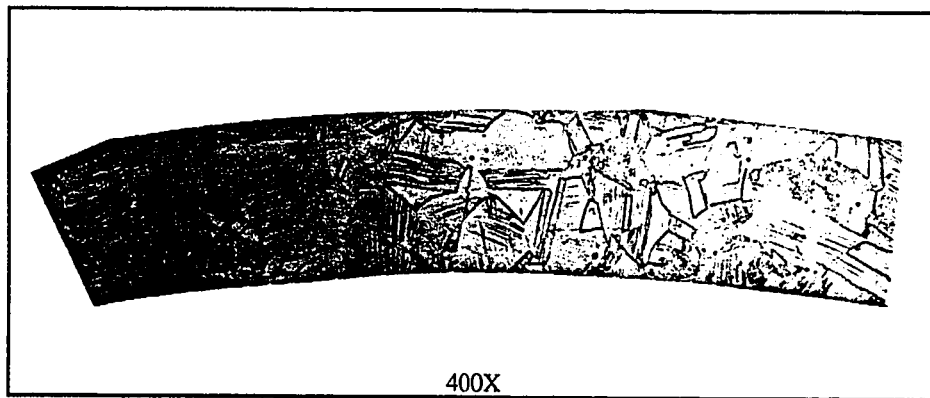
Figure 40. Microstructure of sample from Lot #16, tested for intergranular corrosion.
(DOE ID:1 A: Heat treated at 720°C B: 10% CW C: 0.0635 mm)

[†] Grain boundary thickening due to chromium carbide precipitation.

61
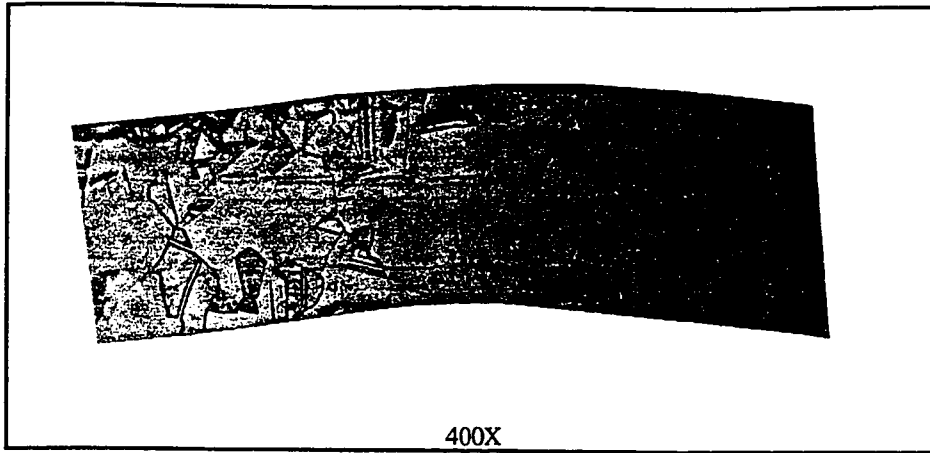
Figure 41. Microstructure of sample from Lot #16, tested for intergranular corrosion.
(DOE ID:2 A: Heat treated at 920°C   B: 10% CW   C: 0.0635 mm)
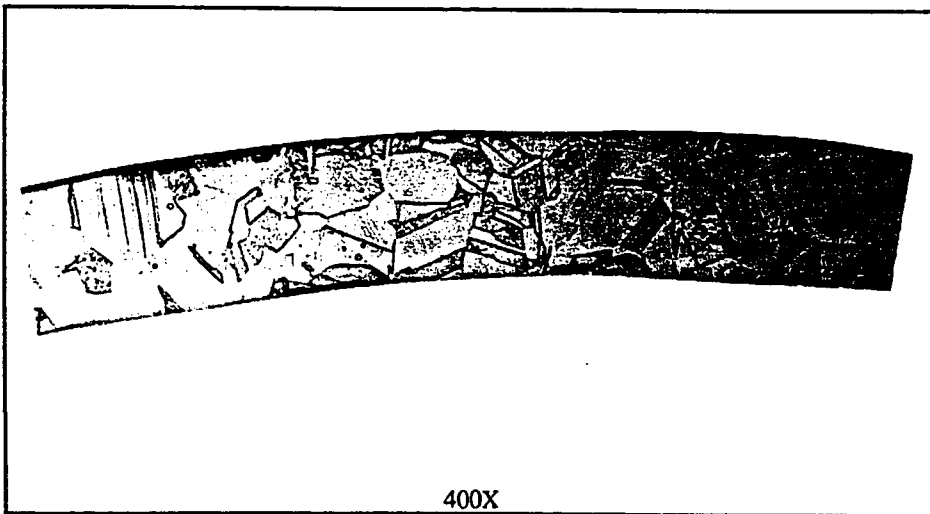
Figure 42. Microstructure of sample from Lot #14, tested for intergranular corrosion.
(DOE ID:3 A: Heat treated at 720°C   B: 24% CW   C: 0.0635 mm)

400X
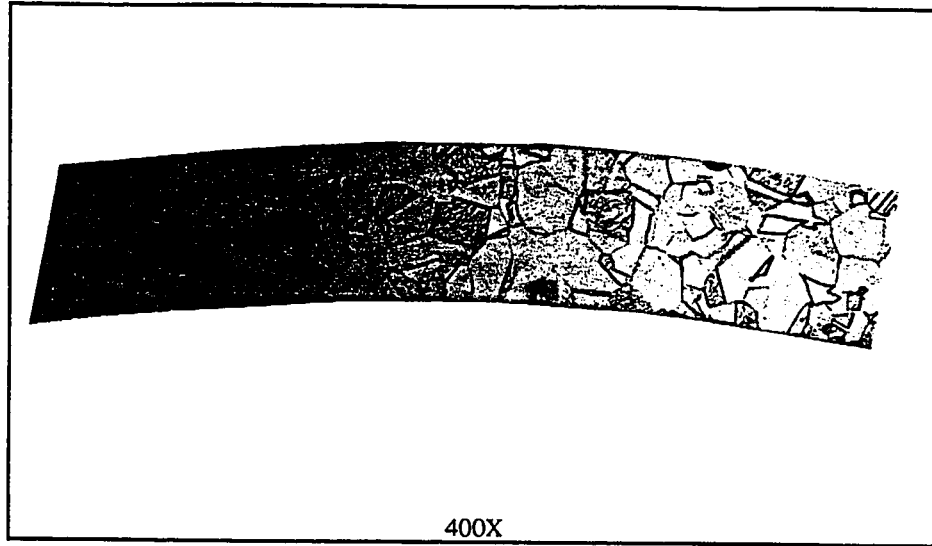
Figure 43. Microstructure of sample from Lot #14, tested for intergranular corrosion.
(DOE ID:4 A: Heat treated at 920°C   B: 24% CW   C: 0.0635 mm)

400X
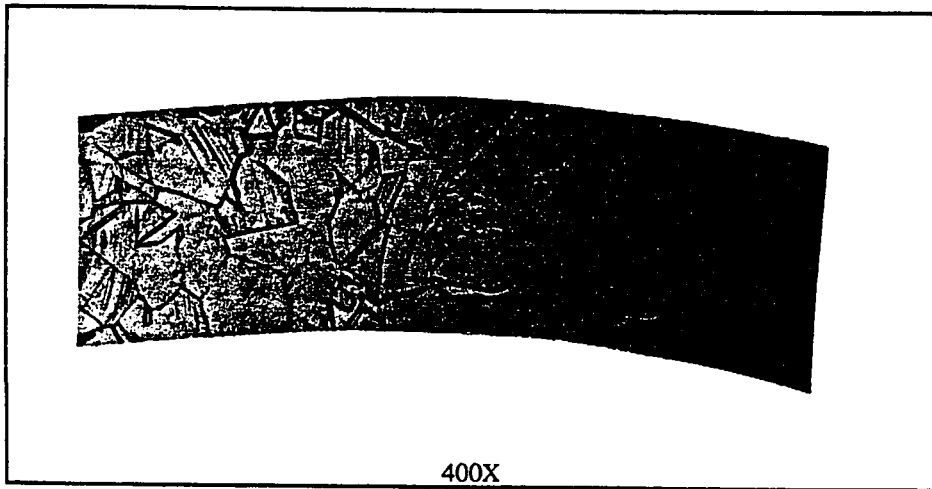
Figure 44. Microstructure of sample from Lot #16, tested for intergranular corrosion.
(DOE ID:5 A: Heat treated at 720°C   B: 10% CW   C: 0.1016 mm)

63
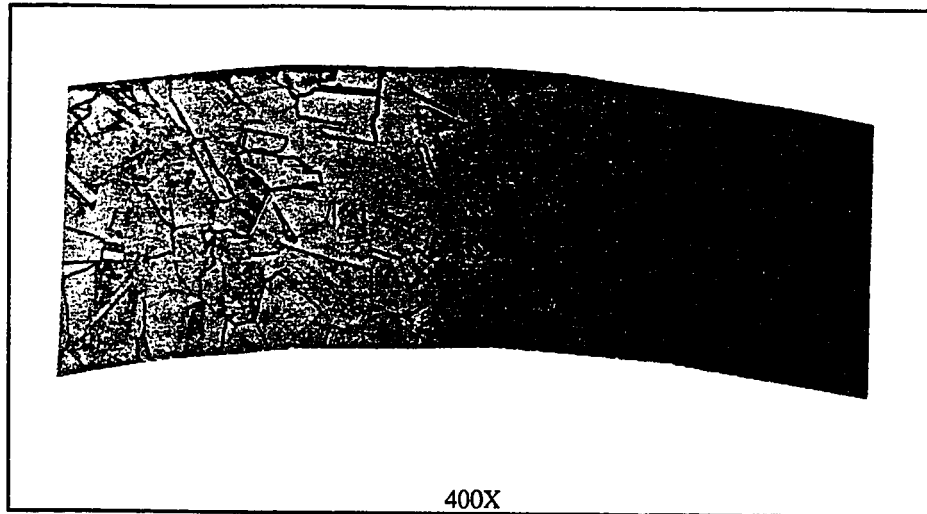
Figure 45. Microstructure of sample from Lot #16, tested for intergranular corrosion.
(DOE ID:6 A: Heat treated at 920°C B: 10% CW C: 0.1016 mm)
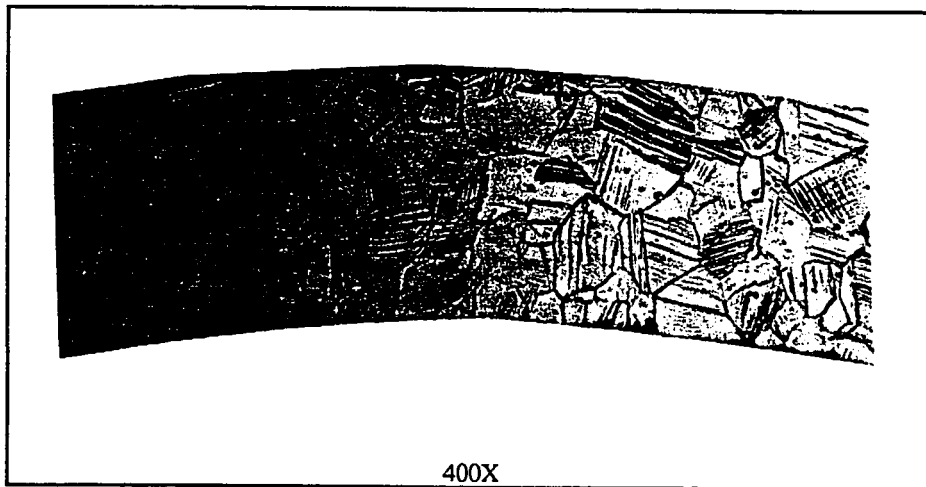
Figure 46. Microstructure of sample from Lot #14, tested for intergranular corrosion.
(DOE ID:7 A: Heat treated at 720°C B: 24% CW C: 0.1016 mm)

400X
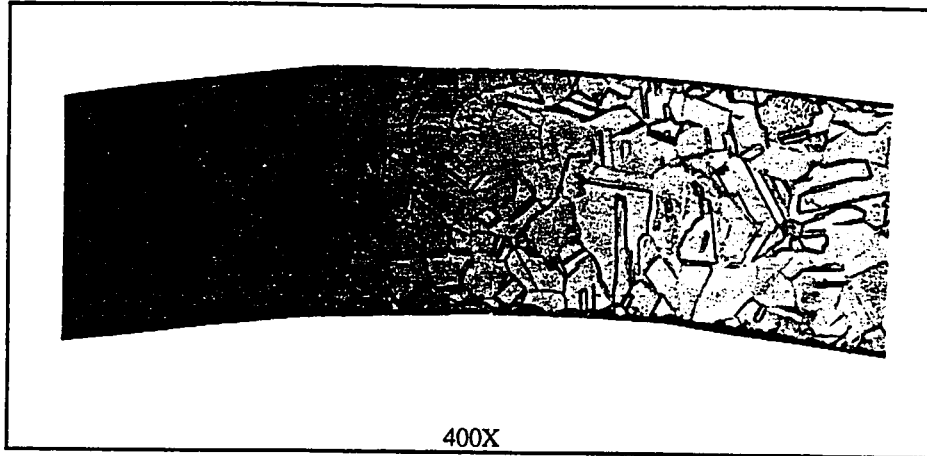
Figure 47. Microstructure of sample from Lot #14, tested for intergranular corrosion.
(DOE ID:8 A: Heat treated at 920°C   B: 24% CW   C: 0.1016 mm)

Table 11. Summary of results of grain size measurement and corrosion test on
DOE samples

DOE Id: CW, Wall, H.T.Temp.	ASTM Grain Size +/- 0.5	Intergranular Attack Susceptibility
1: 10%, 0.0635mm, 720°C	8.0	passed
2: 10%, 0.0635mm, 920°C	7.5	passed
3: 24%, 0.0635mm, 720°C	8.0	Passed
4: 24%, 0.0635mm, 920°C	7.5	passed
5: 10%, 0.1016mm, 720°C	7.5	passed
6: 10%, 0.1016mm, 920°C	7.5	passed
7: 24%, 0.1016mm, 720°C	8.0	passed
8: 24%, 0.1016mm, 920°C	7.5	passed

65

CHAPTER 5

DISCUSSION OF RESULTS

5.1. Introduction

This discussion of the results addresses the effects of the manufacturing variables, or factors, on the mechanical properties, grain size, and corrosion resistance of stainless steel hypotubing. The manufacturing variables included heat treatment temperature, extent of initial cold working, and wall thickness of hypotubings.

5.2. Effect of Factors on Ultimate Tensile Strength

Figure 48 shows the stress-strain curves for stainless steel hypotubing samples from Lot # 16 in the as-received condition, heat treated at 720°C and at 920°C. These specimens had an initial cold working of 10%.
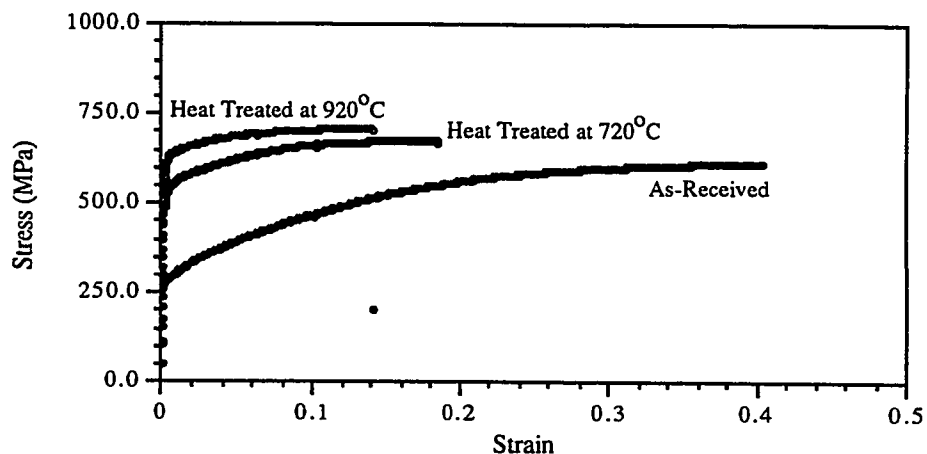
Figure 48. Stress-strain curves for stainless steel hypotubing with 10% cold work (Samples from Lot #16)

Similarly, Figure 49 shows the stress-strain curves for stainless steel hypotubing samples from Lot # 14 in the as-received condition, heat treated at 720°C and at 920°C. These specimens had an initial cold working of 24%.
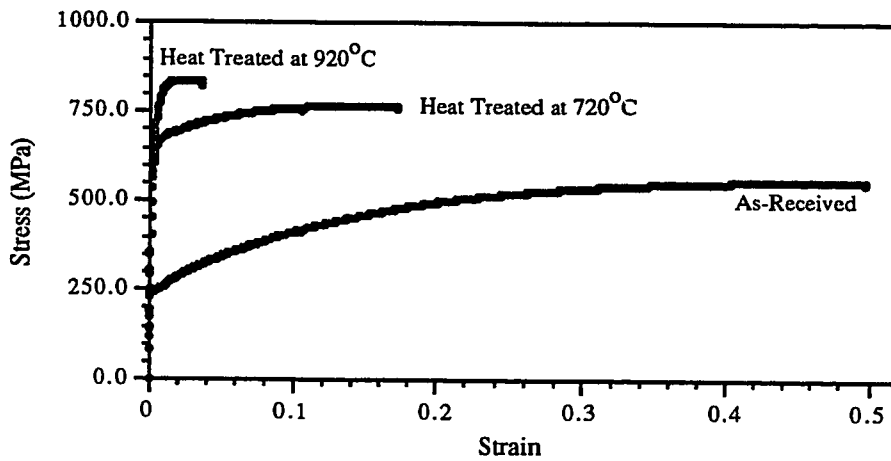
Figure 49. Stress-strain curves for stainless steel hypotubing with 24% cold work (Samples from Lot #14)

As was presented in Table 10, the heat treatment temperature had the most significant effect on the ultimate strength of the material. However, this factor also had interactions with the initial cold working. This was due to the higher stored internal energy of the material, which arises from cold working.

In the cold working process a small fraction of the expended energy is stored in the material as strain energy and the amount of this energy increases with increasing deformation. The free energy of the deformed metal is greater than that of an annealed metal by an amount approximately equal to the stored energy. Therefore, there is a greater tendency (driving force) for the deformed material to go back to its annealed state (lower total free energy). The kinetics of the reaction is the Arrhenius exponential-type, which can be accelerated greatly by heating (temperature). Depending on the temperature, the heat treatment process contains three different steps: recovery, recrystallization, and grain growth. Recovery is the early step, which happens in the low temperature range when the energy from heating is consumed by decreasing the dislocation density. Recrystallization is the next step, where new strain-free crystals are formed, and a significant amount of stored energy is released. And finally, in grain growth certain grains start to grow at the expense of other grains.

In this study the heat treatment process at the low temperature level (720°C) was done in the recovery region, and because the heating was done over a short time, not much stored energy was released. But at the high level temperature (920°C), recrystallization happened, and a major part of the stored energy was released. Here the amount of the internal energy overcame the effect of temperature. In other words, the material with greater cold working released more energy than the material with less cold working. Figure 50 shows the extent of stress relief for stainless steel hypotubings Cold worked to three different extents, and at two levels of heat treatment temperature.
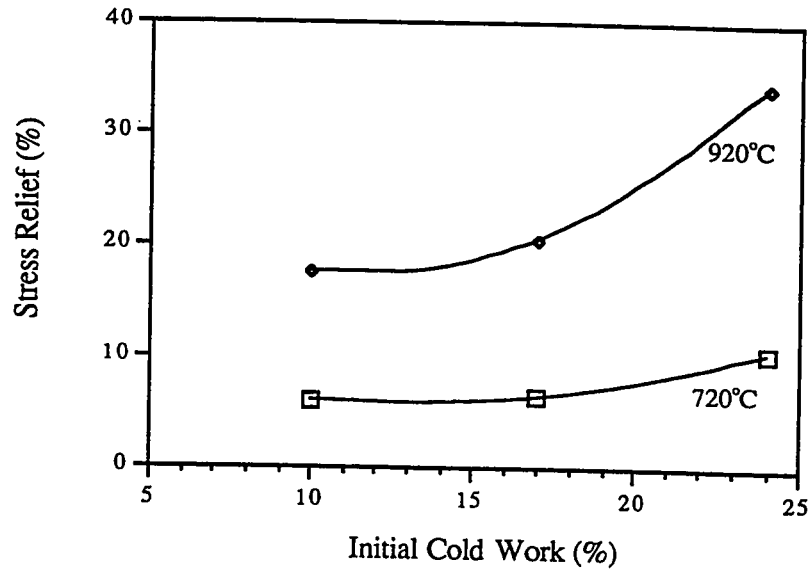
Figure 50. Effect of percent of initial cold working on the extent of stress relief during heat treatment process at 720°C and 920°C for stainless steel hypotubing

Cold working was a driving force for relieving the stress. This effect was more significant at the higher level of heat treatment temperature than at the lower level.

Wall thickness, as was presented in Table 10, did not affect the strength of the material significantly. This was due to the fact that during an ideal grinding process, no deformation or structural change happens. But due to the relatively thin walls of these hypotubings, a small amount of cold working did occur due to the grinding process, resulting in the strength of the thinner hypotubing being slightly higher.

5.3. Effect of Factors on Yield Strength

Heat treatment temperature had the greatest effect on the yield strength, as was shown in Table 10. Here the reduction of the dislocation density, due to the heating, lowered the yield strength of the material.[†] The heat treatment temperature had the same interaction with cold working, as was the case with ultimate tensile strength. The heat treatment temperature had interactions with the wall thickness as well. At the low temperature level, because of lower wall thickness, the thinner hypotubing had less ability to deform elastically. In other words, the material with a thinner wall had a lower yield point. But at the high temperature level this effect was overcome by the heat treatment temperature.

Cold work and wall thickness had interactions as shown in Table 10. At the low level of cold working, the wall thickness did not have a significant effect. However, at the high cold work level the effect of thinner walls and cold working added up and resulted in a lower yield point in the hypotubing with thinner walls.

5.4. Effect of Factors on Ductility

In the case of ductility of the material, or simply elongation, again the heat treatment temperature had the most significant effect. Here, increasing the temperature increased the ductility of the material significantly.

As mentioned in the preliminary study of the factors and presented in Table 10, wall thickness had a negative effect and hypotubings with thinner walls had lower ductilities. This was due to the thinness of the wall hypotubings where there were only 4 to 5 grains per wall. Therefore, by grinding the hypotubing there were fewer grains per wall. Since

---

[†] Yield strength is the stress corresponding to the minimum strain beyond which the material deforms plastically. The amount of this strain is generally considered to be 0.002.

metals deform plastically by the slip phenomenon, which is caused by dislocations or line defects, the traveling distance of the slip was reduced in the thinner wall hypotubing. This effect can be explained macroscopically as well. The total amount of elongation that was used as the response for this study included uniform and localized deformation, which starts after necking. Here, the elongation due to the localized deformation was reduced due to lack of material thickness.

The heat treatment temperature and cold working had the same interaction that was explained for the ultimate tensile strength. At the low temperature level a small amount of stress relieving happened and the material with higher cold working still had lower ductility. But at the high level of temperature the effect of greater cold working as the driving force for the stress relieving process overcame the effect of temperature, and the higher cold worked material had more ductility.

5.5. Effect of Factors on Microstructure

As was shown in Figures 30 to 39, the factors in this experiment did not affect the microstructure of the material significantly. The heat treatment time and temperature range covered only the recovery and recrystallization steps, thus resulting in no grain growth.

5.6. Effect of Factors on Corrosion Properties

Intergranular attack susceptibility of the material was tested as another response for the designed experiments. Figures 40 to 47 showed the results of these tests. There was no chromium carbide precipitation on the grain boundaries, and the material passed the test. This was mainly due to the low carbon concentration in this grade of stainless steel. Not

enough carbon is available for carbide formation during the short heat treatment time (5 min). As was pointed out in Chapter 4, the longer heat treatment times (over one hour) caused some chromium carbide precipitation, which was due to the time available for diffusion of the components.

CHAPTER 6
CONCLUSION

316L stainless steel hypotubing is one of the raw materials used for the production of surgical implant devices in the field of cardiology. The objective of this project was to investigate the structure-properties-processing relationships of 316L stainless steel hypotubing and develop characterization techniques to verify these relationships. These techniques were done in accordance with the FDA's requirements, which were specified as ASTM standards, and according to any requirements regarding the application of these hypotubings. Proper characterization techniques were developed in the course of this project. In order to investigate the structure-properties-processing relationships, factors that contribute to the properties of the material were identified, and designed experiments were performed. As a result of these experiments the correlations between the specified factors and mechanical properties of the material were determined.

The material under investigation was 316L stainless steel hypotubing, which is used for the manufacture of intravascular stents, a mesh type tubing that can be expanded in a narrowed section of an artery to keep it from reclosure due to the build-up of plaque. The chemical composition of this grade of stainless steel satisfies the biocompatibility requirements. The other important requirements are that the material be ductile enough to deform, up to the expanded shape, without fracture and that it be strong enough to withstand the pressure that arises from the reclosure of the vessel.

These hypotubings are manufactured in two forms: seamless and welded. In both cases the final step is tube drawing. Because of this common final step, the properties of the material, regardless of whether seamless or welded, are not significantly different. The standard requirement for the surface finish is that it be the "best possible finish". This reduces the chance for any chemical or mechanical surface reaction. Therefore both of

these manufacturing variables, manufacturing method and surface finish, were blocked out of the study.

It was found that the amount of initial cold working, done during the manufacturing of the hypotubings, affected the mechanical properties of the hypotubings. A higher cold worked material had a higher strength and a lower ductility. Therefore the amount of cold working was considered as one of the factors in the study, with 10% and 24% as the low and high levels, respectively.

It was also found that the wall thickness of the hypotubings (0.0635 mm to 0.1016 mm) affected the ductility of the hypotubings, with the thinner hypotubings having lower elongations. As a result of this, the wall thickness of the hypotubing was specified as another factor in the study, with values of 0.0635 mm and 0.1016 mm as the low and high levels, respectively.

In order to obtain different states of cold working in the material, the hypotubings were heat treated. The heat treatment process factors were first identified in the course of this project as a preliminary study. These factors included the heat treatment temperature range, heat treatment time, heat treatment environment, and cooling method. The goal was to release the residual stress due to the cold working in the manufacturing process without any change in microstructure, including chromium carbide precipitation and grain growth. As a result of the preliminary study the heat treatment temperature range of 720°C to 920°C, in which the residual stress from cold working process was reduced and heat treatment caused no grain growth, was identified. Heat treatment temperatures of 720°C and 920°C were chosen as the low and high levels for the experiment.

Full factorial experiments with three factors of heat treatment temperature, cold-working, and wall thickness at two levels, as mentioned above, were then designed. The response variables of the experiments were the mechanical properties of the material, which included the ultimate tensile strength, yield strength, and ductility. It was found that the heat treatment process in these experiments caused no grain growth or chromium carbide

precipitation in the material. Lack of chromium carbide precipitation decreased the susceptibility of the material to intergranular attack.

As a result of these experiments a window of operation was developed in order to obtain the required properties. This window of operation was in the form of three mathematical equations for predicting the response values (mechanical properties of stainless steel hypotubings) from the chosen factors. The manufacturing variables, or factors, that were found to affect the mechanical properties of the hypotubings were the heat treatment temperature, initial cold working, and the wall thickness.

It was found that the heat treatment temperature had the most significant effect on the mechanical properties of the stainless steel hypotubings. Increasing the temperature to 920°C resulted in a significant decrease in both the ultimate tensile strength and the yield strength (releasing residual stress), but an increase in the ductility of the material.

The effect of the heat treatment temperature on the mechanical properties depended on the extent of initial cold working in the material. This effect was more significant in the case of the material with a higher initial cold-working. The study showed that, in the case of material with 24% initial cold work, up to 35% of the residual stress can be relieved, and the ductility of the material can be increased up to 60%, by heat treating at 920°C.

It was found that the wall thickness of the hypotubings had a negative effect on only the ductility. In other words, the hypotubings with thinner walls had lower ductilities. The other mechanical properties were found not vary with wall thickness.

REFERENCES

1. Laing, P. G., Galante, J. O., and Lautenschlager, E., "Medical Devices: Measurements, Quality Assurance, and Standards: Chapter 7-Biomaterials: Orthopedic Implants", ASTM Special Technical Publication 800, (1990) pp.74-83.

2. Vander Voort, G. F., and James, H. M., "Wrought Stainless Steels", ASM Metals Handbook, 9th Edition, Vol. 3 , (1984) pp. 279-290.

3. Sutow, E. J., and Pollak, S. R., "The Biocompatibility of Certain Stainless Steels", Handbook of CRC: Biocompatibility of Clinical Implant Materials, Vol. 2, (1991) pp. 453-481.

4. Huber, P. L., "Stress Relieving of Austenitic Stainless Steels", ASM Metals Handbook, 9th Edition, Vol. 4, (1984) pp. 647-649.

5. Gray, R.G., "Metallographic Examinations of Retrieved Intramedullary Bone Pins and Bone Screws from the Human Body", J. Biomed. Mater. Res. Symposium, No. 5, Part 1, (1974), pp. 27-38.

6. Cahoon, J. R. and Paxton, H. W., "A metallurgical survey of current orthopedic implants", J. Biomed. Mater. Res. Symp, No. 4, (1970) pp. 223-230.

7. Weinstein, A., Amstutz, H., Pavon, G., and Franceschini, V., "Orthopedic implants-a clinical and metallurgical analysis", J. Biomed. Mater. Res. Symp, No. 4, (1973), pp. 297-304.

8. Procter, R. P. M. and Seaton, J. F., "An Evaluation of the quality of stainless steel surgical Implants", Injury , No. 8, (1975), pp.102-108.

9. Avadani, A. H., Murr, L. E., Atteridge, D. G., Chelakara, R., and Bruemmer, S. M., "Deformation Effects on Intragranular Carbide Precipitation and Transgranular Chromium Depletion in Type 316 Stainless Steels", Corrosion, Vol. 47, No. 12, (Dec 1991) pp. 939-948.

10. Eckenrod, J. J., and Kovach, C. W., "Effect of Nitrogen on the Sensitization, Corrosion, and Mechanical Properties of 18Cr-8Ni Stainless Steels, Prpoperties of Austenitic Stainless Steels and Their Weld Metals (Influence of Slight Chemistry Variations)", ASTM STP 679, (1979), pp. 17-41.

11. ASTM E122 - 88, "Standard Test Methods for Determining Average Grain Size", Annual Book of ASTM Standard, Vol. 03.01., (June 1993).

12. ASTM E45 - 87, "Standard Practice for Determining the Inclusion Content of Steel", Annual Book of ASTM Standard, Vol. 03.01., (June 1993)

13. ASTM A 370, "Standard Test Methods and Definitions for Mechanical Testing of Steel Product: A2.2. Steel Tubular Products", Annual Book of ASTM Standard, Vol. 01.01., (Jan. 1993)

14. ASTM A 262 - 91, "Standard Practices for Detecting Susceptibility to Intergranular Attack in Austenitic Stainless Steels", Annual Book of ASTM Standard, Vol. 01.03., (Feb. 1993)

15. Vander Voort, G. F.,"Sample Preparation", Metallography: Principles and Practice, McGraw-Hill, (1984), pp. 17-41.

16. Cormia, R. D., Schiefelbein, B., and Olsen, P. A., "Electropolishing of Stainless Steel: Meeting the Materials Requirements for Today's Demanding Applications", Photo Chemical Machining Institute Publication, Presented at the PCMI Annual Meeting, (Feb. 1990).

17. ASTM F 138 - 92, "Standard Specification for Stainless Steel Bar and Wire for Surgical Implant (Special Quality)", Annual Book of ASTM Standard, Vol. 13.01., (Sep. 1993)

18. ASTM F 139 - 92, "Standard Specification for Stainless Steel Sheet and Strip for Surgical Implants (Special Quality)", Annual Book of ASTM Standard, Vol. 13.01., (Sep. 1993)

BIBLIOGRAPHY

Denny, A. Jones, <u>Principles and Prevention of Corrosion</u>, Macmillan Publishing Co., N.Y., (1992).

Dieter, G. E., <u>Mechanical Metallurgy</u>, 2nd Edition, McGraw-Hill, (1976).

Hanson, J. A., <u>An introduction to stainless steels</u>, ASM Publication, (1972).

Huber, P. L., "Stress Relieving of Austenitic Stainless Steels", <u>ASM Metals Handbook</u>, 9th edition, Vol. 4, (1984) pp. 647-649

Krauss, G., <u>Steels, Heat Treatment and Processing Principles</u>, ASM Publication, (1992).

Peckner, D., and Bernstein, I. M., <u>Handbook of Stainless Steels</u>, McGraw-Hill, (1977).

Sutow, E. J., and Pollak, S. R., "The Biocompatibility of Certain Stainless Steels", <u>Handbook of CRC: Biocompatibility of Clinical Implant Materials</u>, Vol. 2, (1991) pp. 453-481.

Topol, E. J., <u>Textbook of Interventional Cardiology</u>, W. B. Saunders Co., (1990).

Vander Voort, G. F., <u>Metallography: Principles and Practice</u>, McGraw-Hill, (1984).

Vander Voort, G. F., and James, H. M., <u>Wrought Stainless Steels, ASM Metals Handbook</u>, Vol. 3, 9th Edition, (1984), pp. 279-290

APPENDIX 1

EFFECT OF GAGE LENGTH AND STRAIN RATE
IN TENSILE TEST

Gage length: Figure A1 shows the result of tensile test on sample #15 with three different sample lengths, and the tensile data are presented in Table A1. The strength of the material was not different but the percent elongation over 5.08 cm (2") increased with the decreasing the grip distance.
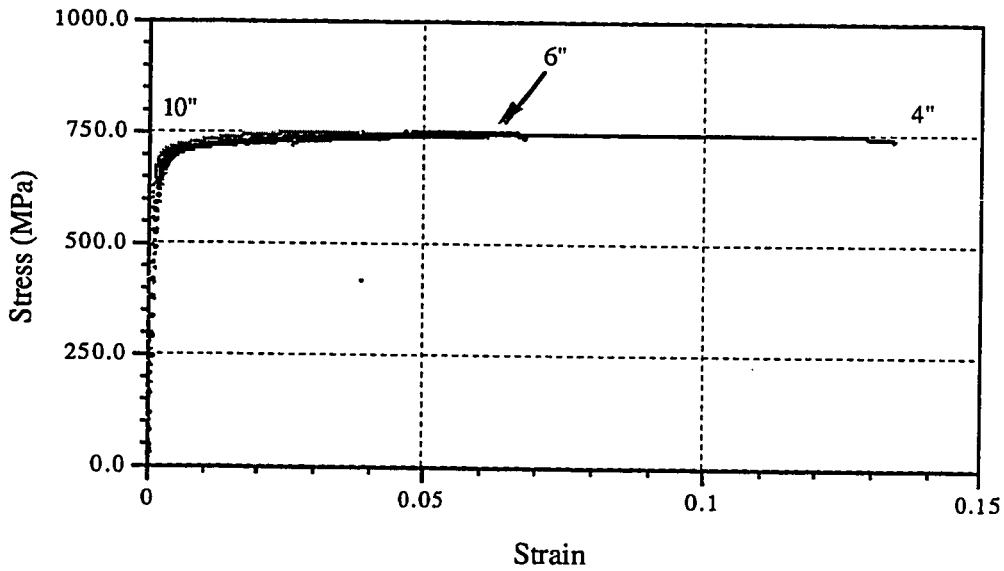
Figure A1. Effect of Grip Distance (Total length of tensile sample) on the Stress-Strain curve of stainless steel hypotubing, Sample #15.

Table A1. Tensile Properties of Sample #15 tested with 10.2, 15.2, and 25.4 cm grip distance.

	10.2 cm	15.2 cm	25.4 cm
UTS (MPa)	748.94	749.63	754.46
Y.S. (MPa)	637.19	640.91	650.55
Elongation (% in 5.08cm)	25	23	22

Strain Rate: For most metallic materials at room temperature, the strain rate has only a small effect on the level of the stress-strain curve. The average strain rate during most tests is in the range of 0.06 to 0.6 min.$^{-1}$.[19] For many materials, the effect of the strain rate on the stress, σ, at a fixed strain rate and temperature can be accounted for by Equation A1, at constant strain and temperature.

$$\sigma = C\, \varepsilon^{\circ\, m} \qquad \text{[A1]}$$

Where m, is the strain rate sensitivity coefficient, ε° is the strain rate in min.$^{-1}$, and C is a constant. So by measuring stress at two different strain rates and at constant strain, m can be calculated from Equation A2..

$$\sigma_2/\sigma_1 = (\varepsilon^{\circ}_2/\varepsilon^{\circ}_1)^{m} \qquad \text{[A2]}$$

At room temperature, the value of m is between -0.005 and +0.015 for most metals.[19] For example, for m = 0.01, a ten-fold increase in strain rate ($\varepsilon^{\circ}_2/\varepsilon^{\circ}_1=10$) raises the level of the stress only 2%. Figure A2 shows the result of tensile test on sample #15 with three different strain rates and value of strain rate sensitivity for stainless steel hypotubing calculated from the value of UTS in the above test.

Figure A2. Effect of Strain Rate on tensile properties of stainless steel hypotubing and strain rate sensitivity measurement.
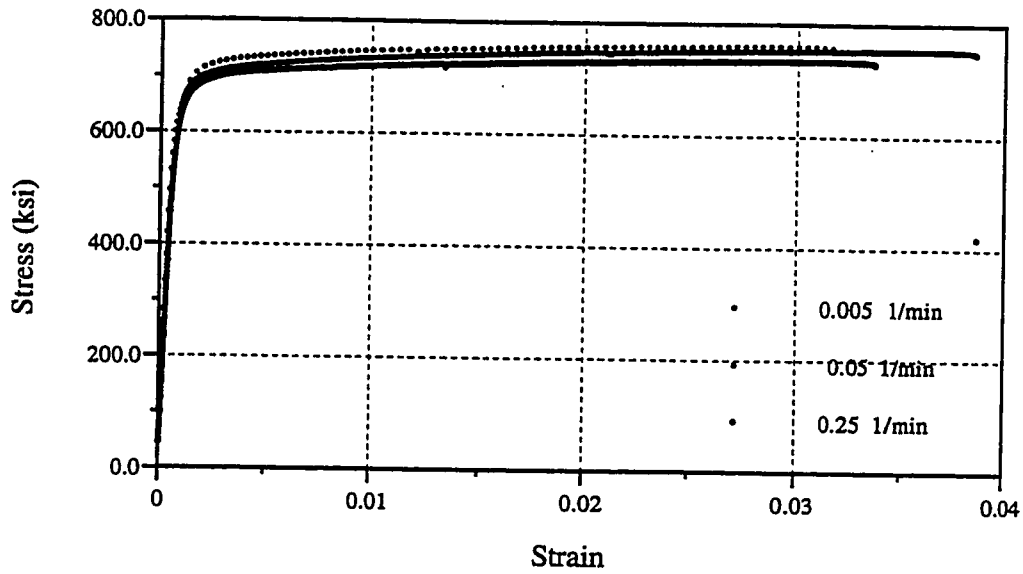
	Strain Rate (min^{-1})		
	0.005	0.05	0.25
UTS (MPa)	732.41	753.77	759.28
Y.S. (MPa)	627.06	653.59	681.35
Elongation in 5.08 cm (%)	20	23	19

$$\sigma = C \, (\, \varepsilon^\circ)^m_{\varepsilon,T}$$

Strain Rate Sensitivity : m = 0.0088

APPENDIX 2

FURNACE TEMPERATURE PROFILE

APPENDIX 3

Priliminary Study for the Heat Treatment Stainless Steel Hypotubing

Table A2 shows the results of the preliminary study of heat treatment factors and response variables. These factors were temperature (Temp.), time (t), furnace environment (Envir.), and cooling method (Cooling). The response variables included the effect of heat treatment on microstructure (grain size and observation of any carbide precipitation), and the mechanical properties of the hypotubings. In order to study the effect of these factors, the properties of the as-received material including grain size, ultimate tensile strength, yield strength, and percent elongation are compared with the properties of the heat treated samples.

Furnace Environment

Heat treatment in vacuum, because of the one hour heating up time and the one hour cooling down time of the furnace under vacuum, caused grain growth and chromium carbide precipitation, and surface of heat treated samples in argon were oxidixed. Finally, heat treatment in mixture of argon and 3.5% hydrogen gave satisfactory resuls

Heat Treatment Temperature and Time

As shown in Table A2, no stress relief (reduction in the strength of the material) happened during heat treatments at low temperatures (from 475°C to 650°C), for both short and long times. Five minutes heat treatment time in the high temperature range of 720°C to 920°C in argon gave satisfactory results where samples with no significant grain growth, reduced stress, and higher percent elongation were obtained. The grain size of these heat treated samples were in the range of 7.5 to 8.0 which is the same as the grain size of the as-received sample. The ultimate tensile strength of the material was reduced

from 708.30 MPa in the as-received condition to 580.96 MPa in the case of the sample heat treated at 920°C (18% stress relief); the percent elongation increased from 31% to 55%.

Cooling Method

Air cooling caused surface oxidation of the sample, but water quenching provided faster cooling and no surface oxidation happened. Water quenching gave the best results where no surface oxidation was observed.

Table A2. Summary of the preliminary study of heat treatment factors

Temp. (C)	t (min)	Envir.	Cooling	Microstructure (Grain Size)	UTS (MPa)	Y.S. (MPa)	Elon. (%)
538	15	vacuum	Argon	8	745.50	619.62	25
538	30	vacuum	Argon	7.5 (Carbide Prec.)	727.58	584.96	27
850	5	vacuum	Argon	6	610.04	261.41	44
950	5	vacuum	Argon	6.5 (Carbide Prec.)	609.83	261.27	42
475	30	Argon	Air Cool.	8	718.28	595.57	24
538	30	Argon	Air Cool	8	713.80	582.83	26
600	15	Argon	Air Cool.	8	705.88	568.01	31
720	5	Argon	W.Quen.	7.5	671.02	490.98	38
800	5	Argon	W.Quen.	7.5	659.44	463.21	41
850	5	Argon	W.Quen.	8	653.65	452.33	40
920	5	Argon	W.Quen.	7	580.96	243.01	55
As Received				8	708.3	560.8	31

APPENDIX 4 TENSILE TEST DATA

Tensile Test on 316L Stainless Steel Hypotubing
New Method by Mazdak Rooein
SI System

Test type: Tensile
Testing System 1.15
Operator name: Mazdak

Instron CorporationSeries IX Automated Materials

Test Date: 14 Feb 1994

Sample Identification: **MAZ8: #8**
Interface Type: 4500 Series
Machine Parameters of test:
Sample Rate (pts/sec):   2.000
Crosshead Speed (mm/min): 12.7000
Extensometer switch value: 10.0000% offset

Sample Type: ASTM

Humidity (%):   50
Temperature (deg. C):   25

Dimensions:

	Spec. 1	Spec. 2	Spec. 3
Area(mm**2)	51075	.51075	.51075
Ext. gauge len (mm)	50.800	50.800	50.800
Spec gauge len (mm)	254.00	254.00	254.00

Out of 3 specimens, 1 excluded.

		UTS (MPa)	Y.S. (MPa)	Elongation (%)
Specimen	*Excluded*	709.4	————	.0017
Number	2	710.4	568.9	33.5700
	3	711.5	586.0	34.5300
	Mean:	711.0	577.5	34.0500
	Standard Deviation:	.7	12.1	.6854

85

Tensile Test on 316L Stainless Steel Hypotubing
New Method by Mazdak Rooein
SI System
Test type: Tensile

Instron Corporation
Series IX Automated Materials Testing System 1.15
Test Date: 13 Mar 1994
Sample Type:

Operator name: Mazdak
Sample Identification: **MAZ8GR   #8Ground**
ASTM
Interface Type: 4500 Series
Machine Parameters of test:
Sample Rate (pts/sec):   2.000
Crosshead Speed (mm/min): 12.7000
Extensometer switch value: 10.0000% offset

Humidity (%):   50
Temperature (deg. C):   25

Dimensions:

	Spec. 1	Spec. 2	Spec. 3
Area (mm**2)	.37698	.37698	.37698
Ext. gauge len (mm)	50.800	50.800	50.800
Spec gauge len (mm)	254.00	254.00	254.00

Out of 3 specimens, 0 excluded.

		UTS	Y.S.	Elongation
		(MPa)	(MPa)	(%)
Specimen	1	721.8	596.3	21.94
Number	2	724.3	572.5	23.67
Mean:		723.5	589.0	23.62
Standard Deviation:		1.5	14.4	1.66

Tensile Test on 316L Stainless Steel Hypotubing
New Method by Mazdak Rooein
SI System

Test type: Tensile

Operator name: Mazdak

Sample Identification: **MAZ9**   **#9**
Interface Type: 4500 Series
Machine Parameters of test:
Sample Rate (pts/sec):   2.000
Crosshead Speed (mm/min): 12.7000
Extensometer switch value: 10.0000% offset

Sample Type: ASTM

Humidity (%):   50
Temperature (deg. C):   25

Dimensions:

	Spec. 1	Spec. 2	Spec. 3
Area (mm**2)	.51075	.51075	.51075
Ext. gauge len (mm)	50.800	50.800	50.800
Spec gauge len (mm)	254.00	254.00	254.00

Out of 3 specimens, 0 excluded.

		UTS (MPa)	Y.S. (MPa)	Elongation (%)
Specimen Number	1	781.2	662.9	26.30
	2	778.8	669.4	21.24
	3	777.6	662.2	26.73
Mean:		779.2	664.8	24.75
Standard Deviation:	1.8	4.0	3.05	

Strain

87

Tensile Test on 316L Stainless Steel Hypotubing
New Method by Mazdak Rooein
SI System

Test type: Tensile
                                                              Instron Corporation
                              Series IX Automated Materials Testing System 1.15
Operator name: Mazdak   Test Date: 13 Mar 1994

Sample Identification: **MAZ9GR #9Ground**   Sample Type: ASTM
Interface Type: 4500 Series
Machine Parameters of test:
Sample Rate (pts/sec):   2.000
Crosshead Speed (mm/min): 12.7000   Humidity (%):   50
Extensometer switch value: 10.0000% offset   Temperature (deg. C):   25
Dimensions:

	Spec. 1	Spec. 2
Area (mm**2)	.37698	.37698
Ext. gauge len (mm)	50.800	50.800
Spec gauge len (mm)	254.00	254.00

Out of 2 specimens, 0 excluded.

		UTS (MPa)	Y.S. (MPa)	Elongation (%)
Specimen	1	723.9	599.5	16.84
Number	2	730.8	615.6	16.85
Mean:		727.4	607.6	16.84
Standard Deviation:		4.9	11.4	.00

Strain

Tensile Test on 316L Stainless Steel Hypotubing
New Method by Mazdak Rooein
SI System
Test type: Tensile

Instron Corporation
Series IX Automated Materials Testing System 1.15

Operator name: Mazdak

Test Date: 14 Feb 1994

Sample Identification: # 2
Interface Type: 4500 Series
Machine Parameters of test:
Sample Rate (pts/sec):   2.000
Crosshead Speed (mm/min): 12.7000
Extensometer switch value: 10.0000% offset
Dimensions:

Sample Type: ASTM

Humidity (%):   50
Temperature (deg. C):   25

	Spec. 1	Spec. 2	Spec. 3	Spec. 4
Area (mm**2)	.41498	.41498	.41498	.41498
Ext. gauge len (mm)	50.800	50.800	50.800	50.800
Spec gauge len (mm)	254.00	254.00	254.00	254.00

Out of 4 specimens, 0 excluded.
Sample comments: #2 Without H.T.

		UTS (MPa)	Y.S. (MPa)	Elongation (%)
Specimen Number	1	982.3	837.2	6.249
	2	973.2	822.0	7.515
	3	971.1	824.3	9.240
	4	963.8	810.7	16.240
	Mean:	972.6	823.6	9.812
Standard Deviation:		7.6	10.9	4.460
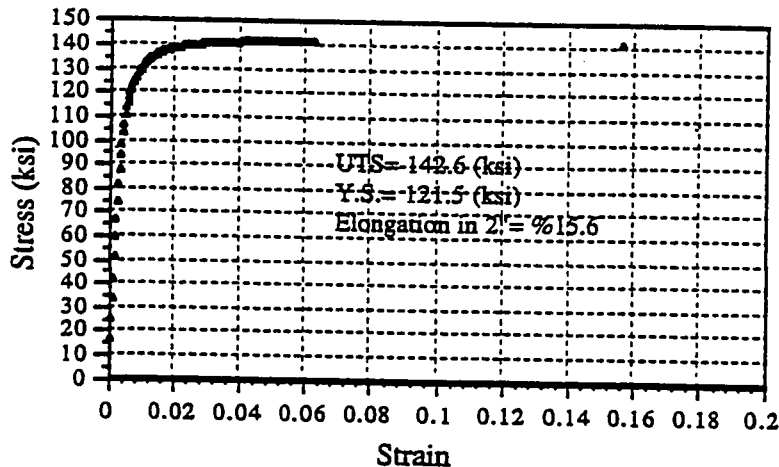
UTS= 142.6 (ksi)
Y.S.= 121.5 (ksi)
Elongation in 2" = %15.6

Stress (ksi) vs Strain

Tensile Test on 316L Stainless Steel Hypotubing
New Method by Mazdak Rooein

89

SI System
Test type: Tensile

Instron Corporation
Series IX Automated Materials Testing System 1.15
Test Date: 13 Mar 1994

Operator name: Mazdak

Sample Identification: **2Ground**
Interface Type: 4500 Series
Machine Parameters of test:
Sample Rate (pts/sec):   2.000
Crosshead Speed (mm/min): 12.7000
Extensometer switch value: 10.0000% offset
    Dimensions:

Sample Type: ASTM

Humidity (%):   50
Temperature (deg. C): 25

	Spec. 1	Spec. 2	Spec. 3
Area (mm**2)	.23511	.23511	.23511
Ext. gauge len (mm)	50.800	50.800	50.800
Spec gauge len (mm)	254.00	254.00	254.00

Out of 3 specimens, 0 excluded.

		UTS (MPa)	Y.S. (MPa)	Elongation (%)
Specimen	1	1192.	1001.0	9.599
Number	2	1178.	986.0	10.420
	3	1162.	1024.0	7.307
Mean:		1177.	1004.0	9.110
Standard Deviation:		15.	19.0	1.614

UTS= 962.53 (MPa)
Y.S.= 807.51 (MPa)
Elongation in 5.08 cm = %10.2

Tesile Test on Stainless Steel Hypotubing (SI System)
New Method by Mazdak Rooein

Test type: Tensile

                                           Instron Corporation
            Series IX Automated Materials Testing System 1.15
Operator name: Mazdak   Test Date: 22 Jul 1994
Sample Identification: **DOE1**   Sample Type: ASTM
Interface Type: 4200 Series
Machine Parameters of test:
Sample Rate (pts/sec):   2.000
Crosshead Speed (mm/min): 12.7000   Humidity (%):   50
Extensometer switch value: 10.0000% offset   Temperature (deg. C):   25

Dimensions:

	Spec. 1	Spec. 2	Spec. 3
Area (mm**2)	.51075	.51075	.51075
Ext. gauge len (mm)	50.800	50.800	50.800
Spec gauge len (mm)	254.00	254.00	254.00

Out of3 specimens,0 excluded.
Sample comments: Run#1,**10%CW,.0004",HT920C**

		UTS (MPa)	Y.S. (MPa)	% Elongation (%)	Modulus (AutYoung) (ksi)
Specimen	1	610.7	283.4	54.50	25620.
Number	2	576.8	244.4	54.50	24340.
	3	584.6	251.5	56.50	20720.
Mean:		590.7	259.7	55.17	23560.
Standard Deviation:		17.7	20.8	1.16	2542.

Strain

91

Tesile Test on Stainless Steel Hypotubing (SI System)
New Method by Mazdak Rooein
Test type: Tensile

Operator name: Mazdak
Sample Identification: **DOE2**
Interface Type: 4200 Series
Machine Parameters of test:
Sample Rate (pts/sec):   2.000
Crosshead Speed (mm/min): 12.7000
Extensometer switch value: 10.0000% offset

Humidity (%):   50
Temperature (deg. C):   25

Dimensions:

	Spec. 1	Spec. 2	Spec. 3
Area(mm**2)	.31162	.31162	.31162
Ext. gauge len (mm)	50.800	50.800	50.800
Spec gauge len (mm)	254.00	254.00	254.00

Out of 3 specimens, 0 excluded.
Sample comments: Run#2:**10%CW,0.0025",HT920C**

		UTS (MPa)	Y.S. (MPa)	Elongation (%)	Modulus (AutYoung) (ksi)
Specimen	1	590.8	269.3	40.50	31370.
Number	2	595.1	264.5	49.50	22340.
	3	587.4	262.6	45.50	31880.
Mean:		591.1	265.5	45.17	28530.
Standard Deviation:		3.9	3.4	4.51	.5366.

Tesile Test on Stainless Steel Hypotubing (SI System)
New Method by Mazdak Rooein
Test type: Tensile

Instron Corporation
Series IX Automated Materials Testing System 1.15
Test Date: 22 Jul 1994
Sample Type: ASTM

Operator name: Mazdak
Sample Identification: **DOE 3**
Interface Type: 4200 Series
Machine Parameters of test:
Sample Rate (pts/sec):   2.000
Crosshead Speed (mm/min): 12.7000
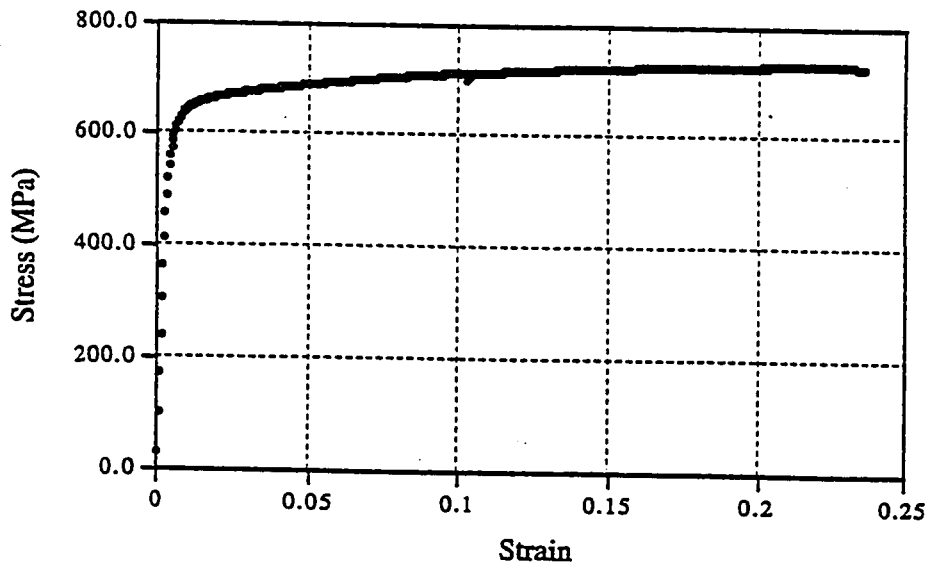Extensometer switch value: 10.0000% offset

Humidity (%):   50
Temperature (deg. C):   25

Dimensions:

	Spec. 1	Spec. 2	Spec. 3
Area(mm**2)	.51075	.51075	.51075
Ext. gauge len (mm)	50.800	50.800	50.800
Spec gauge len (mm)	254.00	254.00	254.00

Out of 3 specimens,   0 excluded.
Sample comments: Run#3: **10%CW,0.004",HT720C**

		UTS (MPa)	Y.S. (MPa)	% Elongation (%)	Modulus (AutYoung) (ksi)
Specimen	1	673.5	525.9	34.50	29550.
Number	2	662.6	476.2	40.50	26210.
	3	669.1	482.9	40.50	26730.
Mean:		668.4	495.0	38.50	27500.
Standard Deviation:		5.5	27.0	3.46	·1797.

Stress (MPa) vs Strain

Strain

Tesile Test on Stainless Steel Hypotubing (SI System)
New Method by Mazdak Rooein
Test type: Tensile   Instron Corporation
                                         Series IX Automated Materials Testing System 1.15
Operator name: Mazdak   Test Date: 02 Aug 1994
Sample Identification: DOE 4   Sample Type: ASTM
Interface Type: 4200 Series
Machine Parameters of test:
Sample Rate (pts/sec):   2.000   Humidity (%):   50
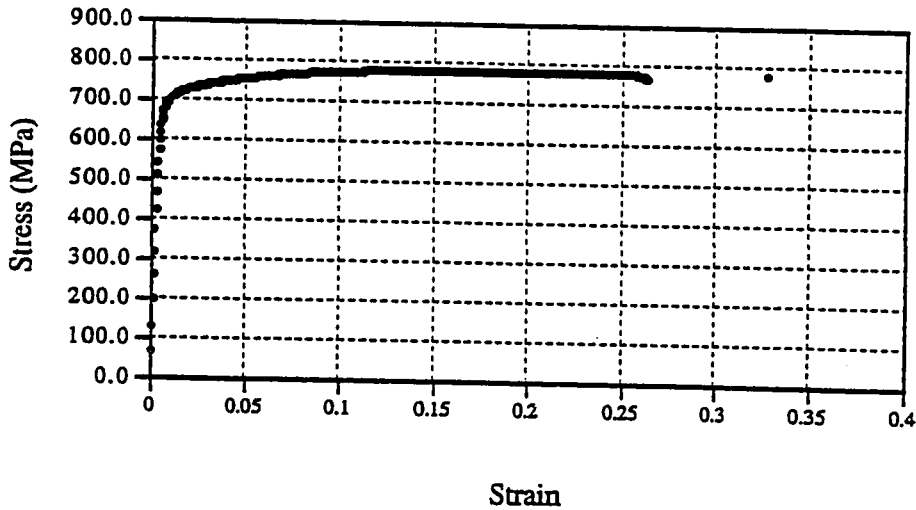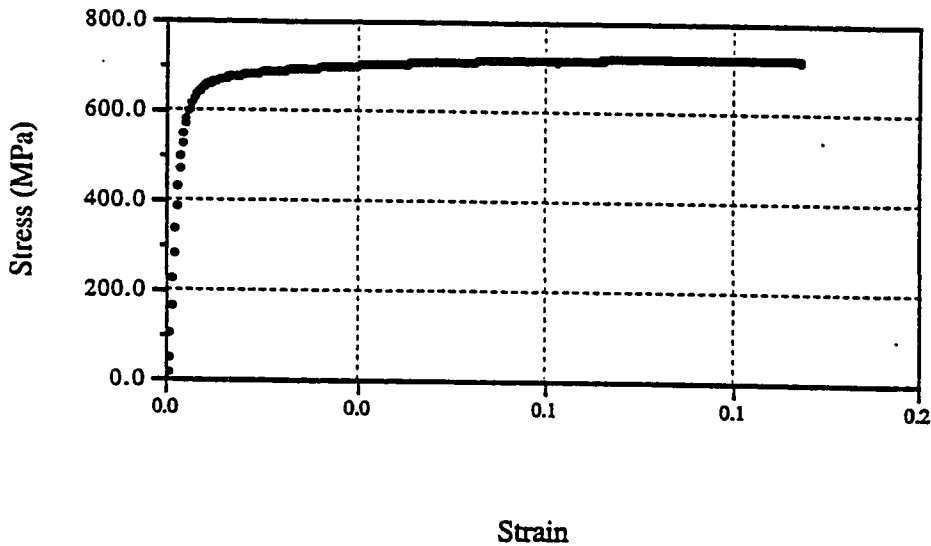Crosshead Speed (mm/min   ):   12.7000   Temperature (deg. C):   25
Extensometer switch value: 10.0000% offset

Dimensions:

	Spec. 1	Spec. 2	Spec. 3
Area(mm**2)	.31162	.31162	.31162
Ext. gauge len (mm)	50.800	50.800	50.800
Spec gauge len (mm)	254.00	254.00	254.00

Out of 3 specimens,   0 excluded.
Sample comments: Run#4 10%CW, 0.0025",HT720C

		UTS (MPa)	Y.S. (MPa)	% Elongation (%)	Modulus (AutYoung) (ksi)
Specimen	1	715.4	553.4	25.00	32100.
Number	2	714.9	543.8	20.50	31390.
	3	719.2	529.8	31.50	29430.
Mean:		716.5	542.3	25.67	30970.
Standard Deviation:		2.4	11.8	5.53	1383.

94

Tesile Test on Stainless Steel Hypotubing (SI System)
New Method by Mazdak Rooein
Test type: Tensile

Instron Corporation
Series IX Automated Materials Testing System 1.15

Operator name: Mazdak
Sample Identification: **DOE5**
Interface Type: 4200 Series
Machine Parameters of test:
Sample Rate (pts/sec):   2.000
Crosshead Speed (mm/min): 12.7000
Extensometer switch value: 10.0000% offset

Test Date: 02 Aug 1994
Sample Type: ASTM

Humidity (%):   50
Temperature (deg. C):   25

Dimensions:

	Spec. 1	Spec. 2	Spec. 3
Area (mm**2)	.31162	.31162	.31162
Ext. gauge len (mm)	50.800	50.800	50.800
Spec gauge len (mm)	254.00	254.00	254.00

Out of 3 specimens,0 excluded.
Sample comments: Run#5: **10%CW, 0.0025", 920C**

		UTS (MPa)	Y.S. (MPa)	Elongation (%)	Modulus (AutYoung) (ksi)
Specimen	1	602.7	280.6	47.00	19830.
Number	2	595.8	276.3	50.00	27950.
	3	624.5	292.4	47.00	24930.
Mean:		607.7	283.1	48.00	24240.
Standard Deviation:		15.0	8.3	1.73	4109.

Tesile Test on Stainless Steel Hypotubing (SI System)
New Method by Mazdak Rooein
Test type: Tensile

Instron Corporation
Series IX Automated Materials Testing System 1.15
Operator name: Mazdak   Test Date: 22 Jul 1994
Sample Identification: **DOE6**   Sample Type: ASTM
Interface Type: 4200 Series
Machine Parameters of test:
Sample Rate (pts/sec):   2.000
Crosshead Speed (mm/min):   12.7000   Humidity (%):   50
Extensometer switch value: 10.0000% offset   Temperature (deg. C):   25

Dimensions:

	Spec. 1	Spec. 2	Spec. 3
Area (mm**2)	.51075	.51075	.51075
Ext. gauge len (mm)	50.800	50.800	50.800
Spec gauge len (mm)	254.00	254.00	254.00

Out of 3 specimens,0 excluded.
Sample comments: Run#6:**10%CW,0.004",HT750C**

		UTS (MPa)	Y.S. (MPa)	Elongation (%)	Modulus (AutYoung) (ksi)
Specimen	1	667.5	511.9	31.50	32320.
Number	2	669.1	498.6	34.50	27230.
	3	668.9	493.0	36.00	28560.
Mean:		668.5	501.2	34.00	29370.
Standard Deviation:		.9	9.7	2.29	.2639.

96

Tesile Test on Stainless Steel Hypotubing (SI System)
New Method by Mazdak Rooein

Test type: Tensile   Instron Corporation
Series IX Automated Materials Testing System 1.15
Operator name: Mazdak
Sample Identification: **DOE7**
Interface Type: 4200 Series
Machine Parameters of test:
Sample Rate (pts/sec):   2.000
Crosshead Speed (mm/min):   12.7000
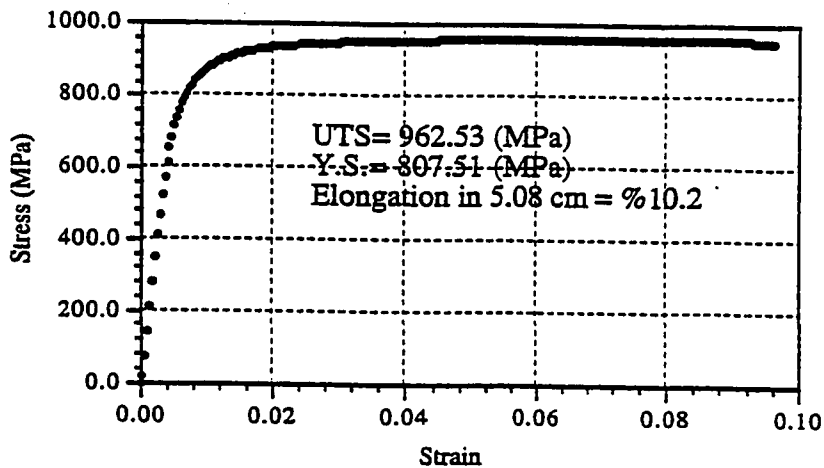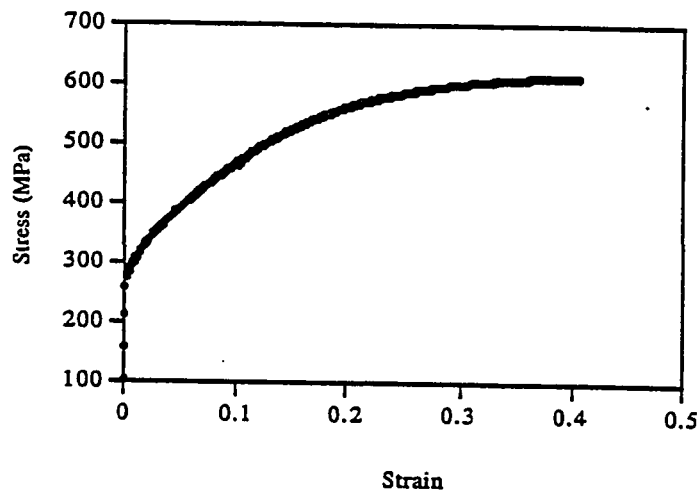Extensometer switch value: 10.0000% offset

Test Date: 22 Jul 1994
Sample Type: ASTM

Humidity (%):   50
Temperature (deg. C):   25

Dimensions:

	Spec. 1	Spec. 2	Spec. 3
Area (mm**2)	.51075	.51075	.51075
Ext. gauge len (mm)	50.800	50.800	50.800
Spec gauge len (mm)	254.00	254.00	254.00

Out of 3 specimens, 0 excluded.
Sample comments: Run#7:24%CW,0.004",HT920C

		UTS (MPa)	Y.S. (MPa)	% Elongation (%)	Modulus (AutYoung) (ksi)
Specimen	1	558.7	249.8	58.00	22670.
Number	2	546.7	256.2	-100.00	23160.
	3	562.8	253.0	59.50	27420.
Mean:		556.1	253.0	5.83	24420.
Standard Deviation:		8.4	3.2	91.66	2614.

Tesile Test on Stainless Steel Hypotubing (SI System)
New Method by Mazdak Rooein

Test type: Tensile   Instron Corporation
Series IX Automated Materials Testing System 1.15
Operator name: Mazdak
Sample Identification: **DOE9**
Interface Type: 4200 Series
Machine Parameters of test:
Sample Rate (pts/sec):   2.000
Crosshead Speed (mm/min):   12.7000
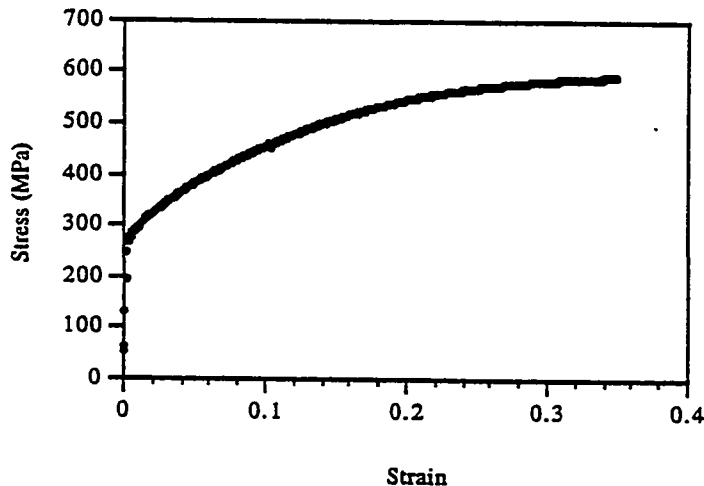Extensometer switch value: 10.0000% offset

Test Date: 03 Aug 1994
Sample Type: ASTM

Humidity (%):   50
Temperature (deg. C):   25

Dimensions:

	Spec. 1	Spec. 2	Spec. 3
Area (mm**2)	.31162	.31162	.31162
Ext. gauge len (mm)	50.800	50.800	50.800
Spec gauge len (mm)	254.00	254.00	254.00

Out of 3 specimens, 0 excluded.
Sample comments: Run#9:24%CW,0.0025",HT920C

		UTS (MPa)	Y.S. (MPa)	Elongation (%)	Modulus (AutYoung) (ksi)
Specimen	1	611.5	274.5	56.50	28320.
Number	2	527.4	263.5	-100.00	25340.
	3	620.4	282.6	47.00	27230.
Mean:		586.4	273.5	1.17	26970.
Standard Deviation:		51.3	9.6	87.74	1510.

98

Tesile Test on Stainless Steel Hypotubing (SI System)
New Method by Mazdak Rooein
Test type: Tensile

Series IX Automated Materials Testing System 1.15

Instron Corporation

Test Date: 03 Aug 1994
Sample Type: ASTM

Operator name: Mazdak
Sample Identification: **DOE10**
Interface Type: 4200 Series.
Machine Parameters of test:
Sample Rate (pts/sec):   2.000
Crosshead Speed (mm/min): 12.7000
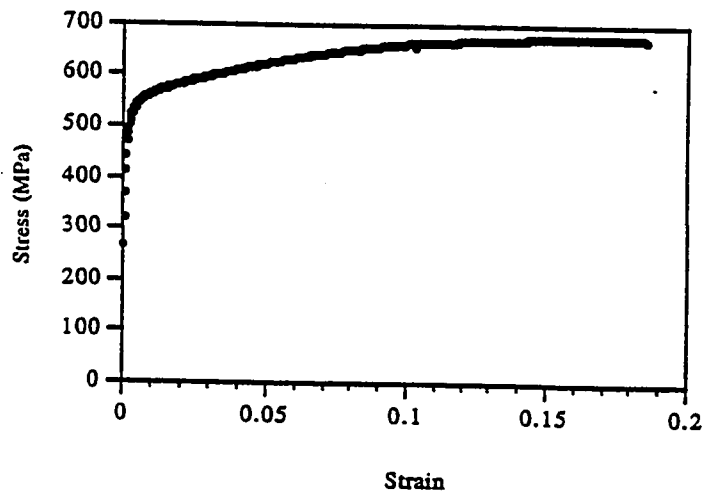Extensometer switch value: 10.0000% offset

Humidity (%):   50
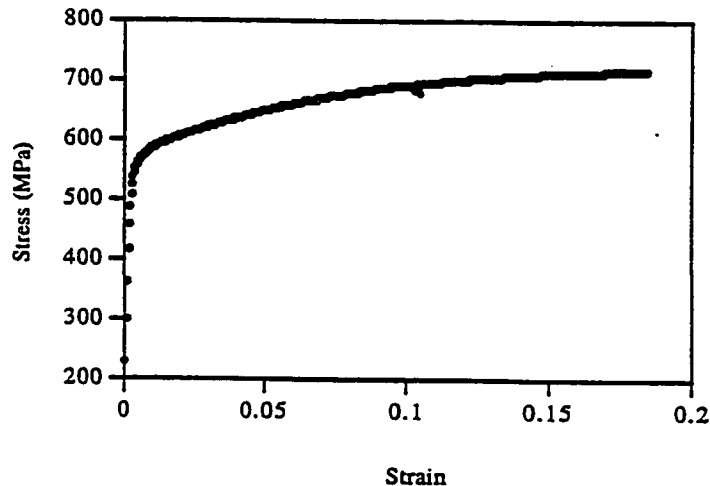Temperature (deg. C):   25

Dimensions:

	Spec. 1	Spec. 2	Spec. 3
Area (mm**2)	.31162	.31162	.31162
Ext. gauge len (mm)	50.800	50.800	50.800
Spec gauge len (mm)	254.00	254.00	254.00

Out of 3 specimens, 0 excluded.
Sample comments: Run#10:24%CW,0.0025",HT920C

		UTS (MPa)	Y.S. (MPa)	Elongation (%)	Modulus (AutYoung) (ksi)
Specimen	1	803.0	668.2	15.50	28290.
Number	2	841.3	712.7	17.00	29640.
	3	834.1	714.2	-100.00	26670.
Mean:		826.1	698.4	-22.50	28200.
StandardDeviation:		20.4	26.1	67.12	.1489.

99

Tesile Test on Stainless Steel Hypotubing (SI System)
New Method by Mazdak Rooein
Test type: Tensile

Instron Corporation
Series IX Automated Materials Testing System 1.15
Test Date: 03 Aug 1994
Sample Type: ASTM

Operator name: Mazdak
Sample Identification: **DOE11**
Interface Type: 4200 Series
Machine Parameters of test:
Sample Rate (pts/sec): 2.000
Crosshead Speed (mm/min): 12.7000
Extensometer switch value: 10.0000% offset

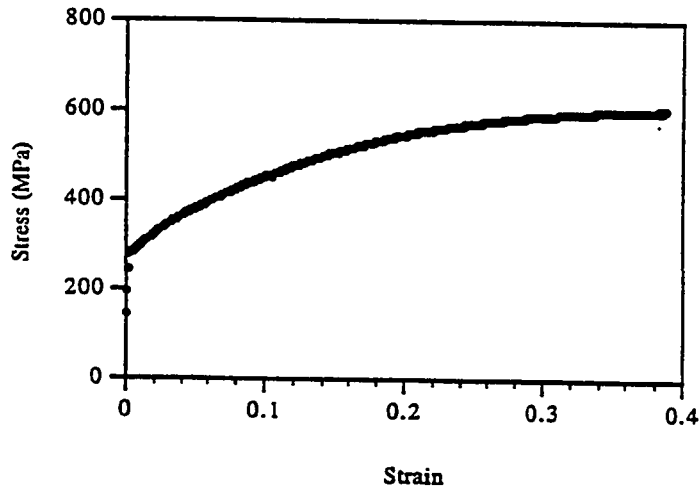Humidity (%): 50
Temperature (deg. C): 25

Dimensions:

	Spec. 1	Spec. 2	Spec. 3
Area(mm**2)	.31162	.31162	.31162
Ext. gauge len (mm)	50.800	50.800	50.800
Spec gauge len (mm)	254.00	254.00	254.00

Out of 3 specimens, 0 excluded.
Sample comments: Run#11:**10%CW,0.0025",HT920C**

		UTS (MPa)	Y.S. (MPa)	Elongation (%)	Modulus (AutYoung) (ksi)
Specimen	1	634.5	309.1	49.50	22460.
Number	2	585.1	261.6	45.50	32290.
	3	587.0	263.2	45.50	28390.
Mean:		602.2	278.0	46.83	27710.
Standard Deviation:		28.0	27.0	2.31	4953.
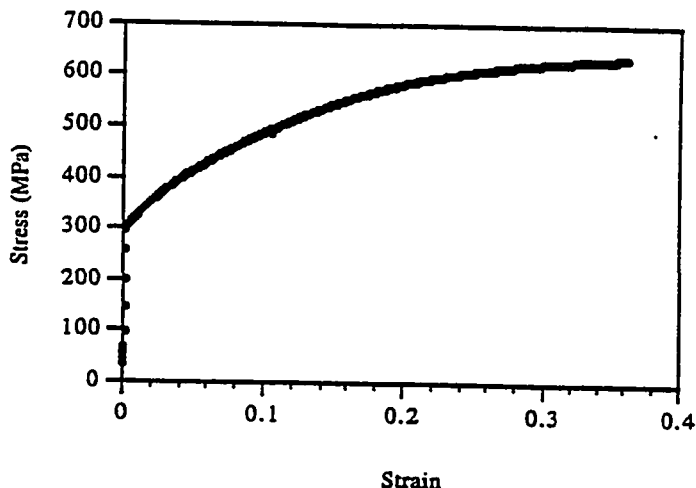
Tesile Test on Stainless Steel Hypotubing (SI System)
New Method by Mazdak Rooein
Test type: Tensile
Series IX Automated Materials Testing System 1.15
Operator name: Mazdak
Sample Identification: **DOE Run 12**
Interface Type: 4200 Series
Machine Parameters of test:
Sample Rate (pts/sec):   2.000
Crosshead Speed (mm/min   ):   12.7000
Extensometer switch value: 10.0000% offset

Instron Corporation

Test Date: 22 Jul 1994
    Sample Type: ASTM

Humidity (%):   50
Temperature (deg. C):   25

Dimensions:

	Spec. 1	Spec. 2
Area(mm**2)	.51075	.51075
Ext. gauge len (mm)	50.800	50.800
Spec gauge len (mm)	254.00	254.00

Out of 2 specimens, 0 excluded.
Sample comments: Run#12 **24% CW, 0.004", HT720C**

		UTS (MPa)	Y.S. (MPa)	% Elongation (%)	Modulus (AutYoung) (ksi)
Specimen	1	766.1	650.7	20.50	24570.
Number	2	768.9	655.6	20.50	25910.
Mean:		767.5	653.1	20.50	25240.
Standard Deviation:		2.0	3.5	.00	947.

Tensile Test on Stainless Steel Hypotubing (SI System)
New Method by Mazdak Rooein
Test type: Tensile
Series IX Automated Materials Testing System 1.15
Operator name: Mazdak
Sample Identification: **DOE13**
Interface Type: 4200 Series
Machine Parameters of test:
Sample Rate (pts/sec):   2.000
Crosshead Speed (mm/min):   12.7000
Extensometer switch value: 10.0000% offset

Instron Corporation

Test Date: 02 Aug 1994
Sample Type: ASTM

Humidity (%):   50
Temperature (deg. C):   25

Dimensions:

	Spec. 1	Spec. 2	Spec. 3
Area (mm**2)	.31162	.31162	.31162
Ext. gauge len (mm)	50.800	50.800	50.800
Spec gauge len (mm)	254.00	254.00	254.00

Out of 3 specimens, 0 excluded.
Sample comments: Run#13:**10%CW,0.0025",HT720C**

		UTS (MPa)	Y.S. (MPa)	Elongation (%)		Modulus (AutYoung) (ksi)
Specimen	1	705.0	536.6	25.00		24810.
Number	2	704.3	535.0	28.00		28410.
	3	722.7	542.4	33.00		28370.
Mean:		710.6	538.0	28.67	27190.	
Standard Deviation:		10.4	3.9	4.04	2066.	
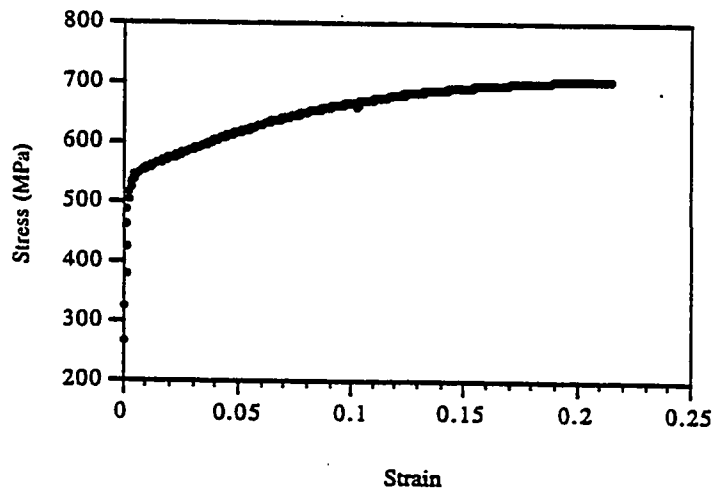
Tesile Test on Stainless Steel Hypotubing (SI System)
New Method by Mazdak Rooein
Test type: Tensile

Instron Corporation
Series IX Automated Materials Testing System 1.15
Test Date: 22 Jul 1994
Sample Type: ASTM

Operator name: Mazdak
Sample Identification: **DOE14**
Interface Type: 4200 Series
Machine Parameters of test:
Sample Rate (pts/sec):   2.000
Crosshead Speed (mm/min): 12.7000
Extensometer switch value: 10.0000% offset

Humidity (%):   50
Temperature (deg. C):   25

Dimensions:

	Spec. 1	Spec. 2
Area (mm**2)	.51075	.51075
Ext. gauge len (mm)	50.800	50.800
Spec gauge len (mm)	254.00	254.00

Out of 2 specimens, 0 excluded.
Sample comments: Run#14,10%CW,0.0004",HT920C

		UTS (MPa)	Y.S. (MPa)	Elongation (%)	Modulus (AutYoung) (ksi)
Specimen	1	554.2	249.7	-100.00	23630.
Number	2	586.0	249.5	59.50	24000.
Mean:		570.1	249.6	-20.25	23820.
Standard Deviation:		22.5	.1	112.80	258.

103

Tesile Test on Stainless Steel Hypotubing (SI System)
New Method by Mazdak Rooein

Test type: Tensile

Instron Corporation
Series IX Automated Materials Testing System 1.15

Operator name: Mazdak

Test Date: 22 Jul 1994

Sample Identification: **DOE15**
Interface Type: 4200 Series
Machine Parameters of test:

Sample Type: ASTM

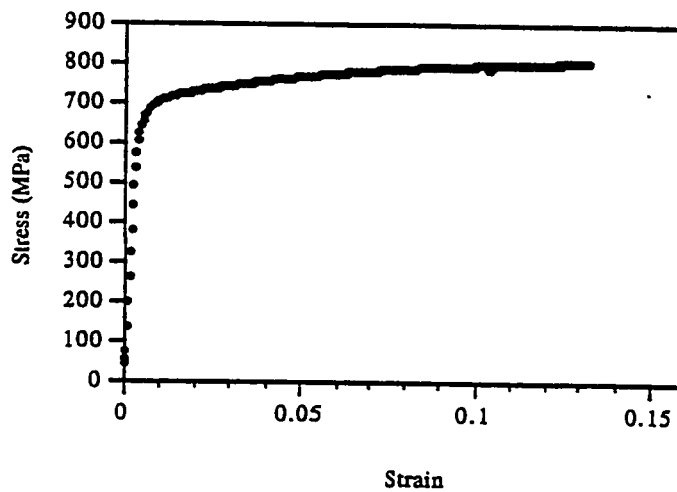| Sample Rate (pts/sec): | 2.000 | Humidity (%): | 50 |
| Crosshead Speed (mm/min): | 12.7000 | Temperature (deg. C): | 25 |
| Extensometer switch value: | 10.0000% offset | | |

Dimensions:

	Spec. 1	Spec. 2	Spec. 3
Area(mm**2)	.51075	.51075	.51075
Ext. gauge len (mm)	50.800	50.800	50.800
Spec gauge len (mm)	254.00	254.00	254.00

Out of 3 specimens, 0 excluded.
Sample comments: Run#15, **10% CW, 0.0004", HT720C**

		UTS	Y.S.	Elongation	Modulus (AutYoung)
		(MPa)	(MPa)	(%)	(ksi)
Specimen	1	666.8	498.6	37.50	28470.
Number	2	668.4	487.4	40.50	29080.
	3	668.4	501.2	36.00	27850.
Mean:		667.9	495.7	38.00	28470.
Standard Deviation:		.9	7.3	2.29	613.

Strain

Tesile Test on Stainless Steel Hypotubing (SI System)
New Method by Mazdak Rooein
Test type: Tensile

Operator name: Mazdak
Sample Identification: **DOE16**
Interface Type: 4200 Series
Machine Parameters of test:
Sample Rate (pts/sec):   2.000
Crosshead Speed (mm/min):   12.7000
Extensometer switch value: 10.0000% offset

Instron Corporation
Series IX Automated Materials Testing System 1.15
Test Date: 02 Aug 1994
Sample Type: ASTM

Humidity (%):   50
Temperature (deg. C)   25

Dimensions:

	Spec. 1	Spec. 2	Spec. 3
Area (mm**2)	.31162	.31162	.31162
Ext. gauge len (mm)	50.800	50.800	50.800
Spec gauge len (mm)	254.00	254.00	254.00

Out of 3 specimens,0 excluded.
Sample comments: Run#16:**10% CW,0.0025",HT720C**

		UTS (MPa)	Y.S. (MPa)	Elongation (%)	Modulus (AutYoung) (ksi)
Specimen	1	701.1	531.4	15.50	30760.
Number	2	714.5	531.7	29.50	28410.
	3	704.3	542.4	28.00	27710.
Mean:		706.6	535.1	24.33	28960.
Standard Deviation:		7.0	6.3	7.69	.1599.
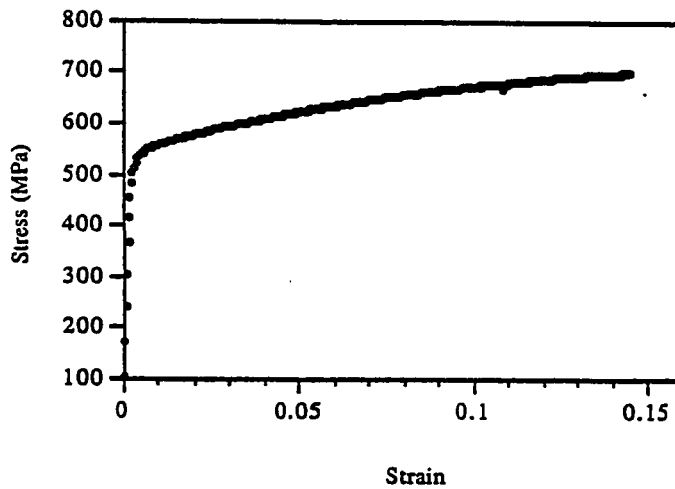
Strain

105

Tesile Test on Stainless Steel Hypotubing (SI System)
New Method by Mazdak Rooein

Test type: Tensile   Instron Corporation
                                        Series IX Automated Materials Testing System 1.15
Operator name: Mazdak   Test Date: 03 Aug 1994

Sample Identification: **DOE17**   Sample Type: ASTM
Interface Type: 4200 Series
Machine Parameters of test:
Sample Rate (pts/sec):   2.000   Humidity (%):   50
Crosshead Speed (mm/min): 12.7000   Temperature (deg. C):   25
Extensometer switch value: 5.0000% offset

Dimensions:

	Spec. 1	Spec. 2	Spec. 3
Area(mm**2)	.31162	.31162	.31162
Ext. gauge len (mm)	50.800	50.800	50.800
Spec gauge len (mm)	254.00	254.00	254.00

Out of 3 specimens, 0 excluded.
Sample comments: Run#17:24%CW,0.0025,HT720C

		UTS (MPa)	Y.S. (MPa)	Elongation (%)	Modulus (AutYoung) (ksi)
Specimen	1	843.6	729.9	14.00	27920.
Number	2	837.9	744.4	12.50	27880.
	3	839.1	749.8	12.50	26370.
Mean:		840.2	741.4	13.00	27390.
Standard Deviation:		3.0	10.3	.87	883.

106

Tesile Test on Stainless Steel Hypotubing (SI System)
New Method by Mazdak Rooein
Test type: Tensile

Operator name: Mazdak

Sample Identification: **DOE18**
Interface Type: 4200 Series
Machine Parameters of test:

Sample Type: ASTM

Sample Rate (pts/sec):	2.000	Humidity (%):	50
Crosshead Speed (mm/min):	12.7000	Temperature (deg. C):	25
Extensometer switch value:	10.0000% offset		

Dimensions:

	Spec. 1	Spec. 2	Spec. 3
Area (mm**2)	.31162	.31162	.31162
Ext. gauge len (mm)	50.800	50.800	50.800
Spec gauge len (mm)	254.00	254.00	254.00

Out of 3 specimens, 0 excluded.
Sample comments: Run#18:24%CW,0.0025",HT920C

		UTS (MPa)	Y.S. (MPa)	Elongation (%)	Modulus (AutYoung) (ksi)
Specimen	1	615.0	278.9	56.50	29380.
Number	2	612.4	278.9	47.00	29350.
	3	581.7	265.1	50.00	30120.
Mean:		603.0	274.3	51.17	29620.
Standard Deviation:		18.5	8.0	4.86	438.
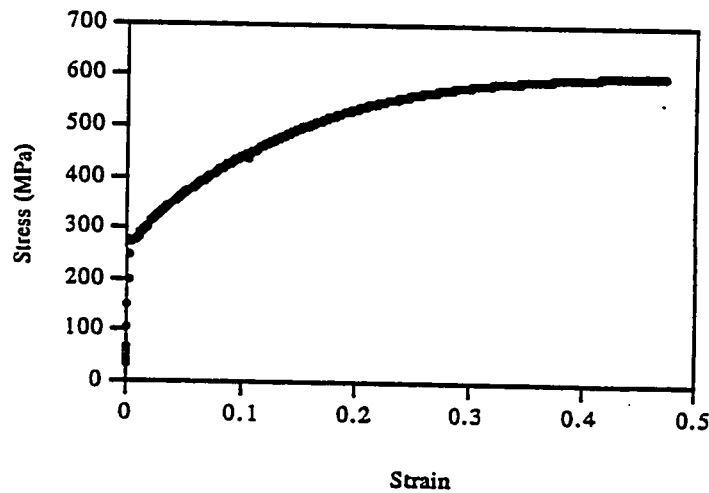
107

Tesile Test on Stainless Steel Hypotubing (SI System)
New Method by Mazdak Rooein
Test type: Tensile

Instron Corporation
Series IX Automated Materials Testing System 1.15

Operator name: Mazdak
Sample Identification: **DOE19**
Interface Type: 4200 Series
Machine Parameters of test:

Test Date: 03 Aug 1994
Sample Type: ASTM

Sample Rate (pts/sec):   2.000
Crosshead Speed (mm/min): 12.7000
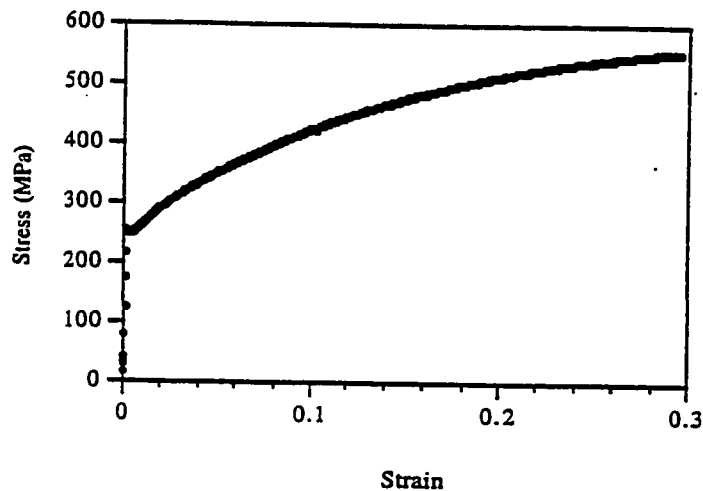Extensometer switch value: 10.0000% offset

Humidity (%):   50
Temperature (deg. C):   25

Dimensions:

	Spec. 1	Spec. 2	Spec. 3
Area(mm**2)	.31162	.31162	.31162
Ext. gauge len (mm)	50.800	50.800	50.800
Spec gauge len (mm)	254.00	254.00	254.00

Out of 3 specimens,   0 excluded.
Sample comments: Run#19:**24%CW, 0.0025, HT920C**

		UTS (MPa)	Y.S. (MPa)	Elongation (%)	Modulus (AutYoung) (ksi)
Specimen	1	579.7	264.2	47.00	30320.
Number	2	533.2	270.7	-100.00	30090.
	3	602.7	271.1	53.00	32180.
Mean:		571.9	268.6	.00	30860.
Standard Deviation:		35.4	3.9	86.65	1149.

108

Tesile Test on Stainless Steel Hypotubing (SI System)
New Method by Mazdak Rooein
Test type: Tensile

Instron Corporation
Series IX Automated Materials Testing System 1.15

Operator name: Mazdak
Sample Identification: **DOE20**
Interface Type: 4200 Series
Machie Parameters of test:

Test Date: 22 Jul 1994
Sample Type: ASTM

Sample Rate (pts/sec):   2.000
Crosshead Speed (mm/min   ):   12.7000
Extensometer switch value: 10.0000% offset

Humidity (%):   50
Temperature (deg. C):   25

Dimensions:

	Spec. 1	Spec. 2	Spec. 3
Area (mm**2)	.51075	.51075	.51075
Ext. gauge len (mm)	50.800	50.800	50.800
Spec gauge len (mm)	254.00	254.00	254.00

Out of 3 specimens,   0 excluded.
Sample comments: Run#20:24%CW,0.0004",**HT920C**

		UTS (MPa)	Y.S. (MPa)	Elongation (%)	Modulus (AutYoung) (ksi)
Specimen	1	566.3	252.0	59.50	23310.
Number	2	550.7	246.2	56.50	25630.
	3	559.5	249.9	59.50	22420.
Mean:		558.8	249.3	58.50	23790.
Standard Deviation:		7.9	2.9	1.73	1660.
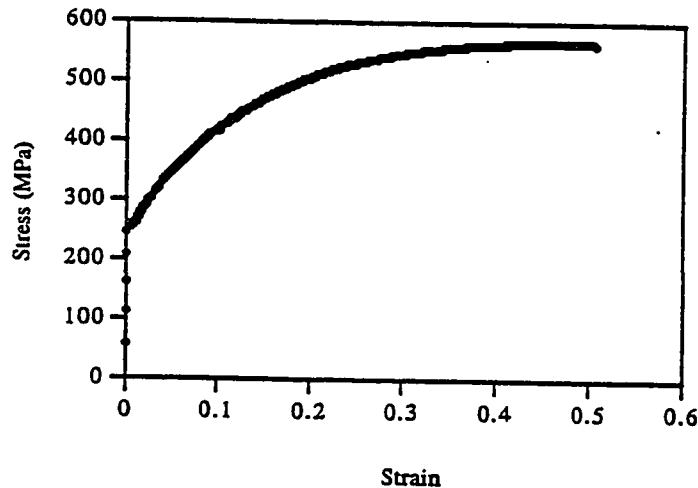
109

Tesile Test on Stainless Steel Hypotubing (SI System)
New Method by Mazdak Rooein
Test type: Tensile

Instron Corporation
Series IX Automated Materials Testing System 1.15

Operator name: Mazdak
Sample Identification: **DOE21**
Interface Type: 4200 Series
Machine Parameters of test:

Test Date: 03 Aug 1994
Sample Type: ASTM

Sample Rate (pts/sec):   2.000
Crosshead Speed (mm/min): 12.7000
Extensometer switch value: 5.0000% offset

Humidity (%):   50
Temperature (deg. C):   25

Dimensions:.

	Spec. 1	Spec. 2	Spec. 3
Area (mm**2)	.31162	.31162	.31162
Ext. gauge len (mm)	50.800	50.800	50.800
Spec gauge len (mm)	254.00	254.00	254.00

Out of 3 specimens,   0 excluded.
Sample comments: Run#21: **24%, 0.0025", HT720C**

		UTS (MPa)	Y.S. (MPa)	Elongation (%)	Modulus (AutYoung) (ksi)
Specimen	1	847.0	727.2	14.00	30770.
Number	2	829.8	712.7	15.50	27450.
	3	797.7	680.5	19.00	28810.
Mean:		824.8	706.8	16.17	29010.
Standard Deviation:		25.0	23.9	2.57	.1669.

Strain

Tesile Test on Stainless Steel Hypotubing (SI System)
New Method by Mazdak Rooein
Test type: Tensile

Instron Corporation
Series IX Automated Materials Testing System 1.15

Operator name: Mazdak
Sample Identification: **DOE 22**
Interface Type: 4200 Series
Machine Parameters of test:

Test Date: 22 Jul 1994
Sample Type: ASTM

Sample Rate (pts/sec):   2.000
Crosshead Speed (mm/min): 12.7000
Extensometer switch value: 5.0000% offset
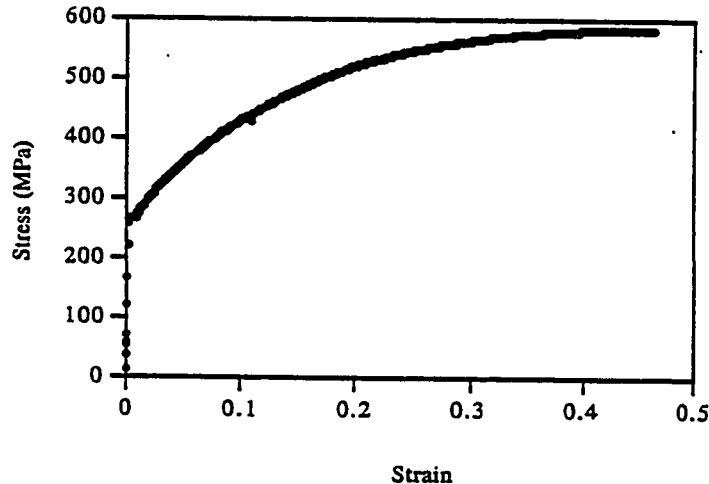
Humidity (%):   50
Temperature (deg. C):   25

Dimensions:

	Spec. 1	Spec. 2	Spec. 3
Area (mm**2)	.51075	.51075	.51075
Ext. gauge len (mm)	50.800	50.800	50.800
Spec gauge len (mm)	254.00	254.00	254.00

Out of 3 specimens,   0 excluded.
Sample comments: Run#22: **24%CW,0.004",HT720C**

		UTS (MPa)	Y.S. (MPa)	Elongation (%)	Modulus (AutYoung) (ksi)
Specimen	1	769.1	672.6	19.00	26540.
Number	2	759.1	642.7	20.50	25190.
	3	756.7	662.1	20.50	24870.
Mean:		761.6	659.2	20.00	25530.
Standard Deviation:		6.6	15.2	.87	884.

111
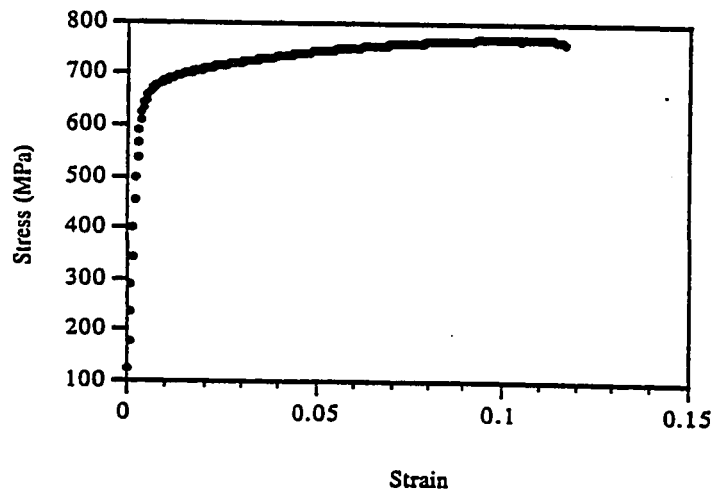
Tensile by Mazdak
Test type: Tensile

Operator name: Mazdak
Sample Identification: **DOE23**
Interface Type: 4200 Series
Machine Parameters of test:

Sample Type: ASTM

Sample Rate (pts/sec):	2.000	Humidity (%):	50
Crosshead Speed (in/min):	.5000	Temperature (deg. C):	25
Extensometer switch value:	5.0000% offset		

Dimensions:

	Spec. 1	Spec. 2	Spec. 3
Area (in**2)	.00079	.00079	.00079
Ext. gauge len (in)	SEPARATE		
Spec gauge len (in)	10.000	10.000	10.000

Out of 3 specimens,0 excluded.
Sample comments: Run#23:24%CW,0.004",HT720C

		UTS (Ksi)	Y.S. (Ksi)	Gauge Length (in)	Final G.L (in)	% Elongation (%)	Modulus (AutYoung) (ksi)
Specimen	1	109.0	94.20	2.000	2.380	19.00	25730.
Number	2	112.7	96.51	2.000	2.390	19.50	26410.
	3	108.2	94.00	2.000	2.380	19.00	24970.
0							
Mean:		110.0	94.90	2.000	2.383	19.17	25700.
Standard Deviation:		2.4	1.39	.000	.006	.29	724.
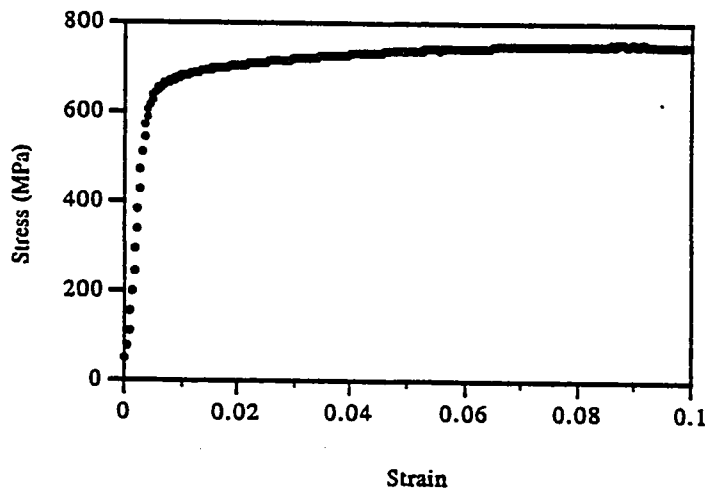
Strain

112

Tesile Test on Stainless Steel Hypotubing (SI System)
New Method by Mazdak Rooein
Test type: Tensile

Instron Corporation
Series IX Automated Materials Testing System 1.15
Test Date: 22 Jul 1994

Operator name: Mazdak
Sample Identification: **DOE24**
Interface Type: 4200 Series
Machine Parameters of test:

Sample Type: ASTM

Sample Rate (pts/sec):   2.000
Crosshead Speed (mm/min):   12.7000
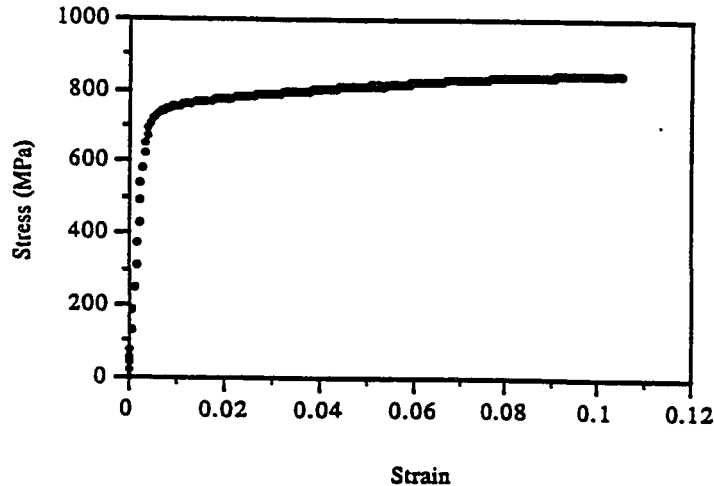Extensometer switch value: 10.0000% offset

Humidity (%):   50
Temperature (deg. C):   25

Dimensions:

	Spec. 1	Spec. 2
Area (mm**2)	.51075	.51075
Ext. gauge len (mm)	50.800	50.800
Spec gauge len (mm)	254.00	254.00

Out of 2 specimens,   0 excluded.
Sample comments: Run#24: **24%CW,0.004",HT920C**

		UTS (MPa)	Y.S. (MPa)	% Elongation (%)	Modulus (AutYoung) (ksi)
Specimen	1	556.6	247.7	58.00	22640.
Number	2	560.3	249.7	59.50	26670.
Mean:		558.4	248.7	58.75	24650.
Standard Deviation:		2.6	1.5	1.06	2849.

113
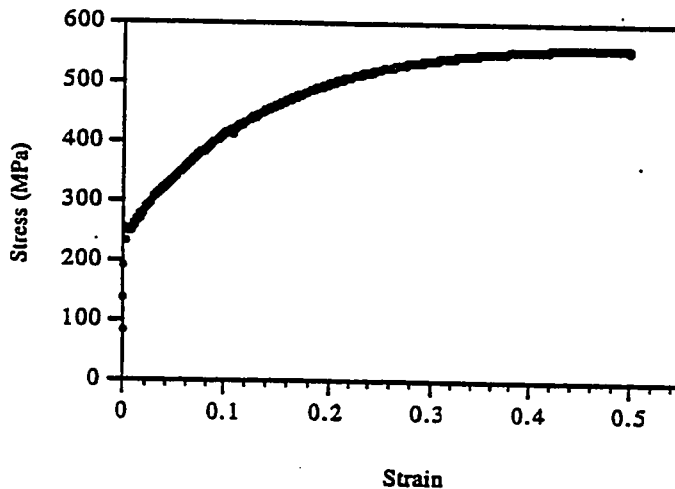
APPENDIX 5
DOE ANOVA

```
---------------------------
Analysis of Elongation                    MRDOE1.DE3   Anova Results   8/15/94
---------------------------
```

SOURCE	SUM OF SQUARES	DF	MEAN SQUARE	F VALUE	PROB > F
MODEL	6071.4263	7	867.35	323.18	< 0.0001
RESIDUAL	42.9400	16	2.68		
*PURE ERROR	42.9400	16	2.68	.	
COR TOTAL	6114.3663	23			

ROOT MSE	1.6382	R-SQUARED	0.99	
DEP MEAN	38.9875	ADJ R-SQUARED	0.99	
C.V. %	4.2019	PRED R-SQUARED	0.98	

Predicted Residual Sum of Squares (PRESS) =   96.62

* Residual = Lack-Of-Fit + Pure Error

FACTOR	COEFFICIENT ESTIMATE	DF	STANDARD ERROR	t FOR HO COEFFICIENT=0	PROB > $\|t\|$
INTERCEPT	38.98750	1	0.33440		
A	-2.80417	1	0.33440	-8.39	< 0.0001
B	14.46250	1	0.33440	43.25	< 0.0001
C	4.12083	1	0.33440	12.32	< 0.0001
AB	4.20417	1	0.33440	12.57	< 0.0001
AC	-1.00417	1	0.33440	-3.00	0.0084
BC	0.27917	1	0.33440	0.83	0.4161
ABC	0.45417	1	0.33440	1.36	0.1933

Final Equation in Terms of Coded Factors

Elongation =

```
          38.9875
    -      2.8042  * A
    +     14.4625  * B
    +      4.1208  * C
    +      4.2042  * A * B
    -      1.0042  * A * C
    +      0.2792  * B * C
    +      0.4542  * A * B * C
```

Final Equation in Terms of Uncoded Factors

Elongation =

```
         -46.7692
    -      2.3984  * Cold Work
    +      0.0782  * H.T. Temp.
    +  17753.0159  * Wall Thick.
    +      0.0032  * Cold Work * H.T. Temp.
    -    900.6349  * Cold Work * Wall Thick.
    -     10.9841  * H.T. Temp. * Wall Thick.
    +      0.8651  * Cold Work * H.T. Temp. * Wall Thick.
```

OBS ORD	ACTUAL VALUE	PREDICTED VALUE	RESIDUAL	LEVER	STUDENT RESID	COOK'S DIST.	OUTLIER T VALUE	RUN ORD
1	24.30	26.23	-1.93	0.333	-1.445	0.131	-1.501	22
2	25.70	26.23	-0.53	0.333	-0.399	0.010	-0.388	1
3	28.70	26.23	2.47	0.333	1.844	0.213	2.012	15
4	16.20	15.13	1.07	0.333	0.797	0.040	0.788	18
5	13.00	15.13	-2.13	0.333	-1.595	0.159	-1.684	23
6	16.20	15.13	1.07	0.333	0.797	0.040	0.798	24
7	48.00	47.10	0.90	0.333	0.673	0.028	0.661	3
8	46.50	47.10	-0.60	0.333	-0.449	0.013	-0.437	6
9	46.80	47.10	-0.30	0.333	-0.224	0.003	-0.218	11
10	51.80	51.00	0.80	0.333	0.598	0.022	0.586	16
11	51.20	51.00	0.20	0.333	0.150	0.001	0.145	13
12	50.00	51.00	-1.00	0.333	-0.748	0.035	-0.737	17
13	34.00	36.83	-2.83	0.333	-2.118	0.280	-2.418	8
14	38.00	36.83	1.17	0.333	0.872	0.048	0.865	20
15	38.50	36.83	1.67	0.333	1.246	0.097	1.270	7
16	20.00	19.90	0.10	0.333	0.075	0.000	0.072	9
17	19.20	19.90	-0.70	0.333	-0.523	0.017	-0.511	10
18	20.50	19.90	0.60	0.333	0.449	0.013	0.437	5
19	55.20	57.00	-1.80	0.333	-1.346	0.113	-1.384	2
20	59.50	57.00	2.50	0.333	1.869	0.218	2.047	21
21	56.30	57.00	-0.70	0.333	-0.523	0.017	-0.511	14
22	58.80	58.70	0.10	0.333	0.075	0.000	0.072	4
23	58.80	58.70	0.10	0.333	0.075	0.000	0.072	12
24	58.50	58.70	-0.20	0.333	-0.150	0.001	-0.145	19

SOURCE	SUM OF SQUARES	DF	MEAN SQUARE	F VALUE	PROB > F
MODEL	4031.7552	7	575.97	567.61	< 0.0001
RESIDUAL	16.2354	16	1.01		
*PURE ERROR	16.2354	16	1.01		
COR TOTAL	4047.9906	23			

ROOT MSE	1.0073	R-SQUARED	1.00	
DEP MEAN	96.5179	ADJ R-SQUARED	0.99	
C.V. %	1.0437	PRED R-SQUARED	0.99	

Predicted Residual Sum of Squares (PRESS) =   36.53

* Residual = Lack-Of-Fit + Pure Error

FACTOR	COEFFICIENT ESTIMATE	DF	STANDARD ERROR	t FOR H0 COEFFICIENT=0	PROB > |t|
INTERCEPT	96.51792	1	0.20562		
A	3.40542	1	0.20562	16.56	< 0.0001
B	-11.27208	1	0.20562	-54.82	< 0.0001
C	-3.04292	1	0.20562	-14.80	< 0.0001
AB	-4.27125	1	0.20562	-20.77	< 0.0001
AC	-0.97208	1	0.20562	-4.73	0.0002
BC	0.93375	1	0.20562	4.54	0.0003
ABC	-0.11542	1	0.20562	-0.56	0.5824

Final Equation in Terms of Coded Factors

UTS =

$$
\begin{aligned}
& 96.5179 \\
+\ & 3.4054 * A \\
-\ & 11.2721 * B \\
-\ & 3.0429 * C \\
-\ & 4.2713 * A * B \\
-\ & 0.9721 * A * C \\
+\ & 0.9337 * B * C \\
-\ & 0.1154 * A * B * C
\end{aligned}
$$

Final Equation in Terms of Uncoded Factors

UTS =

$$
\begin{aligned}
& 141.7149 \\
+\ & 5.5058 * Cold\ Work \\
-\ & 0.0616 * H.T.\ Temp. \\
-\ & 14183.1111 * Wall\ Thick. \\
-\ & 0.0054 * Cold\ Work * H.T.\ Temp. \\
-\ & 4.8889 * Cold\ Work * Wall\ Thick. \\
+\ & 16.1873 * H.T.\ Temp. * Wall\ Thick. \\
-\ & 0.2198 * Cold\ Work * H.T.\ Temp. * Wall\ Thick.
\end{aligned}
$$

OBS ORD	ACTUAL VALUE	PREDICTED VALUE	RESIDUAL	LEVER	STUDENT RESID	COOK'S DIST	OUTLIER T VALUE	RUN ORD
1	102.60	103.23	-0.63	0.333	-0.770	0.037	-0.760	22
2	104.00	103.23	0.77	0.333	0.932	0.054	0.928	1
3	103.10	103.23	-0.13	0.333	-0.162	0.002	-0.157	15
4	119.30	120.30	-1.00	0.333	-1.216	0.092	-1.236	18
5	121.90	120.30	1.60	0.333	1.945	0.237	2.156	23
6	119.70	120.30	-0.60	0.333	-0.730	0.033	-0.718	24
7	88.20	87.13	1.07	0.333	1.297	0.105	1.327	3
8	85.80	87.13	-1.33	0.333	-1.621	0.164	-1.717	6
9	87.40	87.13	0.27	0.333	0.324	0.007	0.315	11
10	89.40	87.58	1.82	0.333	2.217	0.307	2.579	16
11	87.52	87.58	-0.06	0.333	-0.069	0.000	-0.067	13
12	85.81	87.58	-1.77	0.333	-2.148	0.288	-2.465	17
13	97.03	96.99	0.04	0.333	0.045	0.000	0.043	8
14	96.94	96.99	-0.05	0.333	-0.065	0.000	-0.063	20
15	97.01	96.99	0.02	0.333	0.020	0.000	0.020	7
16	110.50	110.63	-0.13	0.333	-0.162	0.002	-0.157	9
17	110.00	110.63	-0.63	0.333	-0.770	0.037	-0.760	10
18	111.40	110.63	0.77	0.333	0.932	0.054	0.928	5
19	85.74	85.09	0.65	0.333	0.790	0.039	0.781	2
20	85.05	85.09	-0.04	0.333	-0.049	0.000	-0.047	21
21	84.48	85.09	-0.61	0.333	-0.742	0.034	-0.731	14
22	81.05	81.18	-0.13	0.333	-0.162	0.002	-0.157	4
23	81.39	81.18	0.21	0.333	0.251	0.004	0.244	12
24	81.11	81.18	-0.07	0.333	-0.089	0.000	-0.086	19

SOURCE	SUM OF SQUARES	DF	MEAN SQUARE	F VALUE	PROB > F
MODEL	16357.028	7	2336.7	1040.09	< 0.0001
RESIDUAL	35.947	16	2.2		
*PURE ERROR	35.947	16	2.2		
COR TOTAL	16392.974	23			

ROOT MSE	1.499	R-SQUARED	1.00	
DEP MEAN	62.719	ADJ R-SQUARED	1.00	
C.V. %	2.390	PRED R-SQUARED	1.00	

Predicted Residual Sum of Squares (PRESS) =   80.9

* Residual = Lack-Of-Fit + Pure Error

FACTOR	COEFFICIENT ESTIMATE	DF	STANDARD ERROR	t FOR H0 COEFFICIENT=0	PROB > |t|
INTERCEPT	62.71917	1	0.30596		
A	5.91583	1	0.30596	19.34	< 0.0001
B	-24.51167	1	0.30596	-80.11	< 0.0001
C	-2.60667	1	0.30596	-8.52	< 0.0001
AB	-6.14833	1	0.30596	-20.10	< 0.0001
AC	-0.33833	1	0.30596	-1.11	0.2852
BC	0.97417	1	0.30596	3.18	0.0058
ABC	0.25250	1	0.30596	0.83	0.4214

Final Equation in Terms of Coded Factors

Y.S. =

```
+        62.7192
+         5.9158 * A
-        24.5117 * B
-         2.6067 * C
-         6.1483 * A * B
-         0.3383 * A * C
+         0.9742 * B * C
+         0.2525 * A * B * C
```

Final Equation in Terms of Uncoded Factors

Y.S. =

```
         147.4690
+          9.5386 * Cold Work
-          0.1114 * H.T. Temp.
-       6326.4127 * Wall Thick.
-          0.0103 * Cold Work * H.T. Temp.
+        458.8254 * Cold Work * Wall Thick.
+          4.8127 * H.T. Temp. * Wall Thick.
+          0.4810 * Cold Work * H.T. Temp. * Wall Thick.
```

OBS ORD	ACTUAL VALUE	PREDICTED VALUE	RESIDUAL	LEVER	STUDENT RESID	COOK'S DIST	OUTLIER T VALUE	RUN ORD
1	77.67	78.16	-0.49	0.333	-0.398	0.010	-0.387	22
2	78.71	78.16	0.55	0.333	0.452	0.013	0.441	1
3	78.09	78.16	-0.07	0.333	-0.054	0.000	-0.053	15
4	100.20	103.47	-3.27	0.333	-2.669	0.445	-3.470	18
5	107.60	103.47	4.13	0.333	3.377	0.713	6.103	23
6	102.60	103.47	-0.87	0.333	-0.708	0.031	-0.697	24
7	41.09	39.99	1.10	0.333	0.902	0.051	0.896	3
8	38.53	39.99	-1.46	0.333	-1.190	0.089	-1.207	6
9	40.34	39.99	0.35	0.333	0.289	0.005	0.280	11
10	40.43	39.69	0.74	0.333	0.602	0.023	0.590	16
11	39.81	39.69	0.12	0.333	0.095	0.001	0.092	13
12	38.84	39.69	-0.85	0.333	-0.697	0.030	-0.686	17
13	72.74	72.18	0.56	0.333	0.460	0.013	0.449	8
14	71.95	72.18	-0.23	0.333	-0.185	0.002	-0.180	20
15	71.84	72.18	-0.34	0.333	-0.275	0.005	-0.267	7
16	95.67	95.12	0.55	0.333	0.447	0.012	0.435	9
17	94.90	95.12	-0.22	0.333	-0.182	0.002	-0.177	10
18	94.80	95.12	-0.32	0.333	-0.264	0.004	-0.256	5
19	37.70	36.89	0.81	0.333	0.659	0.027	0.647	2
20	36.22	36.89	-0.67	0.333	-0.550	0.019	-0.538	21
21	36.76	36.89	-0.13	0.333	-0.109	0.001	-0.106	14
22	36.09	36.26	-0.17	0.333	-0.136	0.001	-0.132	4
23	36.49	36.26	0.23	0.333	0.191	0.002	0.185	12
24	36.19	36.26	-0.07	0.333	-0.054	0.000	-0.053	19